Building a 3D model of the human keratoconic cornea

Thomas Volatier, BSc MSc MPhil

Doctor of Philosophy (PhD)

Institute of Biomedicine

Faculty of Medical Sciences

Newcastle University

Declaration of work

I declare that this thesis is based on my own work and has not been submitted in any form for another degree at any university or any other tertiary education. Information derived from published and unpublished work of others has been acknowledged in the text and the list of reference given in the bibliography.

Abstract

Keratoconus is a corneal disease characterized by the affected tissue adopting a conical shape, leading to loss of vision and compromised structural integrity. The disease is manageable in its early stage with lenses or glasses and can be treated in its later stages with surgery or crosslinking. The underlying cause of the disease is still poorly understood, a model would aid the exploration of this disease. In this study, primary stromal cells harvested from healthy and keratoconic corneas using a variety of extraction methods were cultured in compressed collagen gels and serum-free medium containing retinoic acid to simulate the cornea's natural environment. The survival of stromal cells and their gene expression was assayed, paying special attention to genes related to differentiation and ECM maintenance. Among healthy cells, differences were identified between limbal and central population while central keratoconic cells more closely resembled healthy limbal cells. Use of retinoic acid as a medium supplement allowed for the culture of cells in serum-free conditions and caused gene expression that resembled *in vivo* behaviour. The final addition of ECM in the form of curved, compressed collagen gels to this culture system caused the stromal cells to radically change their behaviour and reaction to retinoic acid. Overall, this study identified a stromal tissue model as well as the multiple considerations in the construction of such a model. The use of this model in keratoconus research may lead to breakthroughs in attempts to better understand the disease.

Acknowledgements

I would like to thank my supervisor Prof. Che J. Connon for his support, patience and guidance throughout my PhD. It has been a privilege to learn from him and I could not have found a better group to integrate than his team of intelligent and motivated researchers.

I would like to thank my second supervisor, Prof. Francisco Figueiredo for lending his expertise in corneal surgery and anatomy as well as his great service in the provision of corneal tissue.

I would also like to thank our collaborator Dr. Shukti Chakravarti at NYU Langone Health for her expertise and work on RNA-Seq.

I would like to thank Prof. Mark Birch-Machin and Dr. Kataryzna Pirog, my panel members from Newcastle University for their support and the suggestions that I received during my annual meeting.

I would also like to thank my friends and colleagues from Newcastle University. Particularly Dr. Ricardo Gouveia, whose experience and practical skills have been invaluable in helping me progress through my PhD. I would like to thank Dr. Martina Miotto, Ms/Miss Olla Al-Jaibaji, Dr. Fadhilah Zainal Abidin, Miss Anastassia Kostenko, Dr. Andrei Constantinescu and Dr. Steven Swioklo for their support throughout the years.

I would like to thank all of my friends in France, Belgium and the UK who have encouraged and supported me outside the lab.

Finally, I would like to thank my family for being a source or love and encouragement throughout my life. My parents in particular have been very supportive and have pushed me to achieve more than I thought possible.

Table of Contents

Abstract ii

Acknowledgements iii

Table of Contents iv

Table of Figures vii

Index of Tables viii

Chapter 1: Introduction 1

1. Thesis abstract 1

2. Thesis structure 1

Chapter 2. Literature review 1

Chapter 3. General methodology 1

Chapter 4. Isolation of stromal cells from different parts of the cornea 2

Chapter 5. Culturing Stromal Cells in Serum-Free Conditions 2

Chapter 6. Engineering a 3D culture system 2

Chapter 7. Validation of the artificial stroma model 2

Chapter 8. Conclusions and future directions 3

3. List of abbreviations 3

Chapter 2: Literature review 4

1. Anatomy of the human cornea 4

1.1 Tear fluid 5

1.2. Epithelium 6

1.3. The Bowman layer 6

1.4. Stroma 7

1.5. Descemet's membrane 7

1.6. Endothelium 7

2. Keratocytes 8

2.1. Keratocytes during morphogenesis 8

2.2. Homeostasis 9

2.3. Wound healing 9

3. Keratoconus 10

3.1. Incidence and associated factors 10

3.2. Pathophysiology and molecular signalling 11

3.3. Diagnosis and treatment 16

4. Corneal tissue engineering 19

4.1. Models of the stroma 19

4.2. Models of keratoconus 19

Chapter 3: General Methodology 21

1. Tissue Culture 21

1.1. Stromal cell growth medium 21

1.2. Stromal cell serum-free medium 21

1.3. Preparation of retinoic acid aliquots and addition to cell cultures 21

1.4. Stromal cell culture 21

1.5. Stroma enzyme digestion 22

1.6. Stromal explant migration 23

1.7. Keratoconic cell sources 23

1.8. Freezing and thawing stromal cells 24

1.9. Culturing cells serum-free conditions 24

1.10. Culturing cells in compressed collagen gels 24

2. Assays and Analysis 26

2.1. Alamar blue: Resazurin fluorescence to count cells 26

2.2. Reverse Transcription Polymerase Chain Reaction 27

2.3. RNA extraction from adherent cells 27

2.4. RNA extraction from cells in collagen gels 28

2.5. Synthesis of complementary DNA 29

2.6. Primer design 29

2.7. Quantitative PCR 30

2.8. Statistical Analysis 32

Chapter 4: Isolation of stromal cells from different parts of the cornea 33

1. Abstract 33

2. Introduction 33

2.1. Stromal cell population within the stroma 33

2.2. Activation and differentiation of stromal cells 34

2.3. Stromal cell extraction methods 36

2.4. Aims 36

3. Methods 37

3.1. Isolating cells from central and limbal stroma with collagenase 37

3.2. Isolating cells from central and limbal stroma via explant migration- 37

3.3. Extracting non-mobile cells from explants post-migration 37

3.4. Survival in serum-free conditions 37

..... 39

3.5. Quantitative PCR 40

4. Results 40

4.1. Serum-free survival of healthy and keratoconic stromal cells 40
4.2. Gene expression of healthy and keratoconic stromal cells 42
..... 45
5. Discussion 46
Chapter 5: Culturing Stromal Cells in Serum-Free Conditions 50
1. Abstract 50
2. Introduction 50
2.1. Reproducing the stromal cell native environment 50
2.2. Modelling the corneal stroma 50
2.3. Medium supplementation 51
2.4. Retinoic Acid 53
2.5. Aims 54
3. Methods 54
3.1. Preparation of RA 54
3.2. Cell survival in RA-supplemented medium 54
3.3. Stromal cell gene expression in RA-supplemented medium 55
4. Results 55
4.1. Survival of healthy and keratoconic stromal cells with RA 55
..... 57
4.2. Gene expression of healthy and keratoconic stromal cells with RA 57
..... 59
5. Discussion 60
Chapter 6: Engineering a 3D Culture System 65
1. Abstract 65
2. Introduction 65
2.1. Stromal architecture and function 65
2.2. Influence of stromal ECM on cell behaviour 66
2.3. Use of collagen gels in model building 66
2.4. Curvature as an environmental cue 67
2.5. Model specifications and requirements 67
2.6. Aims 67
3. Methods 68
3.1. Gel making and cell encapsulation 68
3.2. Curved gel culture 68
3.3. Retinoic acid supplementation 68
3.4. Stromal cell gene expression in compressed collagen gels 68

4. Results **69**
5. Discussion **79**
5.1. Comparison of 2D to CCG culture 79
5.2. Comparison of CCG with and without RA 82
5.3. Comparison of flat and curved CCG in the presence and absence of RA 84
Chapter 7: Validation of the Artificial Stromal Model **87**
1. Abstract **87**
2. Introduction **87**
2.1. Hallmarks of keratoconus gene expression in vivo 87
2.2. Previous keratoconus models and their validity 89
2.3. Aims 90
3. Method **91**
3.1. Quantitative PCR 91
3.2. RNA-Seq 91
4. Results **92**
4.1. Quantitative PCR 92
4.2. RNA-Seq 95
5. Discussion **98**
Chapter 8: Conclusions and Future Directions **102**
1. Conclusions **102**
2. Future directions **105**
References **106**

Table of Figures

Figure 1: Anatomy of the human eye 4
Figure 2: Schematic cross-section of the tissue layers in the central cornea 5
Figure 3: Preparation of compressed collagen gels. 25
Figure 4: Preparation of compressed collagen gels and subsequent culture on dome. 26
Figure 5: Schematic representation of the methods of stromal cell extraction. 39
Figure 6: Survival of healthy and keratoconic stromal cells. 41
Figure 7: Fold change in gene expression for healthy stromal cells cultured in serum-free medium. 42
Figure 8: Fold change in gene expression for healthy stromal cells and keratoconic stromal cells cultured in serum-free medium. 45

Figure 9: Survival of explant migrated and enzyme digested healthy stromal cells in retinoic acid serum- free medium 56
Figure 10: Survival of keratoconic stromal cells in RA serum- free medium 57
Figure 11 : Fold change in gene expression for healthy stromal cells and keratoconic fibroblasts cultured in serum-free medium without RA or with RA 59
Figure 12: Survival of keratoconic cells and enzyme digested limbal and central stromal cells in CCG with and without retinoic acid 70
Figure 13: Fold change in gene expression for healthy limbal and central stromal cells and keratoconic fibroblasts cultured in serum-free medium on flat plastic or within a compressed collagen gel. 72
Figure 14: Fold change in gene expression for healthy limbal and central stromal cells and keratoconic fibroblasts cultured in CCG with serum-free medium either without RA or with RA CCG 74
Figure 15: Fold change in gene expression for healthy limbal stromal cells and keratoconic fibroblasts cultured either in flat CCG or in curved CCG . Each type of gel was subjected to culture without RA.. 77
Figure 16: Fold change in gene expression for healthy limbal stromal cells and keratoconic fibroblasts cultured either in flat CCG or in curved CCG. Each type of gel was subjected to culture with RA.. 78
Figure 17: Gene expression of enzyme-digested healthy limbal stromal cells in various culture conditions relative to freshly extracted limbal stromal cells.. 93
Figure 18: Principal component analysis showing transcriptional variance among the two patient groups and the model 95
Figure 19: Heat map of all significantly enriched and depleted genes for Saudi Arabian patient samples vs model and European Caucasian patient samples vs model 96

Index of Tables

Table 1: Description of primers used in qPCR for keratocyte gene expression analysis. 30
Table 2: Results of multiple t-tests comparing the freshly isolated limbal stromal cells to the cells cultured in the various model conditions. 94
Table 3: Fold change and associated p value for genes of interest as gathered by RNA-Seq comparing model samples and each of the two patient groups. 97
Table 4: RNA-Seq selection of European Caucasian patient genes that showed particularly large fold changes relative to the model. 98

Table 5: RNA-Seq selection of Saudi Arabian patient genes that showed particularly large fold changes relative to the model. 98

Chapter 1: Introduction

1. Thesis abstract

Keratoconus is a corneal disease characterized by the affected tissue adopting a conical shape, leading to loss of vision and compromised structural integrity. The disease is manageable in its early stage with lenses or glasses and can be treated in its later stages with surgery or crosslinking. The underlying cause of the disease is still poorly understood, a model would aid the exploration of this disease. In this study, primary stromal cells harvested from healthy and keratoconic corneas using a variety of extraction methods were cultured in compressed collagen gels and serum-free medium containing retinoic acid to simulate the cornea's natural environment. The survival of stromal cells and their gene expression was assayed, paying special attention to genes related to differentiation and ECM maintenance. Among healthy cells, differences were identified between limbal and central population while central keratoconic cells more closely resembled healthy limbal cells. Use of retinoic acid as a medium supplement allowed for the culture of cells in serum-free conditions and caused gene expression that resembled *in vivo* behaviour. The final addition of ECM in the form of curved, compressed collagen gels to this culture system caused the stromal cells to radically change their behaviour and reaction to retinoic acid. Overall, this study identified a stromal tissue model as well as the multiple considerations in the construction of such a model. The use of this model in keratoconus research may lead to breakthroughs in attempts to better understand the disease.

2. Thesis structure

Chapter 2. Literature review

In this chapter, we reviewed the anatomy of the healthy human cornea as well as catalogued diagnostic signs and molecular pathways of keratoconus. Current approaches and existing challenges in the construction of 3D culture systems and disease models were also mentioned.

Chapter 3. General methodology

In this chapter we described the culture conditions and extraction methods used to isolate primary stromal cells from donor tissue. The fabrication of the 3D culture system and the assays used to monitor cell survival or gene expression were also mentioned. The imitations

and initial troubleshooting involved in some of these methods was also discussed. Lastly, statistical analysis and data processing methods were explained.

Chapter 4. Isolation of stromal cells from different parts of the cornea

In this chapter we investigated the effects that the isolation method and location had on the final population extracted cells. Through 3 distinct methods and 2 distinct pieces of tissue, it was possible to isolate a total of 6 different populations of stromal cells. After analysis of survival and gene expression it became clear that isolation method and location had significant effects on the cells extracted. Lastly, keratoconic cells were factored into this comparison and we observed great similarity between the central, explant-migrated keratoconic cells and the limbal, enzyme-digested healthy cells.

Chapter 5. Culturing Stromal Cells in Serum-Free Conditions

In this chapter the use of retinoic acid was explored as a medium supplement to maintain cell survival in serum-free conditions. Assays determined that retinoic acid had a significant effect on survival and gene expression of both healthy and keratoconic cells. The expression profiles of healthy cells seemed to mimic *in vivo* behaviour, suggesting that retinoic acid is a useful addition to the model system.

Chapter 6. Engineering a 3D culture system

In this chapter the use of compressed collagen gels was investigated as a means to produce stroma-like tissue to house the primary cells extracted previously. The survival and gene expression of the cells were assayed, showing distinct shifts in behaviour from culture on flat plastic in both healthy and keratoconic cells. Addition of retinoic acid and curving the compressed collagen gels were also explored as means to better model stromal conditions. Retinoic acid did seem to have a beneficial effect while the effect of curvature was more complex to interpret.

Chapter 7. Validation of the artificial stroma model

In this chapter the validity of the culture system developed as a model was assayed using qPCR and RNA-Seq. The gene expression of healthy cells cultured in the model was compared to freshly isolated cells while keratoconic cells cultured in the model were compared to patient samples. Key differences between the model cultures and their respective baselines were highlighted.

Chapter 8. Conclusions and future directions

This chapter summarizes the main findings of this thesis and the potential implications for corneal research. Potential future developments and interesting new challenges are also detailed.

3. List of abbreviations

enzdL - enzyme digested limbal stromal cell

enzdC - enzyme digested central stromal cell

exmL – explant migrated limbal stromal cell

exmC – explant migrated central stromal cell

exenzdL – “explant” enzyme digested limbal stromal cell

exenzdC - “explant” enzyme digested central stromal cell

CCG – compressed collagen gel

cCCG – curved compressed collagen gel

RA – retinoic acid

ECM – extra cellular matrix

PCR – polymerase chain reaction

Chapter 2: Literature review

1. Anatomy of the human cornea

The front of the eye is protected by a clear spherical cap of tissue called the cornea (Fig. 1). The clarity and shape of the cornea are both essential to allow transmission of light into the eye and to the retina. The cornea also serves as a physical barrier and protects the inner contents of the eye. The human cornea is made up of five distinct layers (Fig. 2). The anterior-most layer is the cell-rich epithelium. The epithelium's basal cells reside on an underlying fibrous mesh of collagen called the Bowman layer. Posterior to the Bowman layer is the collagen-rich stroma, contributing the majority of the cornea's volume. Posterior to the stroma is the acellular Descemet's membrane. The final and posterior-most layer of the cornea is the single cell layer of endothelium that separates the cornea from the aqueous humour in the eye (Schwarz and Keyserlingk, 1966, Maurice, 1957).

The centre of the cornea is avascular and is sustained by nutrients provided from the aqueous humour and tear film. The periphery of the cornea, referred to as the limbus, has some blood supply due to the proximity to the vascularized conjunctiva that covers the rest of the eye's surface (Sridhar, 2018). The corneal structure does vary between species, particularly in terms of Bowman layer and Descemet's membranes, to accommodate different needs and adaptations, although in all cases the cornea fulfils the basic roles of protection and refraction (Hayashi et al., 2002a).

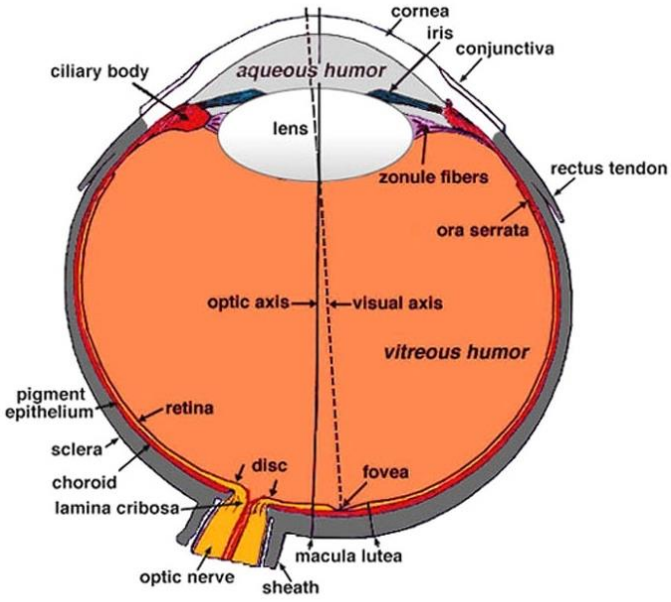

Figure 1: Anatomy of the human eye (Kolb, 1995).

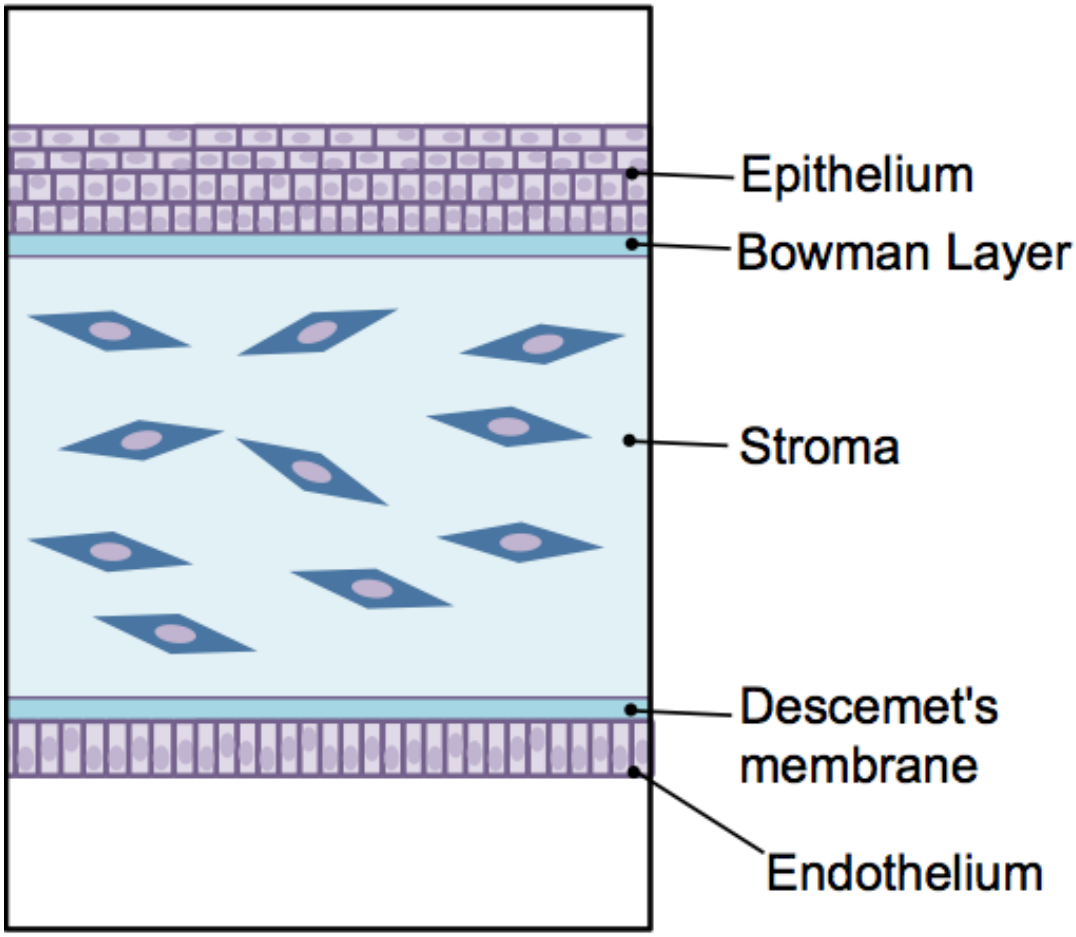

Figure 2: Schematic cross-section of the tissue layers in the central cornea and the approximate shape of cells within each layer. The Bowman layer and Descemet's membrane are both devoid of cells

1.1 Tear fluid

A thin film of tear fluid covers every part of the eye that is exposed to the outside world. This fluid is full of lipids, proteins and salts that fulfil many functions: lubrication, microbial defence, inflammatory regulation and wound healing (Kijlstra and Kuizenga, 1994, Georgiev et al., 2017). The fluid that covers the cornea specifically is termed the precorneal tear fluid (Mishima, 1965). This tear film can be considered the most dynamic structure of the cornea, with the most rapid production and turnover (Rolando and Zierhut, 2001). During wounding events, factors that are normally kept from penetrating into the corneal tissue by the epithelium can enter the stroma and disturb the cells within.

1.2. Epithelium

The corneal epithelium covers the anterior portion of the corneal stroma and is composed of stratified, non-cornified, squamous cells. The epithelium's basal layer of cuboidal cells adheres to the top of the Bowman layer (Tong et al., 2006) via a basement membrane. Like in all parts of the human anatomy, the main purpose of the epithelium is to form a protective barrier to the outside. Along with its protective role, the corneal epithelium has also been found to produce cytokines that influence keratocyte behaviour. Epithelial wounding events may cause loss of cells that can then allow infiltration of previously isolated cytokines into the posterior layers or the loss of pre-existing signals (Lackner et al., 2014). An example is TGFβ in its three isoforms, which can increase ECM production and proliferation of stromal keratocytes; or interleukins 1 and 6 that may trigger ECM remodelling and antagonize TGFβ signalling. The maintenance of the corneal ECM structure and transparency is an active and dynamic process that requires continuous communication between the stromal keratocyte and the neighbouring cells located at separate layers of the cornea. Distinct populations of cells in the epithelium, stroma and endothelium use cytokine-mediated interactions to communicate across the Bowman layer and Descemet's membrane (Wilson and Hong, 2000). The stromal-epithelial crosstalk is the most thoroughly characterized set of cell interactions in the cornea, as evidenced by the greater amount of research attention and publication it has received over the last few years.

1.3. The Bowman layer

The Bowman layer is a condensed acellular layer of collagen fibres. The layer presents a smooth interface to the epithelia, to which epithelial cells adhere, and a less distinct posterior surface that merges into the stromal collagen. Unmyelinated nerves penetrate into the Bowman layer to then innervate the epithelium (Lagali et al., 2009). The exact purpose of the Bowman layer is unclear although it shows clear difference from stromal collagen. The layer seems to function as an intermediate "ligament" between the protective epithelium and the structural stroma. Congenital absence of the Bowman layer does not seem to be associated with otherwise abnormal or hazy corneas and the layer is in fact absent in some species (Wilson and Hong, 2000). The layer itself is only around 12μm thick and, if damaged, isn't replaced (Patel et al., 2001). Instead, stromal collagen populated with cells may fill the gap left behind.

1.4. Stroma

The stroma's complex network of hydrated extracellular matrix (Fujii et al., 2015) makes up over 80% of the cornea's total volume. The tissue is composed of interwoven fibrous proteins, mainly collagens type I and V. Binding the fibres together are glycosaminoglycans such as chondroitin, dermatan, keratan, and heparan sulphates (Pacella et al., 2015). These glycosaminoglycans have many roles: they regulate hydration, arrange fibre distance, bind cytokines and cations, and support structural integrity (Fini and Stramer, 2005). The collagen fibrils in the human cornea are highly organized and tightly packed into bundles called lamellae (Smith and Frame, 1969). These lamellae were arranged parallel to the corneal surface and were interwoven with adjacent lamellae. In the anterior part of the cornea, the fibres undergo a high degree of interweaving, forming a compact fibrillar network. At the stroma's posterior, the lamellae undergo less splitting and less interweaving, these features coincide with a lower concentration of cells and increased swelling properties (Komai and Ushiki, 1991, Mikula et al., 2018). The parallel alignment of the collagen fibrils within the lamellae contributes to the cornea's transparency; the strands of collagen are woven and spaced by glycosaminoglycans and other collagen types. This results in a local order forming a pseudo-crystalline structure that facilitates the passage of light through the cornea (Maurice, 1957). The concentrations and distributions of glycosaminoglycans in the corneal stroma vary along the anterior-posterior gradient. This results in parts of the corneal stroma reacting to stress and swelling differently (Muller et al., 2001).

1.5. Descemet's membrane

There exists another acellular membrane in the cornea, made up of multiple types of collagen. This membrane, called Descemet's membrane, is made and maintained by the endothelial cells. This membrane seems to be a physical barrier against infections and infiltration as well as the basal structure to which the endothelium adheres (Hayashi et al., 2002b). Impairment to Descemet's membrane through infections, wounds or the hereditary conditions known as Fuchs's corneal dystrophy can lead to corneal thickening and cloudiness (Siggel et al., 2019).

1.6. Endothelium

The final layer of the cornea positioned on the posterior side of the Descemet's membrane and separating the cornea from the aqueous humour is the endothelium. This is an avascular, single layer of hexagonal cells. While interactions between the endothelium cells and stromal keratocytes have been the subject of relatively little investigation, the principal function of the

endothelium has been documented as being active transport of water out from the stroma into the anterior chamber of the eye using ATPase pumps (Tuft and Coster, 1990). This movement of fluids prevents stromal swelling and opacity, maintaining transparency. The endothelium also traffics glucose and other essential nutrients into the stroma to feed the cell within (Adamis et al., 1993). Whilst it is known that endothelial cells produce modulatory cytokines such as interleukin 18 and platelet-derived growth factor 7, the exact nature of any biochemical signal exchanged between stromal cells and endothelial cells is unknown (Kim et al., 1999).

2. Keratocytes

Within the stroma, between the collagen lamellae, reside the cells thought responsible for the construction and maintenance of the stromal tissue. These cells are the keratocytes. Typically quiescent and evenly spaced out, these cells will become active in response to injury and slowly repair the specialized ECM (Jester et al., 1999). While fibroblastic in nature, the keratocytes do possess some traits that make them unique, like their crystalline-rich cytoplasm (Jester, 2008). The majority of these keratocytes are positioned in the anterior portion of the cornea, near the epithelium and nerves as well as where injury is most likely to occur (Poole et al., 2003).

2.1. Keratocytes during morphogenesis

The mammalian eye is constructed during development from the neural crest, itself yielding three sources of precursor eye cells: neural ectoderm, surface ectoderm and periocular mesenchyme (Williams and Bohnsack, 2015, Gage et al., 2005). The periocular mesenchyme specifically will derive the stromal cells that maintain the construct the stroma and will later become keratocytes (Yoshida et al., 2006). The cells in the periocular mesenchyme initially build and remodel ECM into stroma, with its unique structure and deposited proteins that make it transparent (Quantock et al., 2003). As the tissue takes form, the cells will undergo apoptosis and the small population that remains will express proteins key to corneal stromal cell function, like crystallins (Jester, 2008). The differentiation from neural crest cell into the quiescent keratocyte can be traced using the disappearance of PAX6, a marker of early eye development, and appearance of CD34, a general marker of mesenchymal stem cells (Funderburgh et al., 2005). Expression of CD34 does decrease when the quiescent keratocytes become activated in the event of an injury (Funderburgh et al., 2003). This loss of expression

is particularly evident in vitro where CD34 expression disappears almost entirely upon keratocyte activation (Toti et al., 2002a).

2.2. Homeostasis

The specialized form of fibroblasts, called keratocytes, are normally found embedded within the stromal ECM in a quiescent state, becoming activated as a response to any disruption to the stroma such as trauma or infection. The activation process is mediated by growth factors like TGFβ, FGF and PDGF (Ljubimov and Saghizadeh, 2015). The majority of these quiescent keratocytes reside in the anterior portion of the stroma, closest to the epithelium. The adjacent epithelium provides the stroma and the cells within with growth factors, such as hepatocyte growth factor (HGF) and keratinocyte growth factor (KGF) (Wilson et al., 1999, Reinach and Pokorny, 2008). As with almost every cell population in the body, there needs to be a stock of progenitor cells to maintain a large enough population of functional cells. For the corneal stromal cells, this population is found in the limbus. Analysis of CD34 expression in particular shows that the limbus hosts a greater percentage of CD34 positive stromal cells (Branch et al., 2012).

2.3. Wound healing

During wounding, replacement of lost keratocytes requires activation of nearby keratocytes; this active state is characterized by a change in morphology to more typically fibroblastic traits like a larger spindle-like shape, increased organelle content and a loss of cytoplasmic granules (Fini and Stramer, 2005). This is in contrast to normal keratocyte morphology where quiescent cells are stellate or dendritic with a triangular body (Espana et al., 2003). The newly activated cells then migrate into the wound area and remodel the ECM with matrix-degrading enzymes and new matrix components. The fibroblasts also express smooth-muscle actin and desmin, becoming contractile to stimulate wound closure (Chaurasia et al., 2009).
Activated keratocytes lose expression of proteins associated with cellular transparency such as ALDH1A1 and crystallins (Jester et al., 1999). Activated keratocytes may also become myofibroblasts and express alpha smooth muscle actin (αSMA). These terminally differentiated, contractile cells are typically found only at wound sites to aid in closure by enlarging and spreading. Myofibroblasts will also produce some ECM crosslinkers and MMPs to remodel damaged stroma (Ebihara et al., 2007). While the myofibroblasts and fibroblasts play an essential role in wound healing of the cornea, persistence of these differentiated cell states are also associated with multiple pathological processes like corneal

haze and scarring (Connon et al., 2003). Studies into the behaviour of stromal cells during surgical wound events found that stromal cells near the wound would differentiate into myofibroblasts, resulting in a fibrotic haze, The fibrous matrix would resolve itself into a more transparent matrix over the two following months as the myofibroblasts were replaced with the quiescent keratocytes (Kivanany et al., 2018). Conserving the undifferentiated state of stromal keratocytes until fibroblastic differentiation is required as a vital role of signalling factors in the stroma.

3. Keratoconus

3.1. Incidence and associated factors

An estimated 1 in 2000 individuals is affected by keratoconus with varying degrees of severity. Keratoconus' onset is typically observed and initially diagnosed between the ages of 15 and 25. A steady decline in the incidence of the disease is observed with age, likely due to tissue stiffening making the hallmark corneal deformation less likely. The disease has a higher reported prevalence in males, with around 60% of cases occurring in males (Godefrooij et al., 2017). Initial reports on keratoconus observed that the disease seemed to affects all ethnic groups equally. However, a significantly increased incidence was later reported for patients of middle-eastern and north African descents. In a retrospective study, North-Pakistani, Iranian and Saudi Arabian ethnicities in particular were identified as groups particularly at risk of developing keratoconus (Georgiou et al., 2004, Ziaei et al., 2012, Assiri et al., 2005). The high incidence of consanguineous marriages has been proposed as a likely cause for the increased occurrence of keratoconus among these groups (Assiri et al., 2005). The occurrence of keratoconus in some patients may sometimes coincide with other systemic diseases, such as Down's syndrome and Leber's congenital amaurosis (Elder, 1994, Rochels, 1979, Cullen and Butler, 1963). However, no conclusive genetic link has been established between keratoconus and these other conditions. It should also be taken into account that any disease or habit that results in excessive eye rubbing, such as atopy or wearing of hard contact lenses, could exacerbate pre-existing keratoconus into manifesting diagnostic signs (Wang et al., 2000). Keratoconus may initially weaken or deform the cornea, allowing further mechanical or inflammatory stress to worsen the condition and accelerate the need for treatment.

The genetic presentation associated with keratoconus shows great variance. Genetic and epigenetic factors are likely at fault and in some case have been found to associate with specific ethnic groups at times. Large-scale genetic studies of keratoconus may be impeded by

small sample sizes and catchment areas as well as some variation in disease presentation. This leads to varying reports in genes associated with keratoconus. Undertaking large-scale cooperative efforts in genomic studies would no doubt aid in understanding keratoconus genetically, particularly in Southern Asia where the disease is currently most present (Kok et al., 2012). Some candidate genes have already been identified in relation keratoconus pathogenesis due to their reoccurrence across several studies and patient groups. Genes like: Visual system homeobox 1 (VSX1), superoxide dismutase 1 (SOD1) and lysyl oxidase (LOX) all have documented evidence of mutations being associated with increased keratoconus susceptibility (Gordon-Shaag et al., 2015, Zhang et al., 2015).

3.2. Pathophysiology and molecular signalling

Stromal thinning is seen in all cases of keratoconus and multiple factors are to blame. An increase matrix degradation by proteolytic enzymes would break down the collagen while a drop in stromal cell population would delay replacement of lost extracellular matrix (ECM) (Romero-Jimenez et al., 2010). As a consequence of this ECM structural weakening, the mechanical properties of the matrix would be altered, providing new cues to differentiating keratocytes and progenitor cells. More severe stromal deformation may also affect the epithelial cells that reside above. The epithelium may be partly lost due to excessive eye rubbing. Beyond providing some structural support to each other, epithelial cells and stromal cells also communicate via a multitude of secreted factors. The implications of this relationship between the two cell types is that, should one be damaged or lost, the other will likely be affected in some manner (Tsubota et al., 1995). While epithelial loss often affects the stroma in some manner, keratoconus has not been reported as always presenting thinned epithelium prior to loss of ECM or stromal cells.

A common diagnostic sign of keratoconus is Fleischer's ring. This is made of iron aggregated by ferritin, an intracellular iron storage protein and then deposited in the basal epithelium (Loh et al., 2009). Tear fluid is the likely source of the deposited iron as lactoferrin normally binds the iron in the tears. A hypothesis of "tear-pooling" has been proposed where the collection of tears along the lines of lid closure lead to repeated concentration of iron in specific location in the cornea. Altered iron metabolism may occur within keratoconic tissue. Iron is a required cofactor for the formation of amino acid hydrolysine, which is then used to regulate collagen fibre diameter. In keratoconic tissue, hydroxylysine content in particular is reportedly lower (Cannon and Foster, 1978); indicating that iron metabolism may be

disrupted upstream although the exact pathway is unclear. There are no reports of the accumulated iron affecting cell behaviour either in the epithelium or the stroma.

In the past, research has shown that keratoconus is a multifactorial disease with both genetic and environmental components at play. There is evidence that a genetic predisposition to the disease may exist, allowing environmental triggers to induce some inflammatory components (Galvis et al., 2015). While the magnitude of inflammation's role in keratoconus remains uncertain, its involvement in some way has been documented as evident. Specific pro-inflammatory factors have been identified in aberrant amounts, either at the gene or protein level, within the stroma and epithelium. This increased production undoubtedly causes stress to the cells within the stroma and nearby. Interleukin 1 (IL-1) is a family of 11 cytokines that regulate immune and inflammatory responses, particularly during corneal wound healing. IL-1α and IL-1β are the main cytokines found during corneal injuries and both induce remodelling through apoptosis and MMP up-regulation. IL-1α is secreted by corneal epithelial cells and then diffuses both into the tear film and into the stroma (Wilson et al., 1996). According to Bureau et al., IL-1α and IL-1β are both present in greater concentrations in the keratoconic stroma, and stromal fibroblasts also display elevated levels of IL-1α receptors on their surface (Bureau et al., 1993). It is also known that IL-1α and IL-1β can induce apoptosis in conjunction with tumour necrosis factor alpha (TNFα); therefore, the loss of keratocytes in keratoconic corneas is likely to be secondary to increased levels of IL-1 within the stroma. Furthermore, IL-1 decreases production of superoxide scavenger SOD3, increases production of prostaglandin and increases production of MMPs (Balasubramanian et al., 2010). Those factors together would contribute to lower rates of cell survival, premature differentiation, stem cell depletion and matrix degradation, as seen in keratoconus.

Interleukin 6 (IL-6) is a pro-inflammatory cytokine mainly expressed by T cells and macrophages. IL-1 stimulates production of IL-6 in order to amplify inflammatory signal and wound healing. While IL-6 is expressed in greater quantities in tears of patients with keratoconus, its level does not increase with disease severity. Instead, friction events such as eye rubbing and contact lens wear seem to have the greatest effect on IL-6 production (Balasubramanian et al., 2013). Ebihara et al., have shown that IL-6 activity will lead to typical wound healing events such as epithelial cell migration and vascularization via VEGF (Ebihara et al., 2011).

Specific MMPs such as gelatinase A (MMP2) and MMP14 were found to be more active in keratoconus corneas and are likely responsible for matrix degradation during disease progression (Collier, 2001, Davidson et al., 2014). The stroma is composed of stacked collagen fibrils cross-linked with proteoglycans and also contains dispersed keratocytes that are responsible for maintaining the surrounding ECM. Keratocytes normally produce additional collagen as well as breakdown collagen to maintain a specific functional architecture. Sivak and Fini among others have reported that the proteolytic enzymes responsible for this maintenance are the matrix metalloproteinases (MMP) (Sivak and Fini, 2002). MMPs are a family of zinc endoproteinases that typically bind to ECM components as well as some cytokines and cell surface proteins. All MMPs possess three characteristics: zinc is required for activity, a collagen interacting function and the inhibition by endogenous tissue inhibitor of metalloproteinases (TIMP) (Nagase and Woessner, 1999). Their activity is required for processes such as angiogenesis and inflammation but also for proteolytic activation of cytokines such as TNFα, an inflammatory factor, and transforming growth factor beta (TGFβ), a cell growth and proliferation factor (Gearing et al., 1994, Yu and Stamenkovic, 2000). In keratoconus, MMPs are overexpressed while TIMP presence is decreased (Ionescu et al., 2016). This means that ECM degradation is less restricted in keratoconic corneal tissue due to an imbalance in the MMP-to-TIMP ratio.

Increased inflammatory activity and enzymatic digestion of ECM is caused by an increase in total activation and production of digestive enzymes. A loss of inhibitory control on matrix metalloproteinases and interleukins also sustains structurally damaging activity. In the cornea, Galectin-1 (Gal-1) and Galectin-3 (Gal-3) were identified as anti-inflammatory regulators by research done in models of conjunctivitis, uveitis and retinopathies (Romero et al., 2006, Mello et al., 2015). Although it was never used in a clinical therapy, administration of Gal-1 to the cornea can reduce corneal opacity and lesions brought by virus-driven inflammation (Rajasagi et al., 2012). Exogenous Gal-3 has also been documented as a potent re-epithelialization reagent in corneal healing assays on mice and monkeys, causing epithelial disorganization by increasing MMP-9 production to disrupt tight junctions and allow restructuring epithelia into an even sheet (Cao et al., 2002, Fujii et al., 2015). Both Gal-1 and Gal-2 have been documented at higher concentration in keratoconic corneas, although Gal-1 has been found in greater concentration within the stroma while Gal-3 remains within epithelial cells and keratocytes. The greater amount of Gal-1 may be an effect rather than the cause of the disease itself. In the past keratoconus has been reported as an inflammatory disease and this data continues to support an inflammatory theory (Andrade et al., 2018). Of

note is that UV exposure, particularly that seen during CXL treatment, has shown to an increased Gal-1 expression and decrease overall interleukin and digestive enzyme presence in the cornea (Zanon Cde et al., 2015).

TGFβs are a family of pleiotropic cytokines capable of binding to multiple ligands with varying affinities. In severe keratoconus, elevated presence of TGFβ2 was noted (Priyadarsini et al., 2015). TGFβ2 is the main TGFβ isoform found in aqueous humour, and may have increased presence due to infiltrations. Increased αSMA has been linked to differentiation of keratocyte progenitor populations into myofibroblastic cells incapable of completely supporting the cornea (Engler et al., 2011). TGFβ is a versatile cytokine that possesses three isoforms (TGFβ1, TGFβ2, TGFβ3) and is typically involved in induction of genes responsible for differentiation, proliferation and migration. TGFβ also plays multiple roles in wound healing, acting as a chemoattractant for macrophages and fibroblasts (Amento and Beck, 1991). In the cornea, TGFβ is secreted by epithelial cells and diffuses into the stroma to bind to TGFβ receptors on keratocytes. The basement membrane between the epithelia and stroma acts as a potential barrier for TGFβ, however when the basement membrane is broken or damaged, TGFβ can pass into the stroma and induce fibroblastic differentiation in keratocytes to increase secretion of ECM at injury sites (Wilson, 2012). Additionally, TGFβ will maintain fibroblast viability in the presence of pro-apoptotic factor IL-1 with consequent stromal opacity. TGFβ may also induce some stromal cells to enter a myofibrogenic state, characterized by the marker α smooth muscle actin (αSMA), where unaligned deposition of fibres leads to a more opaque ECM. The secretion of TGFβ1 by myofibroblasts was also found to inhibit the re-innervation of corneal tissue following injury via the phosphorylation of collapsing response mediating protein 2 (Jeon et al., 2018).

There is evidence that different TGFβ isoforms can drive different matrix-producing behaviours. Particularly TGFβ3 was found to stimulate a higher degree of matrix alignment and little collagen type 3 or αSMA production. TGFβ1 and 2 on the other hand, lead to increased collagen type 3 and αSMA production (Karamichos et al., 2011). This suggests that TGFβ3 triggers different pathways of ECM production and is capable of driving the construction of clearer ECM. A decrease in matrix contraction was observed in keratoconic stromal cell culture and was rescued to healthy stromal fibroblasts levels with the addition of TGFβ isoforms (Lyon et al., 2015).

The multiple isoforms of TGFβ interact with multiple receptors and matrix ligands with varying affinities. TGFβ binds with high affinity to transmembrane receptor II and receptor I to form a heteromeric complex (Wrana et al., 1992). The receptor complex then phosphorylates receptor-regulated SMADs and binds the intracellular SMAD complex that will then act as a transcription factor and modulate gene expression (Otten et al., 2010). TGFβ also binds with matrix molecules like decorin. This binding allows for the neutralization of TGFβ and a mode of control over is bioactivity as the degradation of decorin allows for the release of TGFβ (Jarvelainen et al., 2015). The loss of decorin and general degradation of ECM in the keratoconic cornea impacts the regulation of TGFβ, although the full extent of this dysregulation isn't documented.

A significant link has been established between an HGF gene polymorphism and keratoconus, suggesting that the growth factor is implicated in the corneal deformation. Hepatocyte growth factor (HGF) and keratinocyte growth factor (KGF) are secreted by stromal keratocytes while the receptors to both factors are present on epithelial and stromal cells (Yu et al., 2010). Both factors are secreted in greater quantities following corneal epithelial wounding and increase the proliferation of epithelial cells. KGF receptors are present in stromal cells, but are concentrated at the limbal region where stromal progenitors may reside (Weng et al., 1997). HGF receptors are also present on stromal cells, although the expression of both the receptor and HGF itself are highest at the centre of the cornea (Li and Tseng, 1997). The distribution of c-Met and HGF are also affected in keratoconus, becoming less uniform and showing increased presence in the basal epithelia near the cone (You et al., 2015). The exact effect of HGF and KGF on stromal cells is still unknown due to inconclusive reported evidence (Carrington and Boulton, 2005). Although, no concrete pathway has been established, it has been speculated that IL-6 may be involved (Sahebjada et al., 2014).

In keratoconic cells, a significant decrease in ALDH3 activity leaves the tissue more vulnerable to oxidative damage (Gondhowiardjo et al., 1993). This loss of protection may be the reason why stromal cells experience a decrease in population. The cornea is a transparent physical barrier that separates the eye from the environment. As such the cornea is normally exposed to a multitude of stress factors, particularly UV light. In addition, UV light irradiation stimulates production of reactive oxygen species (Mazzotta et al.) that consequently damage proteins or DNA, that may lead to mutations or cell autophagic malfunction (Heck et al., 2003, Shetty et al., 2017). DNA damage is particularly harmful to cells with a slower turnover rate as mutations are more likely to accumulate (Zierhut et al.,

2008). This is the case with stromal cells but not epithelial cells. While visible light must be able to transit through the cornea and into the eye itself, UV light penetration must be minimized to prevent damage to the retina. To protect the eye from UV light radiation, the cornea mass-produces an isoenzyme of aldehyde dehydrogenase (ALDH3) that acts as a filter to minimize penetration into the eye (Vallabh et al., 2017).

Depending on the species, ALDH3 constitutes 5% to 50% of the total soluble proteins found in the cornea (Pappa et al., 2003). ALDH3 is found highly expressed in the corneas of most mammals with notable exception in rabbits (Piatigorsky, 1998). In the cornea, ALDH3 is strongly expressed on epithelial cells and stromal keratocytes but not in endothelial cells. ALDH3 is part of a protein group called crystallins, that is a lens and corneal proteins that make up a large percentage of water-soluble cell components. ALDH3 also protects cells from oxidative damage by aldehydes. The loss of ALDH3 prevents keratocytes from surviving UV radiation exposure.

In keratoconus, the behaviour of the keratocytes is abnormal, with higher rates of cell death and loss of ECM that could be attributed to an imbalance in the signalling at molecular level from the epithelial cells, which may then be exacerbated by environmental factors or complications such as ruptures in Descemet's membranes and Bowman layer isolating the stroma. Breaks may then lead to infiltrations of neighbouring tissue fluids, such as aqueous humour or tear fluid. Direct contact between the epithelia and stroma may cause long-term wound-like signalling in the stroma. The underlying cause of keratoconus and the large mechanisms that connect the variety of molecular imbalances seen in the disease remain to be fully elucidated. While treatment options currently available have proven effective, current research into keratoconus at the molecular level has been significant and has shown important progress aiming to establishing a detailed understanding of keratoconus as well as leading to novel therapies.

3.3. Diagnosis and treatment

Keratoconus can present with some variable symptoms that change as the disease progresses. The initial symptoms typically include: loss of vision, glare, and distortion of vision among others. Structurally, a common feature of keratoconus is a thinning of the inferior and nasal portions of the corneal stroma. Keratoconus with the cornea protruding conically and an epithelial iron line called Fleisher's ring partially surrounding the base of the cone. The degrees of tissue deformation can vary greatly between patients. Both the anterior and

posterior curvatures of the cornea are affected and tracking changes in the cornea's shape over time is one of the most reliable diagnostic methods of identifying keratoconus and its progression (Schwiegerling, 1997, Tomidokoro et al., 2000).

There are multiple characteristic clinical signs that can be used to set keratoconus apart from other ectatic conditions that affect the cornea (e.g. pellucid marginal degeneration) as well as determining severity of the disease (Sherwin and Brookes, 2004). These signals do not always occur but some combinations are typically observed.

Clinical signs:

1. Central and paracentral thinning of the cornea
2. Vogt's striae, vertical lines located in the superficial stromal layers that occur due to corneal deformation;
3. Fleischer's ring, an iron deposit in the basal epithelium that partially surrounds the base of the corneal cone;
4. Epithelial thinning and a proud nebula, a small build-up of scar tissue at the very centre of the cornea that often results in some loss of vision;
5. Enlarged corneal nerves;
6. Subepithelial fibrillary lines
7. Stromal swelling due to break in Descemet's membrane (i.e. Hydrops)
8. Breaks in the central portion of the Bowman layer;
9. Munson's sign, a wedge-shaped indentation of the lower eyelid by the cornea when patient is looking down. This is common in advanced cases of keratoconus and is due to the conical cornea pushing into the lower eyelid.

As the severity of keratoconus can vary, so can the treatment. Milder, non-progressing cases of the disease can be managed with glasses or contact lenses to correct visual impairment. More advanced or faster progressing cases of keratoconus may require more sophisticated intervention. Cross-linking can be used to stiffen the cornea in earlier stages of disease, fixing the tissue in a shape where vision can still be corrected with glasses or contacts. Crosslinking uses riboflavin administration and non-damaging UV irradiation of the stroma (Spoerl et al., 2007, Raiskup et al., 2015). It should be noted that UV irradiation from the crosslinking treatment has been shown to reduce the number of cells in the treated stroma. Cell numbers do recover in the following months (Mazzotta et al., 2007). In the event that keratoconus has reached a stage where vision can no longer be corrected due to great deformation, corneal scar or unstable gas permeable contact lens fitting, surgery is often recommended. Surgery will

usually involve corneal transplantation or intra-stromal corneal ring (ISCR) implantation to mechanically strengthen the damaged tissue and restore corneal shape as well as slowing, but not arresting, the ectasia (Rabinowitz, 1998, Vega-Estrada et al., 2015).

As previously mentioned, if the disease is found to be progressing but not yet in a severe state, collagen cross-linking treatment is recommended to strengthen the cornea and prevent further deformation. It is well-known however that like most other tissues in humans, the human cornea naturally stiffens and cross-links its collagen matrix with age, therefore it is expected that natural cross linking could slow or even arrest the progression of keratoconus (Robins, 2007). If the cornea is incapable of compensating for keratoconus by naturally toughening the remaining stromal ECM, then UV cross linking treatment can aid in slowing disease process by hardening the collagen matrix (Snibson, 2010). The cross-linking treatment uses photosensitizing riboflavin drops in the stroma and exposes these to UV radiation, forming molecular links between the collagen fibres of existing matrix in the cornea (Wollensak et al., 2003). The effects of UV irradiation are multiple, there is a marked increase in crosslinking proteoglycans like lumican, mimecan and decorin as well as a decrease in MMPs, these added consequences of UV irradiation also aid in strengthening the ECM (Sharif et al., 2018). Pre-treating patient corneas with only UV has been shown to regress invasive lymphatic and blood vessels, reducing subsequent graft rejection (Hou et al., 2018).

In cases of advanced keratoconus where contact lenses no longer fit or where scar tissue occupies a significant portion of the cornea affecting the visual axis, a corneal transplant also known as keratoplasty (i.e. penetrating or deep anterior lamellar) would be recommended (Jhanji et al., 2011). Following penetrating keratoplasty, 70% of patients develop keratometric astigmatism in the 10 years that followed suture removal with most cases occurring after 7 years (de Toledo et al., 2003). The recurrence of keratoconus following deep anterior lamellar keratoplasty has not yet been fully investigated, although a case has been reported where signs of keratoconus re-emerged 49 months after surgery (Feizi et al., 2012). All of the current treatment options, from glasses to transplants, only address secondary deficiencies in the corneal structure rather than directly dealing with the primary pathogenic faults in cellular behaviour and molecular pathways.

4. Corneal tissue engineering

4.1. Models of the stroma

Modelling the cornea in vitro offers some unique opportunities when it comes to more closely studying cell interactions. In vitro models can use human cells and are far cheaper than animal or human studies. It should also be noted that the structure of the cornea varies across species with the thickness and existence of certain tissue layers found in the human cornea changing from among animal models. Cell culture models are normally the first step in any biological research. For the cornea and its stroma, multiple models have been constructed and used, from the very crude immortalised cell culture to more 3D culture of multiple primary cell types. Most of the recent work done on the cornea tends to focus on epithelial and stromal cells, often using collagen as a substrate. Ideally, the collagen matrix would be produced and maintained by the keratocytes as this would most closely resemble the natural matrix. However, this method of matrix production is time consuming, requiring many months to form a suitable piece of tissue (Gouveia et al., 2017). The use of collagen mimics the tissue the cells are typically found on or within and allows the cells to more easily manipulate their surroundings in long-term cultures (Reichl et al., 2004, Suuronen et al., 2004). Collagen as the substrate does have the limitation of low mechanical stiffness, but that could be overcome with compression (Roeder et al., 2002). Compressing the collagen increases the concentration of collagen fibres. Although the high density and geometry of a natural cornea still cannot be easily mimicked, simple compression provides an inexpensive method of approaching the stroma's complexity. The compressed collagen gels may further resemble the stroma by incorporating specific thicknesses and curving (Miotto et al., 2019)

4.2. Models of keratoconus

Although a great amount of research has been undertaken investigating the etiology of keratoconus, the cause and disease pathways remain unclear (Maguire and Bourne, 1989). In the past, cultures of keratoconic stromal cells identified some differences with healthy stromal cells, particularly in regards to gene expression and protein secretion (Gouveia and Connon, 2013). Critically, these *in vitro* studies aim to replicate the environment of the corneal stroma with supplements. Taken a step further, a model of keratoconus was a previously constructed using 3D scaffold to investigate the relevance of 3D culture on the modelling of keratoconus and cell behaviour (Karamichos et al., 2012). Although the culture in question used serum medium when investigating cell behaviour, convincing evidence showed that a 3D culture system might be more desirable if modelling keratoconus.

The aim of this study was to construct a 3D *in vitro* model of keratoconus. To the author's knowledge, this is the first 3D *in vitro* model which use serum-free conditions, similar to the cornea's own environment. This model was then be compared to several types of healthy stromal cells to better understand the disease identity. Ultimately, the development of such a model could prove useful in investigating the disease and developing new treatment strategies.

Chapter 3: General Methodology

1. Tissue Culture

1.1. Stromal cell growth medium

The base for the keratocyte expansion medium comprised of 500ml of 1:1 of Dulbecco's modified Eagle medium and Ham's F12 (DMEM/F12) (Gibco, UK). Added to the DMEM/F12 was 50ml of foetal bovine serum (FBS) (FBS; Gibco Invitrogen) and 5ml of 100X Penicillin/Streptomycin (Invitrogen, UK). This expansion medium was used during cell extraction and expansion prior to experiments.

1.2. Stromal cell serum-free medium

Serum-free medium was used to assay cell survival and simulate the stromal environment. This medium also used 500ml of 1:1 of Dulbecco's modified Eagle medium and Ham's F12 as a base. Added to the DMEM/ F12 was 5ml of 1X ITS liquid medium supplement (Sigma-Aldrich), ascorbic acid (Sigma- Aldrich) to a concentration of 10μM and 5ml of penicillin/streptomycin (Invitrogen) for a final concentration of 50 units/mL of penicillin and 50 μl/mL of streptomycin.

1.3. Preparation of retinoic acid aliquots and addition to cell cultures

3 mg retinoic acid (RA) powder (Merck, USA) was solubilized in 10mL of absolute ethanol to produce a 1mM stock solution, which was sterile-filtered and stored in aliquots at −80°C for up to 1 month. RA was added to serum-free medium immediately before use by diluting at a ratio of 1:1000 medium volume for a final concentration of 1μM. While addition of RA to cells cultured on plastic had some positive effects, addition of the same concentration of RA to collagen gel cultures proved toxic. After serial dilution of RA, it was found that halving the concentration to 0.5μM had the most positive effect on cell in gels while 1μM still had the most positive effect for flat culture on plastic. A different concentration of RA was therefore used for each situation.

1.4. Stromal cell culture

Extracted cells were seeded into tissue culture plastic vented flasks at an approximate density of 500 cells per cm^2 in an appropriate amount of growth medium. The flasks containing cells were left in an incubator (37°C, 5% CO_2, 100% humidity) so that the cells may adhere.

Medium was then replaced every 2-3 days until a confluence of around 80% could be seen under a bright field microscope. Cell passaging began with removing the medium and gently washing the cell monolayer with 1X PBS. A solution of 0.5% trypsin/EDTA (Invitrogen, UK) was then added to the cells and the flask was returned to the incubator for 5 minutes, the amount added was enough to cover the cells. After incubation, the flask was observed under a brightfield microscope to ensure cells had detached. If an insufficient number of cells had detached, gentle tapping or an extra minute of incubation was used to dislodge the cells further. To partially neutralize the trypsin, an equal volume of growth medium containing FBS was added to the flask and then washed 2 to 3 times over the culture surface to suspend the cells in the liquid. The cell suspension was then transferred in its entirety to an appropriate centrifuge tube and centrifuged for 5 minutes at 600G to pellet the cells. The supernatant was gently removed to avoid disturbing the pellet. The pelleted cells were resuspended in 1mL of growth medium for counting. Cell number was determined using the Countess II FL Cell Counter (Invitrogen, UK), 10µl of cell suspension was mixed with 10µl of 0.1% trypan blue solution in a small Eppendorf tube. 10µl of the cell-dye mix was added to the chamber of a haemocytometer slide and inserted into the machine. The image was used to determine if any large debris was present and live/dead ratio was determined automatically with the count.

1.5. Stroma enzyme digestion

The study was carried out in accordance with the principles of the Declaration of Helsinki. Whole donor corneas were supplied by NHSBT Manchester Eye Bank in the UK, under a tissue supply agreement for research and met internationally recognised standards. All patients gave general consent to participate in the study and to have the procedures carried out (donor ages: 69, 80, and another 80; all female with no prior history of corneal diseases or ocular trauma). Prior to cell extraction, the corneas were suspended in dextran-containing medium and stored at hypothermic conditions for several weeks.

The corneal centre of whole corneas was isolated using a biopsy punch (diameter=0.8cm). The isolated central and limbal corneal stroma were separately minced using a scalpel. The limbal tissue was solubilized using collagenase digestion [growth medium with 2 g/L (450 units/ml) collagenase type-1 (Invitrogen)] for 5 hours under continuous rotation at 37°C. Initially, no cells could be recovered from the central button when using the same digestion technique as limbal rings. A shorter digestion time of 2h30 proved effective in yielding cells, potentially due to the smaller amount of collagen or more sensitive cells. The isolated keratocytes were initially cultured in tissue culture flasks, fed every two days with growth

medium until reaching 70-80% confluence. Cells were then passaged and further expanded until a high enough population was reached for experimentation.

1.6. Stromal explant migration

The study was carried out in accordance with the principles of the Declaration of Helsinki. Whole donor corneas were supplied by NHSBT Manchester Eye Bank in the UK, under a tissue supply agreement for research and met internationally recognised standards. All patients gave general consent to participate in the study and to have the procedures carried out (donor ages: 69, 80, and another 80; all female with no prior history of corneal diseases or ocular trauma). Prior to cell extraction, the corneas were suspended in dextran-containing medium and stored at hypothermic conditions for several weeks.

The corneal centre was isolated using a biopsy punch (diameter=0.8cm). The separated central stroma and limbal stroma were each separately minced using a scalpel into approximately $1mm^3$ pieces and put into a 12 well plate (4-6 pieces per well). The cornea pieces were then left to dry for 10 minutes in a tissue culture plate until adhered to the plastic. Keratocytes were left to migrate out of the explants in growth medium for 10 to 14 days until 70-80% confluence. Cells were then passaged and further expanded until a high enough population was reached for experimentation.

Any remaining tissue pieces were set aside and underwent enzyme digestion as previously detailed to extract any cells still inside the explant. The “resident” cell population digested out of the explants was then passaged and further expanded until a high enough population was reached for experimentation.

1.7. Keratoconic cell sources

Keratoconic fibroblasts (KF), isolated from human keratoconic corneas (n = 3; courtesy of Dr Dimitrios Karamichos, USA) were maintained using growth medium. The frozen cells were shipped to the UK in aliquots of $1x10^6$ cells/mL and stored in liquid nitrogen upon arrival. Upon thawing, the cells were then passaged and further expanded until a high enough population was reached for experimentation. Patient data could not be obtained, and it is assumed that the keratoconic tissue was sourced from a graft procedure where the disease severity required intervention. Previous studies on the demographics of keratoconus (Rafati et al.,2019) suggest that the donors where likely between the ages of 20 and 30, younger than the on-average 75-year-old healthy donors used here. There is also a slightly larger male population with keratoconus, meaning that the donors could be mostly male. As all the

healthy donors used here were older female, this adds two important points to consider when comparing the behaviour of the two cell types. Whether scar tissue was present on the tissue when the cells were extracted is also unknown.

1.8. Freezing and thawing stromal cells

All the previously described cells underwent liquid nitrogen storage for a period of time to maintain a low passage number over the course of experiments. Freezing the cells involved initially detaching and counting the cells as previously described. Cells were then resuspended in an appropriate volume of growth medium and distributed into specialized cryovial, each filled with 1 million cells in a mixture of 700µl growth medium, 200µl FBS and 100µl DMSO. The vials were then tightly sealed and placed in a foam vial holder. The vial holder was left to cool overnight in a -80°C freezer before the tubes were finally transferred to the liquid nitrogen storage units. Thawing involved retrieving the tubes from the liquid nitrogen and placing them in a water bath at 37°C, taking care not to fully submerge the neck of the vial to avoid contamination. The thawed contents of the tubes were then resuspended in growth medium and the cells seeded at an approximate density of 5000 cell/cm^2. The cells in the flask were allowed to adhere for up to 5 hours before gently replacing the medium to remove any DMSO leftover from freezing. The morphology of the cells was monitored to ensure freezing had not damaged the cells and no contamination had occurred.

1.9. Culturing cells serum-free conditions

Cells used for experiments were first grown to approximately 80% confluence in growth medium. The growth medium was then substituted for serum-free medium in order to eliminate the serum from the cells. After the 3 days of serum-starvation, the cells were detached and counted. The cells were resuspended in an appropriate amount of serum-free medium and then seeded at a density of 100000 cells per cm^2 in a 24 well plate. Medium used to feed the cells was either serum-free medium or serum-free medium supplemented with retinoic acid at a concentration of 10µM. The cells were inspected regularly for any signs of contamination or anomalous development.

1.10. Culturing cells in compressed collagen gels

Ice-cold rat-tail collagen type I (2 g/L in 0.6% acetic acid; First Link Ltd, UK) was mixed with 10x Modified Essential Medium (Life Technologies, USA) and neutralised with 1M

NaOH at a 1:7:1 volume ratio. Cells suspended in serum free medium were then added at to the gel mix to a final concentration of 100,000 cells/ml. A millilitre of cold gel mix was pipetted a 24 well-plate wells and allowed to solidify at 37°C for up to 1h. Absorbent inserts (Lonza, Switzerland) were applied to the gel-containing wells and left to compress the gels into thin discs of collagen with a diameter of 15mm and thickness of around 100 microns. Compression took approximately 5 minutes. The resulting compressed collagen gels (CCG) were cultured in serum-free medium on either flat plastic (Fig. 1) or pinned by a metal ring onto a spherical glass cap (Fig. 2). Medium used to feed the cells was either serum-free medium or serum-free medium supplemented with retinoic acid at a concentration of 0.5µM. The cells were inspected regularly for any signs of contamination or anomalous development.

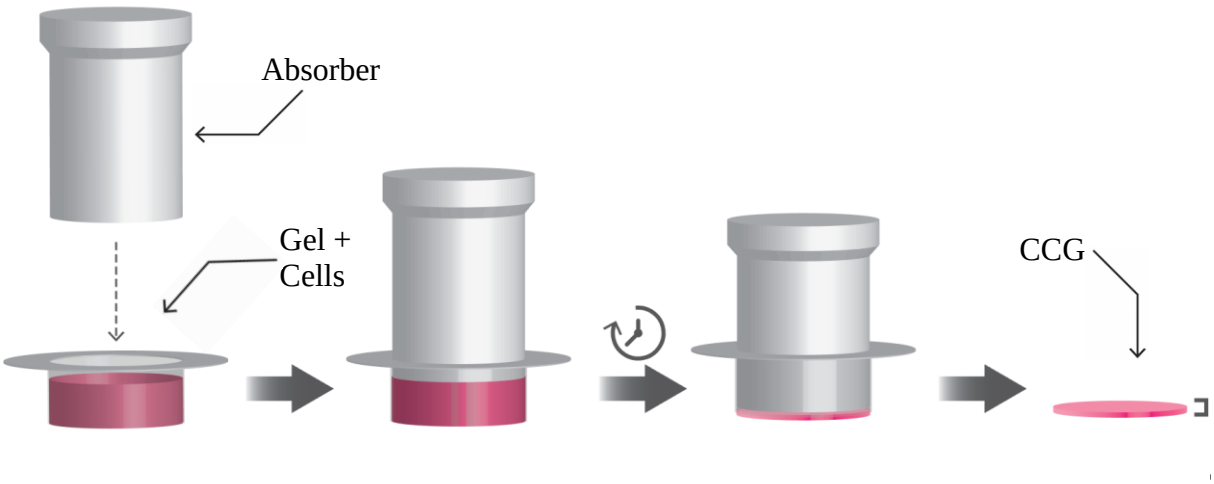

Figure 3: Preparation of compressed collagen gels. A solution of liquid collagen with stromal cells suspended within is initially pipetted into an empty well of a 24 well plate and left to solidify. The specialized absorber was then gently placed onto the solid collagen and allowed to compress the gel. After compression, a thin disc of collagen with stromal cells embedded within was obtained and used in cultures.

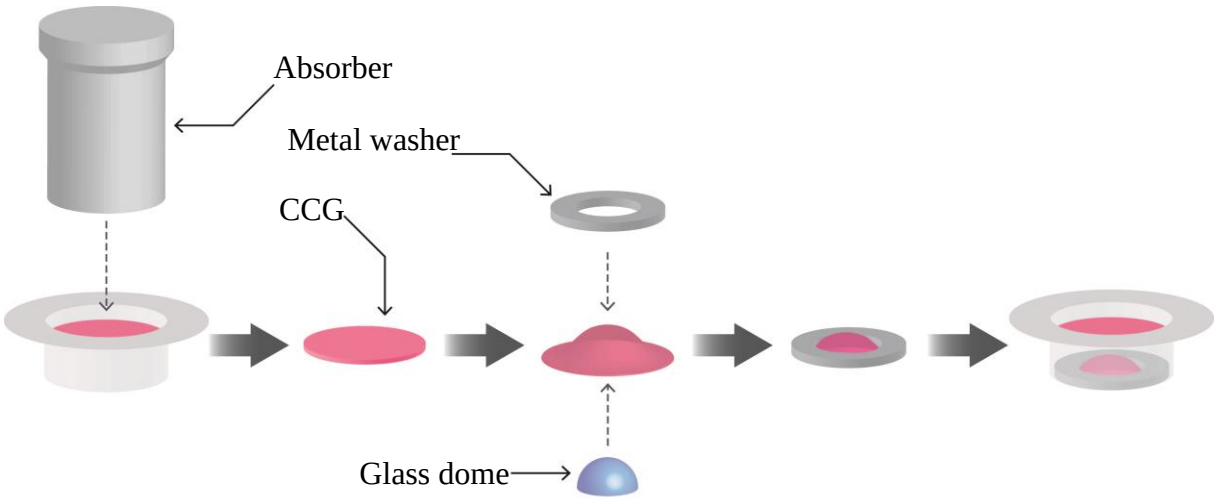

Figure 4: Preparation of compressed collagen gels and subsequent culture on a glass dome pinned by a metal washer to simulate the curvature of the corneal stroma.

2. Assays and Analysis

2.1. Alamar blue: Resazurin fluorescence to count cells

The Alamar blue assay is a primarily metabolic assay that relies of the mitochondrial reduction of resazurin salt to resofurin. Resazurin is not fluorescent but resofurin is and the progressive shift from one to the other is characterized by culture medium shifting from a deep blue to a purple-pink colour. Quantification of this fluorescence gives a reliable measure of the metabolism of a cell population and therefore, through a standard curve, the total number of cells in a well. A stock solution of 0.5mM resazurin salt was prepared in serum-free medium and kept at 8°C for up to two months. When needed, the stock solution would be diluted in a 1:10 working solution in more serum-free medium and used to replace the cell culture medium.

A standard curve had to be prepared for each of the 7 cell types and 2 culture methods assayed throughout this experiment. To make a standard curve, a large number of cells were initially serum starved, detached and counted before seeding into a 24 well plate in increasing amounts. The highest number of cells seeded in a well was 300000 cells while the lowest amount was 1000 cells; a blank well was also used. These cells were allowed to adhere for 3 hours before very gently removing the medium they were seeded in, via a pipette, and replacing it with 250µl Alamar blue working solution. The cells were returned to the incubator for 1h30, by then a colour change was visible with the solution showing a pink-blue gradient correlated with the number of cells seeded. 100µl of the culture supernatant was collected in duplicate and transferred to a clear, flat-bottomed 96 well plate. The plate was

then transferred to a Varioskan LUX multimode microplate reader (ThermoFischer, Franklin, MA) where the supernatant was exposed to a laser at 545nm and fluorescent emission intensity was measured at 580nm. This allowed for the correlation of fluorescent values to population number for each cell type via a standard curve and the slope equation that described the fluorescence/cell-number relationship mathematically. The Alamar blue assay was used to assess keratocyte proliferation and viability in serum-free medium over a period of 11 days for flat plastic cultures and 30 days for CCG cultures.

2.2. Reverse Transcription Polymerase Chain Reaction

The polymerase chain reaction (PCR) is a method that exponentially amplifies copies of DNA to generate a high number of a specific DNA sequence. This method allows for the determination of individual transcripts for specific cells. PCR uses cycles of denaturation to expose the DNA base, annealing to attach primers, and extension by high-temperature TAQ polymerase. The TAQ polymerase synthesizes a matching DNA strand by using the primer-binding site as a site of initial activity. PCR can also be used on the less-stable, single-stranded RNA. In order to do that, total RNA was first extracted and purified. In this study, two methods were used for RNA extraction, these methods are detailed in the next two sections.

2.3. RNA extraction from adherent cells

Cells cultured on plastic proved simplest to extract RNA from. First, medium was removed from the cells and the monolayer was washed with PBS. Then, the cells were detached and centrifuged as previously described in the passaging methodology. The RNeasy kit (Qiagen, UK) provides a lysis buffer that can easily break down the cells once they have been detached and centrifuged into a pellet. Once the supernatant was carefully removed, 350µl of RLT buffer was added. An equal volume of 70% ethanol was added to the now dissolved pellet of lysed cells, this precipitates the nucleic acid content of the lysate mix. The 700µl mixture was transferred to the upper chamber of an RNeasy spin-column and centrifuged at 8000G for 15 seconds; the resulting flow through was discarded. This caused the precipitated nucleic acid, DNA and RNA, to bind to the column's silica membrane.

The columns were then washed with 700µl of the kit's RW1 buffer to remove carbohydrates, proteins and fatty acids that may have adhered non-specifically to the membrane. The column was once again centrifuged at 8000G for 15 seconds. The columns were then washed with 500µl of the kit's RPE buffer twice, with the first centrifugation lasting 15 seconds and the

second centrifugation lasting 1 minute. This step removed traces of salts from the column. The column was then transferred into a new collection tube and centrifuged at maximum speed to dry the membrane. 35µl of RNAse-free water was added to the centre of the membrane and allowed to soak for 1 minute. The column was then transferred to a final collection tube and centrifuged at 8000G for 1 minute. The final product was 35µl of DNA and RNA from the stromal cells.

RNA purity was assayed using a Nanodrop 2000 spectrophotometer (Thermo Scientific, UK) by loading 1µl of the extracted RNA mix to the pedestal. The purity was determined by an A_{260}/A_{280} ratio within the range of 1.7 to 2.0 and an A_{260}/A_{280} above 2:1. Concentration had to be above 75ng/µl for use in later assays. The purified RNA was then either immediately used to make cDNA or stored at -80°C.

2.4. RNA extraction from cells in collagen gels

Extracting RNA from cells cultured in CCG proved more difficult as the RLT buffer could not lyse the ECM to release the cells within, resulting in a clogged membrane in the RNeasy columns. Instead, a previous method that employs TRIZOL (Sigma-Aldrich, UK) to extract RNA from collagen-based constructs was used.

Collagen gels were lifted from their plates and separately minced finely with a scalpel. Small portions of the minced gels were added to an Eppendorf tube filled with 1ml of TRIZOL. A syringe was used to pass the gel pieces through a 21G needle until the gel-TRIZOL suspension was suitably homogenized. The mix was then vortexed and inverted. The now homogenized and mixed cell lysate in TRIZOL had 200µl of chloroform added and was mixed by inversion for 30 seconds. The tube was left to incubate at room temperature for 15 minutes to allow for some initial separation. The lysate was then centrifuged at 18000G for 15 minutes at 4°C. This caused a separation of the lysate into three distinct phases: a bottom red phase of proteins and debris, a middle grey phase of DNA and an upper clear phase of RNA. The RNA phase was carefully removed and transferred to a new collection tube. An equal volume of 100% ethanol was added to the RNA and the RNeasy kit's procedure detailed above could follow with the RW1 buffer, RPE buffer and column purifying the RNA further. Once the RNA was purified, purity and concentration were assayed as previously described using the Nanodrop.

2.5. Synthesis of complementary DNA

The instability of RNA makes it unsuitable for long term storage and frequent handling. Synthesizing complementary DNA (cDNA) by using viral reverse transcriptase yields complementary strands of more stable genetic material for our assays. To do this, the commercially available RT2 First Strand kit was used (Qiagen, UK) with every step being done on ice to minimize the risks of RNA degradation. An initial 8µl of the purified RNA was added to a PCR tube along with 2µl of Buffer GE. The mix was then incubated for 5 minutes at 42°C before being returned to ice for a minute. This incubation eliminated the genomic DNA and left behind only the RNA for reverse transcription. To the RNA, the following reagents were then added: 4µl of 5X Buffer BC3, 3µl of RNase-free water, 2µl of RE3 Reverse transcriptase mix and 1µl of Control P2 primer mix. The tube was then gently tapped to mix the contents and incubated at 37°C for 1 hour and then at 95°C for 5 minutes. 90µl of nuclease-free water was added to the mix to bring the final volume to 110µl of cDNA. Concentration and purity were then assayed as previously mentioned and the total volume was adjusted to bring the final concentration of cDNA to 100ng/µl. The diluted cDNA was stored at -20°C until needed.

2.6. Primer design

Genes of interest were selected based on previous research and literature; primers were designed for these genes according to a set of specifications. These specifications were appropriate binding temperatures, minimal complementary self-assembly and low GC-rich regions. Identification of the transcript of interest was done using the ENSBL genome browser (https://www.ensembl.org/). The Primer3 design software (https://primer3.org/) was used to design relevant primers from the exon data according to our specifications. These primers were 19-22bp long, had a melting temperature as close as possible to 60°C and a GC content below 55%. The designed primers were finally entered into the NCBI primer blast database (https://www.ncbi.nlm.nih.gov/tools/primer-blast/) to identify any potential off-target products. The resulting primers that were used in the experiments are listed below.

Gene	**Primers 5' → 3'**
Decorin (DCN)	F: CTGCTTGCACAAGTTTCCTG R: GACCACTCGAAGATGGCATT
Keratocan (KERA)	F: TATTCCTGGAAGGCAAGGTG R: ACCTGCCTCACACTTCTAGACC

Matrix Metalloproteinase 1 (MMP1)	F: AGGTCTCTGAGGGTCAAGCA R: CTGGTTGAAAAGCATGAGCA
Matrix Metalloproteinase 2 (MMP2)	F: CCAAGCGTCTAGCAATACC R: TCTGGGGCAGTCCAAAGAAC
Matrix Metalloproteinase 3 (MMP3)	F: TGCTTTGTCCTTTGATGCTG R: AAGCTTCCTGAGGGATTTGC
Tissue Inhibitor of Metalloproteinases 1 (TIMP1)	F: ATTGCTGGAAAACTGCAGGAT R: TCCACAAGCAATGAGTGCCA
Retinoic Acid Receptor A (Greenbaum et al.)	F: AGTCCTCAGGCTACCACTAT R: CCTCCTTCTTCTTCTTGTTT
Cluster of Differentiation 34 (CD34)	F: CTTGGGCATCACTGGCTATT R: TCCACCGTTTTCCGTGTAAT
Collagen Type 1 (COL1)	F: CCTGCGTGTACCCCACTCA R: ACCAGACATGCCTCTTGTCCTT
Collagen Type 5 (COL5)	F: ATCTTCCAAAGGCCCGGATG R: AAATGCAGACGCAGGGTACA
Vimentin (VIM)	F: CCTCCTACCGCAGGATGTT R: CTGTAGGTGCGGGTGGAC
α-smooth muscle actin (αSMA)	F: CTGAGCGTGGCTATTCCTTC R: TTCTCAAGGGAGGATGAGGA
Aldehyde dehydrogenase 3 (ALDH3A1)	F: CCCCTTCAACCTCACCATCC R: GTTCTCACTCAGCTCCGAGG
Lumican (Greenbaum et al.)	F: CCTGGTTGAGCTGGATCTGT R: TAGGATGGCCCCAGGA
GAPDH (Housekeeping gene)	F: AGCCGAGCCACATCGCTGAG R: TGACCAGGCGCCCAATACGAC

Table 1: Description of primers used in qPCR for keratocyte gene expression analysis.

2.7. Quantitative PCR

While traditional PCR can inform on whether a gene is being expressed or not, quantitative PCR (qPCR) can provide relative quantitative data related to the expression of genes of interest. The most common form of qPCR uses SYBR green; a commercially available dye that intercalates within double stranded DNA and when excited by blue light will emit a green fluorescence. As the amount of fluorescence is directly proportional to the amount of DNA,

monitoring fluorescence intensity as the PCR progress provides a powerful method of relatively quantifying the amount of expression of particular genes.
With fluorescence and time being plotted, a threshold of detection is set based on a no-template control. The number of doubling cycles required to reach that fluorescence threshold is called the "cycle threshold" or "C_t". For example, comparing the C_t of a particular gene between two cell types: A and B may show that cell type A's C_t preceded that of cell type B by 4 cycles. This means that cell type A contained 2^4= 16 times more of the template gene than cell type B.

The binding efficiency of each primer was calculated by first serially diluting some of the cDNA. Reaction mix was then made from 7µl of 2x SYBR green mastermix (Qiagen, UK), 2µl of forward/reverse primers and 5µl of cDNA for a total reaction volume of 14µl. Various concentrations of cDNA and their mix underwent the following cycles: 10 minutes denaturation at 95°C, followed by 40x cycles of 10 seconds at 95°C, 30 seconds at 60°C and 15 seconds at 72°C. The qPCR reaction was carried out in the Eco Real-Time PCR System (Illumina, USA). This gave a range of C_t that could be correlated to known cDNA concentrations to determine primer efficiency. When plotted against each other, C_t and cDNA dilution factor gave a slope that could input into the following equation:

$$Efficiency\ (E) = 10^{(-1/slope)} - 1$$

This efficiency correction was then used when applying the Pfaffl mathematical model to determine expression profiling (Fleige et al., 2006). The equation for Pfaffl model is expressed below:

$$Fold\ Change = \frac{(E_{target\ gene})^{\Delta Ct\ [target\ gene](control\ sample)}}{(E_{housekeeping\ gene})^{\Delta Ct\ [housekeeping\ gene](control\ sample)}}$$

Negative controls were also done for each primer to account for any baseline fluorescence. Negative controls were also performed for each DNA sample with a reagent mix that contained no fluorophore to account for background fluorescence. No positive controls were used for any of the primers, although all primers did manage to detect their gene of interest in some samples. A potential weakness of the experimental design discussed above is the lake of inter-run calibration. This makes comparison between samples read in different plates weaker, despite the biological repeats. Any differences seen may be due to non-uniform heating of the

metal block, variable reagent reactivity, or fluorometric detector wear over time. Further experiments should aim to control inter-run variation by randomly assigning samples to plates.

2.8. Statistical Analysis

Statistical analysis was carried out using Graphpad Prism 6 (La Jolla, USA). Statistical tests were deemed significant when returning a p value of <0.05. All error bars presented are the standard error of the mean. When assessing the qPCR gene expression data, a one-way ANOVA was used with a post-hoc Dunnett's test to correct for multiple significances. When assessing the cell survival data in serum-free conditions, two-way ANOVA was used with a post-hoc Bonferroni's test to correct for multiple significances. The interaction p-value of the compared sets of survival data was reported and individual comparisons were made within timepoints; these individual comparisons are reported within the graphs. Significant differences are denoted within graphs with asterisk (* for $p<0.05$, ** for $p<0.005$, *** $p<0.0005$ and **** for $p<0.0001$).

Chapter 4: Isolation of stromal cells from different parts of the cornea

1. Abstract

Current research on healthy corneal stromal cells will typically use primary cells isolated from the limbus of discarded donor corneal tissue (due to its relative abundance), whereas keratoconic cells are extracted from central corneal buttons. When comparing healthy and keratoconic cells, the location the cells are harvested from should be kept the same. To this end, stromal cells were extracted from the limbus and central button of healthy corneas. This allows for comparison of keratoconic cells to both central and limbal healthy cells during development of a keratoconus model. Of concern is also the extraction method of stromal cells since the keratoconic cells donated and used in these experiments had been extracted via explant migration rather than the better-defined method using enzyme digestion of the tissue to release the cells. In this study, we explored the behaviour of stromal cells extracted via enzyme digestion and explant migration from central and limbal zones of the cornea in order to better understand the effects extraction method may have had on keratoconic cells.

2. Introduction

2.1. Stromal cell population within the stroma

Intercalated within the lamellae of the stroma is a population of cells called keratocytes. Keratocytes in the stroma secrete and organize transparent matrix components essential for corneal tissue function (Jester et al., 1999). Dendritic processes allow these cells to form a cellular network within the tissue (Muller et al., 1995). The cells themselves possess unique properties among fibroblasts due to their cytoplasmic proteins, particularly crystallins such as ALDH1A, which allow the cell to match the refractive index of its surrounding ECM and minimize light scattering (Jester, 2008). The majority of keratocytes are located in the anterior portion of the cornea, near to the epithelium. This localization is ideal due to the majority of corneal stromal damage occurring in this anterior portion of the stroma (Moller-Pedersen et al., 2000). The position of the stromal cells is partially mediated by epithelial cells' secreted factors that cause persistence in stromal cells closest to the epithelium (Torricelli et al., 2016). Among these secreted factors is the Transforming Growth Factor-β (TGF-β) family, with TGF-β1 and TGF-β2 causing differentiation of keratocytes and preventing their apoptosis while TGF-β3 prevents differentiation while also maintain survival (Karamichos et al., 2013). The survival of stromal also seems to be regulated by the epithelium but the stromal cells also provide support to the epithelial basement membrane by secreting proteins such as perlecan and nidogen-2 (Torricelli et al., 2015). Previous experiments showed that epithelial

debridement invariably lead to stromal cell apoptosis (Zieske et al., 2001). Keratocytes also tend to localize nearest to the sensory nerve fibres that populate the densely innervated the Bowman layer and its sub-basal plexus (Poole et al., 2003, Yang et al., 2018). The sub-basal plexus is itself part of the anterior stroma and there is therefore physical contact between the nerves and stromal cells. There exists a paracrine relationship between the two where stromal cells have been shown to support some regeneration in the damaged nerves, although this was in chickens (Yam et al., 2017).

2.2. Activation and differentiation of stromal cells

Stromal cells are normally found embedded within the stromal ECM in a dormant state, becoming activated when wound healing is required or as a response to any disruption to the stroma such as trauma or infection. When an injury occurs, keratocytes at the wound site or adjacent will undergo apoptosis, this response initiates an inflammatory response and can reduce the chances of viral infection (Wilson et al., 1996). Replacement of lost keratocytes requires activation of adjacent keratocytes during wounding; this active state is characterized by a change in morphology to fibroblasts: larger spindle-like cells, increased organelle content and loss of cytoplasmic granules (Fini and Stramer, 2005). This is in contrast to normal keratocyte morphology where cells are stellate or dendritic with a triangular body (Espana et al., 2003). These cells also break away from cell networks they may have formed while quiescent. The activation process is mediated by growth factors like TGFβ1, FGF and PDGF (Ljubimov and Saghizadeh, 2015). The newly activated cells then migrate to the wound area and begin the remodelling process by producing ECM-digesting enzymes. As the keratocytes lose their quiescent state, common markers of quiescence such as CD34, keratocan, ALDH3, lumican and decorin also begin disappearing (Espana et al., 2003, Fernandez-Perez and Ahearne, 2019). The activated fibroblasts express smooth-muscle actin and desmin, becoming contractile to effect wound closure (Chaurasia et al., 2009). Of note is that only one soluble growth factor has been documented as having quiescence-inducing functions on corneal stromal cells, TGFβ3 (Karamichos et al., 2011). Unpolymerized F-actin in the stromal cell cytoplasm congregates to form stress fibres within the cell (Petroll et al., 2004).

Activated keratocytes lose expression of proteins associated with cellular transparency such as aldehyde dehydrogenase 1A1 and crystallins (Jester et al., 1999). Activated keratocytes may also become myofibroblasts and express increased levels of alpha smooth muscle actin (αSMA). These contractile cells are typically found only at wound sites to aid in closure by

enlarging and spreading. Myofibroblasts will also produce ECM crosslinkers and MMPs to remodel damaged stroma (Ebihara et al., 2007). While the myofibroblasts and fibroblasts play an essential role in wound healing of the cornea, these differentiated cell states are also associated with multiple pathological processes like corneal haze and scarring among others (Connon et al., 2003). Studies into the behaviour of stromal cells during surgical wound events found that stromal cells near the wound would differentiate into myofibroblasts, resulting in a fibrotic haze. The fibrous matrix would resolve itself into a more transparent matrix over the two following months and the differentiated cells would undergo apoptosis (Kivanany et al., 2018). In the case of chronic or particularly severe wounds, the differentiated cells may be unable to undergo apoptosis or revert to a quiescent state. These cells may then produce higher levels of inflammatory cytokines and matrix metalloproteinases, exacerbating corneal damage (Jester et al., 1999). Conserving the undifferentiated state of stromal keratocytes until fibroblastic differentiation is required as a vital role of signalling factors in the stroma.

Keratocytes exhibit low self-renewal capability and need to be replaced by proliferating progenitor cells. In the corneal limbus, there is a posited to be a population of stromal cell progenitors that express markers associated with mesenchymal stem cell function such as ABCG2 and Pax6 (Du et al., 2005). These cells were also found to express genes associated with neural development such as NGFR and CDH2 (Funderburgh et al., 2016). The presentation of neural markers is in line with the neural crest origin of the limbal stromal stem cells (Pinnamaneni and Funderburgh, 2012). Importantly, this population of cells does not express classical hematopoietic or endothelial marker sets, ensuring that this is a distinct population of progenitor cells unique to the cornea. One more marker of note expressed by these limbal stem cells is CD34. Although commonly associated with hematopoietic stem cells due to its discovery in the blood stem cells, CD34 is a common marker for a multitude of progenitors (Sidney et al., 2014). The exact functions of CD34 are not well known due to its extensive post-transcriptional modification although one of the most well-known functions is the regulation of adhesion, particularly immune cells such as mast cells (Nielsen and McNagny, 2008). The expression of CD34 has been shown to decrease in wounded corneal cells and is lost when stromal cells are cultured *in vitro*, likely due to differentiation (Toti et al., 2002b). These limbal stromal stem cells were also able to differentiate into adipocytes and osteocytes in culture when exposed to the appropriate cues, indicating a degree of plasticity (Polisetty et al., 2008). Limbal stromal stem cells are of particular interest for *in vitro* cultures

due to their maintenance of an enhanced potential to become functional keratocytes (Funderburgh et al., 2016).

When extracting cells from the cornea, the limbal ring is typically used (as this is left over from the fairly common keratoplasty procedures). If isolating cells from the whole, intact cornea, it is reasonably assumed that the more proliferative limbal stromal cells will make up the bulk of any extended in vitro culture. The existence of a progenitor population in the limbus suggests that the limbal ring and central portion of the cornea will yield different cell types. Since keratoconic cells are typically isolated from the central portion of the cornea after lamellar keratoplasty such as DALK (deep anterior lamellar keratoplasty), limbal cells may not provide an accurate healthy control (Chwa et al., 2008). Keratoconic cells are also typically compared to cells isolated from the limbus or whole cornea (Karamichos et al., 2012). If there exists a difference in behaviour between limbal and central cells, identifying this difference is important for any future work.

2.3. Stromal cell extraction methods

Prior to being cultured *in vitro,* primary keratocytes are typically extracted via one of two methods: enzyme digestion or explant migration. Enzyme digestion uses collagenase treatment to break down the collagen component of the matrix and release the cells within. Explant migration involves cutting the cornea into small pieces, adhering the tissue pieces to a surface and letting cells migrate out onto this surface (typically tissue culture plastic, but could also be a specialized biomaterial such as amniotic membrane). Both methods have been used to extract cells when investigating keratocyte behaviour in culture, it has been found that the two methods can aid in the isolation of separate populations, albeit with FACS as a final step to isolate a homogenous population. There has not been any investigation to see if isolating via either enzyme digestion or explant migration leads to different populations of cells (Karamichos et al., 2014). It could be assumed that explant migration biases extracted populations towards more migratory cells while enzyme digestion simply collects all cells contained in the tissue.

2.4. Aims

To better understand the effects of extraction method and location, cells were extracted from the cornea centre and limbus via both enzyme digestion and explant migration. Isolated cell populations were then cultured in serum free conditions and their survival was quantified.

Furthermore, it is possible that some cells do not migrate out of the tissue explants. To investigate this potential non-migratory cell population, the explants were digested once the migration had run its course.

3. Methods

3.1. Isolating cells from central and limbal stroma with collagenase

Stromal cells were isolated from donor tissue as previously described in chapter 3, section 1.5. Cells were then passaged and cultured in serum-free medium [DMEM:F12 medium, 1 x ITS liquid medium supplement (Sigma-Aldrich),1 x 10μM ascorbic acid (Sigma- Aldrich), 1% penicillin/streptomycin (Invitrogen)] for three days prior to assays. Each subsequent experiment was performed three independent times using keratocytes from passages three to five from specific donors. The populations extracted via this method are termed enzdL if isolated from the limbal region or enzdC if isolated from the centre. To collect RNA from fresh, non-cultured cells, the RNA extraction protocol was performed on cells immediately after enzyme digestion from either the centre or limbus.

3.2. Isolating cells from central and limbal stroma via explant migration-

Stromal cells were isolated from donor tissue as previously described in chapter 3, section 1.6. Cells were then passaged and cultured in serum-free medium for three days prior to any assays. The populations extracted via the explant migration method are termed exmL if isolated from the limbal region or exmC if isolated from the centre.

3.3. Extracting non-mobile cells from explants post-migration

Tissue pieces were collected and then underwent enzyme digestion as previously detailed in chapter 3, section 1.6 to extract any cells still inside the explant. The "resident" cell population digested out of the explants, after the initial migration phase is termed exenzL if extracted from the limbus and exenzC if extracted from the centre.

3.4. Survival in serum-free conditions

The Alamar blue assay was used to assess keratocyte proliferation and viability in serum-free medium over a period of 11 days. Cells were initially seeded at a density of 100000 cells per cm^2 in a 24 well plate after 3 days of serum starving. The cells were cultured in serum-free medium and assayed with Alamar blue days 1, 4, 6, 8 and 11 of culture. The cells were incubated with resazurin reagent (Sigma-Aldrich; prepared in 1:10 dilution using fresh culture medium) for 90 minutes at 37°C, after which 100 μl of culture supernatants (in triplicate)

were sampled for fluorescence emission analysis at 590nm using Varioskan LUX multimode microplate reader (ThermoFischer, Franklin, MA). The cells were then replenished with fresh, serum-free medium. To evaluate the effects of retinoic acid on cell survival, RA was added to serum free medium at a concentration of 1μM after being initially diluted from a powder stock (Merck, USA) to a concentration of 10mM in ethanol. Cell number was calculated by interpolation using a standard curve for fluorescence values of 150, 100, 80, 60, 40, 20, 10, 5 x 10^4 cells. All values correspond to average ± SD of 3 independent experiments.

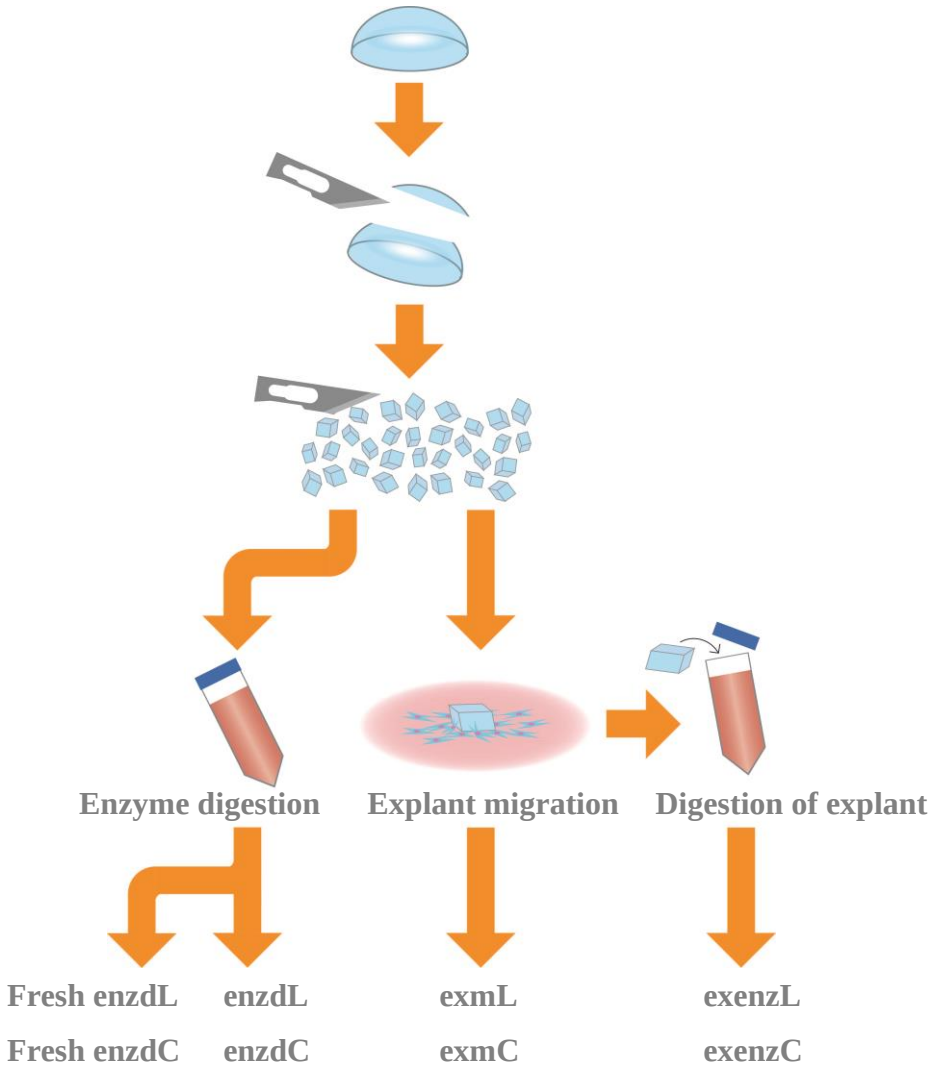

Figure 5: Schematic representation of the methods of stromal cell extraction used and the 8 separate populations of stromal cells assayed. A whole cornea scraped of its endothelium and epithelium is separated into a limbal ring and a central button of 0.8cm diameter. Each of the two pieces is separately minced and undergoes either enzyme digestion or explant migration. The enzyme digested tissue releases cells that can then either be cultured for future experiments (enzdL and enzdC) or immediately used in transcriptional analysis (Fresh enzdL and Fresh enzdC). Cells that migrated out of explants are collected (exmL and exmC) while the tissue is digested to release any final cell that did not migrate (exenzL and exenzC).

3.5. Quantitative PCR

Following 11 days of culture, RNA was extracted from the cells using an RNeasy Mini Kit (QIAGEN, UK) according to manufacturer specifications. The RNA was then treated with DNase to eliminate genomic DNA. Quality assessment of the RNA was performed using a Nanodrop 2000 spectrophotometer (Thermo Scientific, UK) to ensure the A_{260}/A_{280} ratio was within the range of 1.7 to 2.0 and the A_{260}/A_{280} was above 2:1. The RNA was then reverse-transcribed into cDNA with the RT2 First Strand kit (Qiagen, UK) according to manufacturer specifications in a TC-Plus thermal cycler (Techne, Staffordshire, UK). The resulting cDNA was then assessed using the Nanodrop to ensure purity and suitable concentration. The qPCR reaction was carried out using direct dye binding in the Eco Real-Time PCR System (Illumina, USA) and the appropriate primers (Table 1). The following cycles: 10 minute denaturation at 95°C, followed by 40x cycles of 10 seconds at 95°C, 30 seconds at 60°C and 15 seconds at 72°C. All values correspond to average ± SD of 3 independent experiments with expression of each gene of interest normalized to housekeeping gene GAPDH.

4. Results

4.1. Serum-free survival of healthy and keratoconic stromal cells

After cells were enzyme digested from either the centre or limbal region of the cornea, they were cultured in 10% serum medium and allowed to proliferate. Once a large enough number of cells had been reached, serum-free medium was substituted into serum starved cells. After 3 days of serum starvation, cells were seeded at a concentration of 100000 cells per well onto tissue culture plastic and left to survive. A population decline was seen in both enzdC and enzdL populations (Fig. 6A), with a steeper initial decline for central cells.

Cells that were explant migrated from either the centre of limbal region of the cornea, were also cultured in 10% serum medium and allowed to proliferate. Once a large number of cells had been reached, serum-free medium was substituted in to serum starve the cells. After 3 days of serum starvation, cells were seeded onto tissue culture plastic and left to survive. While seeding density was also of 100000, the first 24 hours of culture saw a ~50% reduction in cell number (Fig. 6B). Overall, both populations exhibited similar behaviour and survival rates under these basic cell culture conditions.

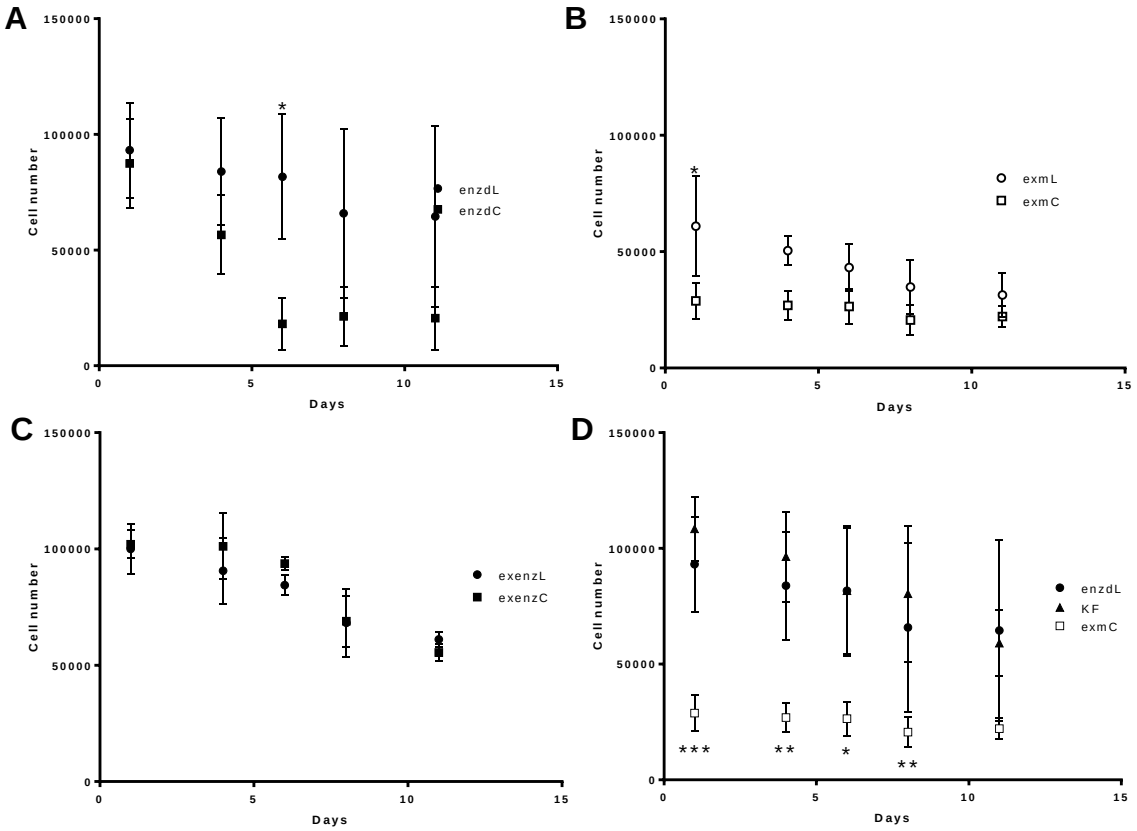

Figure 6: Survival of healthy and keratoconic stromal cells as quantified by Alamar blue assay. Data was obtained from 3 experiments (n=3) per cell type, each with a different donor (** for $p<0.005$, *** for $p<0.0005$).

The explants where left between 10 and 14 days on culture surfaces to allow cells to migrate out. Once cells had migrated out of the explants, the explants were collected and set aside for further processing. Any non-migratory cell that may have remained in the explant was then extracted by enzyme digestion. These cells were then cultured in 10% serum medium and allowed to proliferate. Once an appropriate number of cells had been reached, serum-free medium was substituted to serum starve the cells. After 3 days of serum starvation, cells were seeded onto tissue culture plastic and left to survive. These cells were termed explant enzyme digested limbal (exenzL) and central (exenzC). Both the limbal and central cells showed rates of population decline very similar to an enzyme digested limbal population (Fig. 6C). This suggests that the cells obtained through enzyme digestion will not migrate out of explants and need to be digested out. Interestingly, the corneal centre explants have cells within them that apparently survive longer and die slower if explant migration is performed first. Keratoconic fibroblasts (KF) were previously explant migrated from the centre of the cornea, they were cultured in 10% serum medium and allowed to proliferate. Once a large number of cells had been reached, serum-free medium was substituted in to serum starve the cells. After 3 days of

serum starvation, cells seeded onto tissue culture plastic and left to survive. The rate at which cell population declined amongst KF was most similar to enzdL (Fig. 6D), a surprising similarity as KF are central and explant migrated while enzdL are limbal and enzyme digested.

4.2. Gene expression of healthy and keratoconic stromal cells

Multiple important keratocyte markers were analysed at the gene transcript level and the most common method of stromal cell extraction, enzyme digestion of the limbus or enzdL, was used as a reference. Results showed that the method of extraction and the location of extraction both had a significant effect on the expression of several key genes. When digesting cells out of the centre of the cornea rather than the limbus, significantly higher transcription levels of DCN (368±122 fold increase), LUM (27±1 fold increase), RARA (5±0.7 fold increase), TIMP1 (3±0.01 fold increase) and ALDH3A1 (Fig. 7A, C, J, M and N).

Extracting limbal stromal cells through explant migration also had an effect on gene expression profile of the stromal cell population. Explant migrated limbal cells had increased expression of CD34, LUM (246±45-fold increase), TIMP1 (12±0.3-fold increase) and COL1 (5±0.3-fold increase) (Fig. 7C, E, J and K). Central cells showed rather different transcription profiles when migrated out, with increased expression of ALDH3 and KERA (5.7±1-fold increase). The population of cells that remains in the explant after migration did show some difference in expression, with increased LUM (83±7-fold increase), CD34 and COL1 (4±0.02 fold increase) in the case of limbal cells while central cells showed increased ALDH3 and LUM (9±0.6 fold increase) with decreased CD34 and COL5 (7±0.04 fold decrease) (Fig. 7C, E, F, K and N).

Finally, as all 6 of the previously described cells had been cultured prior to experiments, there was still the question of what gene expression was like *in vivo* or at least in freshly extracted cells. The fresh cells showed the most drastically different profile from the enzdL reference. CD34, a commonly accepted marker of plasticity and stem cell behaviour was much more transcribed in both fresh central (19±4-fold increase) and limbal (7±0.8-fold increase) cells (Fig. 7K). There was massively increased expression of ALDH3 in the limbal cells (366000±120000-fold increase) and smaller but still statistically significant increase in the central cells (Fig. 7N). KERA had significantly increased expression in fresh cells relative to the cultured cells (17000±3600-fold increase) (Fig. 7B). The fresh cells also expressed a larger amount of RARA (19±1-fold increase) (Fig. 7N). A number of genes also seemed inactive in the fresh cells compared to the enzdL reference. COL1 (11±0.5-fold decrease, 100-

fold decrease), COL5 (5±0.2-fold decrease, 2.5±0.4-fold decrease) and αSMA (50±5-fold decrease, 16±4-fold decrease) were all expressed at much lower levels in both limbal and central cells.

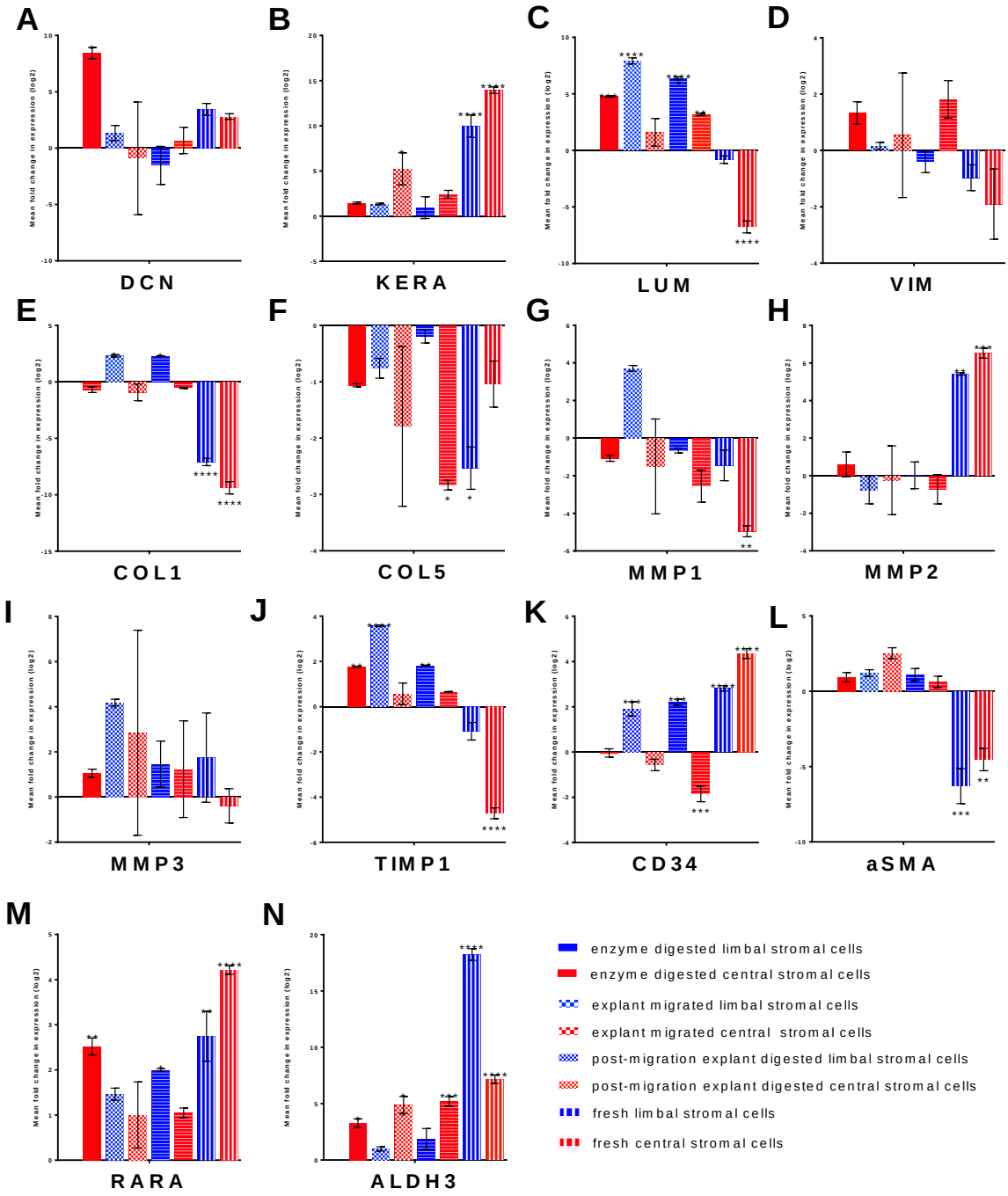

Figure 7: Fold change in gene expression for healthy stromal cells cultured in serum-free medium for 11 days. Gene expression was normalized relative to control group of enzyme digested limbal cells (solid blue fill). Extraction methods were: enzyme digestion (solid fill), explant migration (chequered fill), digestion of explant post-migration (diagonal stripe fill) and analysis immediately after digestion (pinstripe fill). Limbal cells (blue) and central cells (red) were both assayed. Data (mean ±SD) were obtained from three independent experiments (n = 3) and compared to enzdL using t-test (* for $p < 0.05$, ** for p<0.005, *** for p<0.0005, **** for p<0.0001).

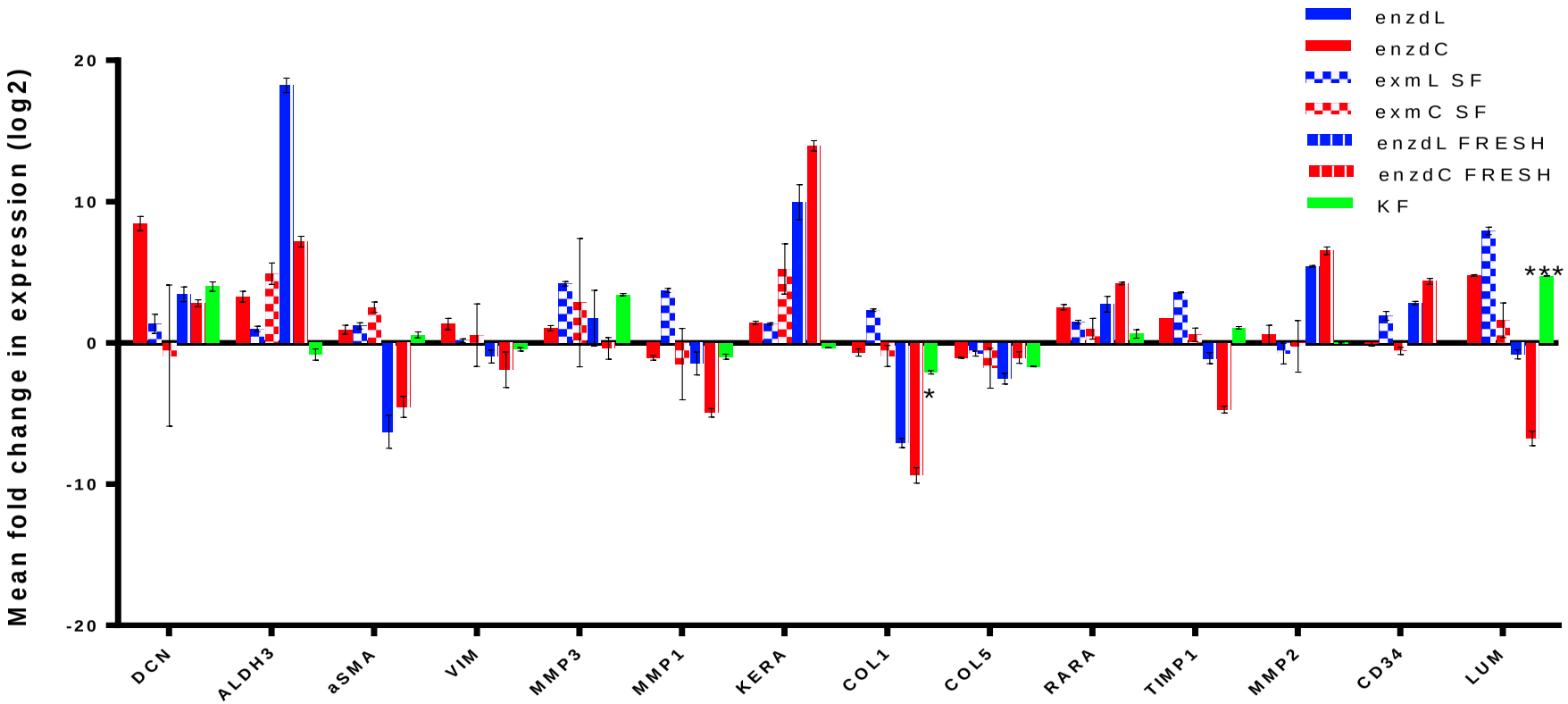

Figure 8: Fold change in gene expression for healthy stromal cells and keratoconic stromal cells (green) cultured in serum-free medium for 11 days. Gene expression was normalized relative to control group of enzyme digested limbal cells (solid blue fill). Extraction methods were: enzyme digestion (solid fill), explant migration (checkered fill) and analysis immediately after digestion (pinstripe fill). Central keratoconic cells (green) Healthy limbal cells (blue) and healthy central cells (red) were both assayed. Data (mean ±SD) were obtained from three independent experiments (n = 3) and compared to enzdL using t-test (* corresponds to $p < 0.05$).

Analysis of the same previously identified keratocyte markers in keratoconic cells showed that, similar to the survival rates of keratoconic stromal cells and healthy enzyme-digested limbal cells, the gene expression profile of the two cell types was also largely similar. However, differences were seen in the increased expression of MMP3 (10±0.6-fold increase) and LUM (26±0.3-fold increase) in keratoconic cells (Fig. 8). Vimentin expression was highest in the cultured central cells, enzdC and exmC, but was lower in the cultured limbal cells. Interestingly, KF were more similar to limbal cells suggesting a "non-central" identity for KF.

5. Discussion

The extraction of corneal stromal cells is a relatively simple procedure, but when using healthy cells as controls in the construction of a 3D model of the stroma, a better understanding of how extraction and culture affects the cells is needed. To this end, three separate stromal cell extraction methods were identified and used to yield a total of 8 different populations of healthy cells. These healthy cells were assayed for survival in a serum-free environment, as would be found in the cornea. These healthy cells were also assayed for the transcription of stromal cell specific genes that relate to various functions and states of differentiation. Finally, keratoconic cells were compared to the healthy stromal cells to find out what differences exist between the diseased cells and the healthy cells. Findings at this stage informed what controls were to be used when designing the keratoconus model system.

The cells extracted from the centre of the cornea appeared to perish faster in culture than cells extracted from the limbal area of the cornea. This is likely due to the presence of a progenitor population of cells with a greater proliferative capacity in the limbus. Although it should be noted that both the central and limbal cells eventually reach similar population numbers, the difference lies in the amount of time it takes to reach that point. The largest amount of variance was seen in the enzyme-digested limbal cells. This was due to some donors yielding cells that survived for a significant amount of time in culture, even proliferating slightly in serum free conditions, even though the cells were serum starved prior to experiments. The cells populations extracted by digesting the pieces of cornea that had been used for explant migration showed longer survival than the explant migrated cells. This suggests that in the case of both the central and limbal cornea, the more proliferative or better surviving cells are not migratory enough to leave the explants. While the limbal population of enzdL and exenzL

appeared similar in respect to their survival, a great difference is seen in the rate at which central population perish. The cells digested from pieces used in explant migration performed much better than cells extracted directly from the intact corneal button. It is possible that allowing cells to first migrate out of the corneal centre and then culturing the small number of cells left behind obtains a more homogenous population of progenitors. This seems contrary to the current prevailing hypothesis of progenitor cells existing only in the limbus. Further investigation into marker profiles and differentiation potential could reveal if the corneal centre does indeed house a small number of progenitor cells that could be isolated.

Extraction method also had an effect on cell survival, explant migrated cells saw faster population reduction in the first few days, faster even that enzyme-digested central cells. These cells showed very little variance among donors and lost the majority of their population in the first day of culture in serum free medium. It is possible that this large loss of cells is due to an inability to adhere. The serum starvation prior to the seeding of the cells occurred after the cells had formed adhesions. Once the cells were starved for three days, they were then transferred to culture plates. As serum free medium doesn't contain the adhesion promoters found in serum medium, it is possible that cells isolated via explant migration cannot build adhesion complexes in serum-free conditions and therefore largely perish when transferred. While this serum-starving step was present in all methodologies and was performed on all cell types assayed, explant migrated cells may be the most responsive due to their migratory and adhesion-based isolation.

Currently, the only method of obtaining a large number of primary corneal stromal cells from human tissue is to expand these cells in serum-containing medium. While this method is simple and robust, the phenotype of the cells is altered drastically due to the new environmental cues and rapid cell cycling (Beales et al., 1999). This is most obvious when observing the fold-changes in αSMA and CD34, a marker of differentiation and a marker of plasticity respectively. The increase in αSMA expression from enzdL and enzdC cells compared to the uncultured Fresh enzdL and Fresh enzdC suggests differentiation towards the more contractile myofibroblast lineage (Chen et al., 2007). A decrease in CD34 expression is also observed after culture in serum medium, with Fresh enzdL and Fresh enzdC cells showing the highest amounts of CD34 mRNA while cultured counterparts showed far lower amounts. In particular, central cells seem to suffer the greatest loss in CD34 transcription following *in vitro* culture. The loss of CD34 could be interpreted either as a differentiation of progenitor cells towards a lineage that lacks the expression of CD34 or as a loss of CD34-

expressing cells due to competition with stromal cells better suited to serum-containing medium. Keratocan, MMP2 and ALDH3 gene expression follow a trend similar to CD34 with higher expression before serum culture while TIMP1 and Collagen type V and Collagen type I follow the pattern of αSMA with lower expression prior to serum culture.

When tissue is retrieved from a donor of keratoconic tissue at the time of keratoplasty, only parts of the central button are harvested. This is because the limbus must remain intact to prevent harmful vascularization of the cornea (Dua and Azuara-Blanco, 2000). This means that keratoconic stromal cells (KF) currently being investigated are all central stromal cells. This is particularly relevant when comparing KF to healthy controls as healthy limbal cells may be different purely due to differences in the location of the tissue of origin rather than due to keratoconus. To better compare KF to healthy cells, central stromal cells were isolated. Following serum and subsequent serum-free culture, these central cells showed clear differences from limbal cells, with greater expression of decorin, lumican, retinoic acid receptor A and TIMP1. This pattern of expression with large proteoglycan RNA production suggests cell behaviour geared towards matrix organization (Chen et al., 2015). Keratoconic cells lacked the higher expression of decorin and RARA but did have increased MMP3. This could be due to a more degradative activity of keratoconic cells in culture.

Keratoconic cells were extracted using explant migration, a method of primary cell isolation that relies on cell movement. Dr. Karamichos performed the extraction of keratoconic cells by culturing the tissue in serum medium to entice the cells out of the tissue and onto plastic (Karamichos et al., 2012). When isolating healthy stromal cells in the same manner, it is not possible to collect a sample of explant migrated cells that were not exposed to serum medium. In order to better understand the effects of explant migration on gene expression, healthy stromal cells were extracted from the limbus of donor corneas via enzyme digestion and explant migration. The resulting two populations were cultured in serum to a large number and then cultured in serum-free conditions. Results showed that exmL retain specific differences with enzdL even after both were subjected to serum culture. Increased expression of lumican, MMP1, MMP3, TIMP1 and Collagen Type I in the exmL population suggest increased matrix-remodelling activity. This is in line with a migratory profile that would require deconstruction and reconstruction of ECM. In central stromal cells, the enzyme digested enzdC and explant migrated exmC also showed some differences although not in the same genes as limbal cells. Lower expression of decorin, lumican, MMP1, MMP3 and TIMP1 were observed in exmC relative to enzdC.

Following a better understanding of the effect of extraction method on stromal cells, the question became: Is the behaviour of keratoconic cells a product of extraction method, extraction location, serum culture or any combination of the three? To best answer this, keratoconic cells were compared to healthy stromal cells extracted from the same location with the same extraction method: explant-migrated central stromal cells. When it came to survival, keratoconic cells outperformed exmC by surviving seeding in greater numbers and lasting for longer. The keratoconic cells seemed most similar to enzdL in respect to survival and some gene expression. When comparing expression profile, KF showed a profile that could not be entirely explained simply by extraction method or location. KF expressed more lumican, MMP1 and MMP3 than exmC while also showing some similar expression patterns to cultured limbal cells like lower ALDH3 and vimentin. It is likely that serum culture and subsequent serum-free culture had an effect on KF, particularly keratocan and CD34 expression, though it cannot be known for sure until freshly extracted cells can be analysed. Overall, KF cells show a distinct set of serum-free survival and expression behaviours that cannot be explained purely by culture, extraction method and location. The difference observed between KF and healthy cells must be due to the disease itself rather than manipulation of the cells.

Chapter 5: Culturing Stromal Cells in Serum-Free Conditions

1. Abstract

Stromal cell behaviour is regulated by the cell's environment. The cornea and the cells within provide a multitude of cues such as nutrient concentrations, oxygen content, matrix physical properties, cytokines and hormones. A wound or disease will change the environmental cues and lead to a change in cell behaviour. When extracting stromal cells and subsequently culturing these cells in serum medium, these *in vivo* cues are lost. Tissue culture plastic lacks the mechanical properties of corneal ECM, specific growth factors are replaced by the broad spectrum that serum provides, oxygen concentration is now unregulated and neighbouring secretory cells are no longer around. If a model is to be built with stromal cells, keratoconic or otherwise, the behaviour of the cells must be returned (as close as practicably possible) to that which it exhibited *in vivo*. This can partially be achieved through the removal of serum and addition of retinoic acid, a metabolite of vitamin A and potent regulator of corneal function.

2. Introduction

2.1. Reproducing the stromal cell native environment

Stromal cells like all cells are dependent on signals provided largely by the ECM and surrounding cells (Wu et al., 2012). These signals determine the way the cells respond during migration, adhesion, proliferation and differentiation. Epithelial cells have been documented as the principal cellular coordinator of stromal cell fate through their two-way communication across the Bowman layer (Wilson et al., 2003). Loss of epithelial cells will exacerbate wound-healing reactions in the stromal cells and lead to increased differentiation (Nakamura et al., 2002). This stromal cell differentiation can be reproduced *in vitro* by simply adding serum to stromal cell cultures (Jester and Ho-Chang, 2003). While it would be desirable to use corneal epithelial cells from keratoconic sources to build a model, these cells pose unique challenges in their acquisition, culture and storage. To compensate for the lack of epithelial cells in the model, serum-free conditions will be used and although the absence of serum drives rapid population decline in stromal cells as seen in Chapter 4, different medium supplementation may be used to overcome cell loss *in vitro*.

2.2. Modelling the corneal stroma

When studying a tissue and the diseases that affect it, a model is typically used. The cornea has multiple existing animal models, each with their own advantages and disadvantages. For example, while rabbits are commonly used as corneal models, the microanatomy of the

cornea has clear differences, particularly in innervation (Ojeda et al., 2001). Mouse corneas also differ from humans by becoming significantly thinner towards the periphery (Henriksson et al., 2009). When attempting to model keratoconus in animals, the problem becomes compounded. Since the exact cause of keratoconus is unknown, it is difficult to replicate the disease in an animal. Although keratoconus or at least a very similar disease has been observed in monkeys (Kodama et al., 2010), there doesn't exist a genetic lineage of animals with keratoconus. To produce animal models of keratoconus, effort has been made to replicate the symptoms of the disease, usually through mutations that causes a keratoconus-like keratopathy (Tachibana et al., 2002). While animal models provide several biological challenges, there are also cost and ethical implications when using animals to study tissue or a disease. Multiple cell culture-based corneal models have been explored with the intended purpose of overcoming the challenges associated with animal experiments and to replace animal models with viable *in vitro* systems.

In vitro models of corneal tissue offer unique advantages for the study of cell behaviour such as simplification of the more complex in vivo environment, lower cost than human or animal models and relatively easy high throughput analysis. *In vitro* models of the cornea have previously been constructed using epithelial cells (Gonzalez-Andrades et al., 2016), stromal cells (Reichl et al., 2004) and, in rare case, endothelial cells (Orwin and Hubel, 2000) or neuronal cells (Suuronen et al., 2004). These cells are typically encased in a substrate that will replicate some of the properties of the highly specialized corneal collagen matrix such as biodegradability, geometry or stiffness. The final component is the medium used to feed the cells; in a model, the formulation should aim to replicate as many of the *in vivo* cues as possible or at least induce cellular behaviour similar to what is observed in the cornea.

2.3. Medium supplementation

When cultured in vitro, the chemical cues and nutrients that allow keratocytes to thrive have to be reproduced. The basal medium formulation used for mammalian cell culture was first set by Harry Eagle, described as being isotonic, pH-neutral and containing molecules necessary for cell survival such as vitamins, amino acids, salts and sugars (Eagle, 1955). A later modified recipe of Eagle medium called modified Eagle medium (Greenbaum et al.), included greater amounts of amino acids and vitamins, increasing nutritional value (Eagle, 1959). One of the later iterations of Eagle medium, modified by Renato Dulbecco, included a fourfold increase in vitamins, amino acids and glucose combined with the new inclusion of iron and pH indicator phenol red (Dulbecco and Freeman, 1959). The sequence of tweaks to

the original basal medium formulation eventually led to the combination of two existing medium recipes (Barnes and Sato, 1980). DMEM and Ham's nutrient mixture F-12 where mixed to combine the high nutritional contents of DMEM with the components of F-12 like bitotin, putrescin, glycine and proline that aren't found in DMEM (Ham and McKeehan, 1979). The medium, known as DMEM/F-12 is typically supplemented with a stabilized form of L-glutamine to prevent ammonia build-up and ensure cell survival during long-term culture (Atanassov et al., 1998). This DMEM/F-12 is the most widely used cell culture medium for keratocytes and can be supplemented with serum. For keratocytes, the presence of serum in DMEM/F-12 has been shown to drive cell proliferation (Priyadarsini et al., 2015).

Historically, serum has been an important part of mammalian cell culture methods. Serum provides growth enhancers and protective elements to cells, allowing cultures to thrive. Adhesion promoters, hormones, protease inhibitors, low molecular weight nutrients, and growth factors are all present in serum (Francis, 2010). When cultured in the presence of serum, keratocyte undergo behavioural changes, shifting from a quiescent dendritic state into fibroblastic proliferating cells. This change resembles the normal wound healing response seen in vivo (Beales et al., 1999, Jester et al., 1999). While serum provides many benefits, there exist multiple reasons why serum-free cultures are desirable. Firstly, the collection of serum is costly and considered inhumane by some (van der Valk et al., 2004). The variance between batches of serum due to seasonal, continental and animal variance affects the reproducibility of experimental results, a crucial requirement for many cell cultures that require defined and non-variable supplement. Furthermore, sera or any reagent of animal origin caries the risk of contamination; viral contamination has been noted in up to 50% of commercial foetal bovine serum (Wessman and Levings, 1999, Levings and Wessman, 1991). A serum-free culture system is therefore desirable to avoid the complications that accompany serum use, although the benefits of serum need to be reproduced to support proliferation and a degree of quiescence.

Instead of serum, the basal medium DMEM/F12 has to be supplemented with different additives. The ITS supplement groups three such additives, namely insulin, transferrin and selenium. The ITS mix first showed promise in enhancing germ cell maturation and embryogenesis when coupled to ascorbic acid (Cordova et al., 2010). It has been shown that medium supplemented with ITS allows for adequate culture of keratocytes (Gouveia and Connon, 2013). The insulin can maintain the keratocyte phenotype during proliferation, delaying appearance of fibroblastic markers (Musselmann et al., 2005). Transferrin is an iron

transfer protein necessary for cell survival in culture. Selenium is a trace element used in anti-oxidative pathways that protect cells (Helmy et al., 2000). What makes ITS particularly attractive as a supplement for keratoconic cells is that each component addresses a pathological facet of the disease. Fibroblastic and myofibroblastic differentiation are both reported in keratocytes extracted from keratoconic patients, insulin reportedly inhibits these phenotypes in culture. Transferrin polymorphisms occur in some cases of keratoconus, supplementing cells with transferrin may offset these polymorphisms (Wojcik et al., 2013). An increase in oxidative stress and a decrease in anti-oxidative pathways are both hallmarks of keratoconus; an antioxidant like selenium may combat this aspect (Arnal et al., 2011). All vitamins necessary for keratocyte survival are present in DMEM/F12, although increasing the amounts of specific vitamins can have positive effects. Ascorbic acid, also known as vitamin C, can be supplemented to basal medium to increase collagen synthesis. The addition of ascorbic acid to a variety of cell types showed effects on differentiation and proliferation (Huijskens et al., 2015, Takahashi et al., 2003). Ascorbic acid doesn't seem to affect growth or directly cause differentiation, instead activating ECM production pathways that lead to new cell behaviour (Builles et al., 2006).

Of final note regarding the composition of medium for stromal cell culture is glucose concentration. The cornea itself is an avascular organ with lower availability of metabolites compared to other tissues. Glucose is a nutrient that the cornea receives very little of. The human cornea has a glucose concentration of around 1g/L while the DMEM/F12 used here and in multiple other stromal cell experiments has a glucose concentration of 4.5g/L. The effects of low glucose were previously investigated to better understand the effect this had on cells (Foster et al., 2015). Compared to high-glucose medium in serum-free conditions, low-glucose medium was found to enhance survival and induce cellular characteristics that closely resemble the keratocyte *in vivo*. Glucose concentration seems to be the most obvious next step in formulating a medium that best replicates the stromal environment in order model the cornea.

2.4. Retinoic Acid

Another vitamin with positive effects on keratocytes is retinoic acid (RA), a metabolite of vitamin A also known as "activated vitamin A". To maintain integrity and proper functionality, the cornea requires RA to regulate transcription of specific genes (Nezzar et al., 2007). Past experiments involving the culture of keratinocytes in the presence of RA have shown that RA can either inhibit and induce proliferation (Marcelo and Madison, 1984). RA

may also drive the expression of differentiation markers in keratocytes, such as keratin (Fuchs and Green, 1981) and filaggrin (Fleckman et al., 1985). This effect on differentiation is not limited to keratinocytes, in culture; RA can stimulate the differentiation of many pluripotent stem cell types. This previous data suggest that RA could be modulating the activation of stem cells to transient proliferating cells. Overall, the effect of RA on proliferation and differentiation seems concentration dependent. Cultures of keratocytes did show that RA would enhance proliferation and stratification while reducing mobility in serum-free conditions (Gouveia and Connon, 2013).

2.5. Aims

To construct a model of keratoconus in vitro, stromal cells need to be cultured in serum-free conditions without perishing. To this end, RA was used to keep cells alive as it is a significant molecular cue of the cornea during development and maintenance of the tissue.

3. Methods

3.1. Preparation of RA

3 mg RA powder (Merck, USA) was solubilized in 10mL of absolute ethanol to produce a 1mM stock solution, which was sterile-filtered and stored in aliquots at −80°C for up to 1 month. RA was added to medium immediately before use by diluting in serum-free DMEM/F12 at a ratio of 1:1000 medium volume for a final concentration of 1μM.

3.2. Cell survival in RA-supplemented medium

The Alamar blue assay was used to assess keratocyte proliferation and viability in RA-supplemented serum-free medium over a period of 11 days. Cells were initially seeded at a density of 100000 cells per cm^2 in a 24 well plate after 3 days of serum starving. The cells were cultured in serum-free medium supplemented with RA. The cells were assayed with Alamar blue at days 1, 4, 6, 8 and 11 of culture. The cells were incubated with resazurin reagent (Sigma-Aldrich; prepared in 1:10 dilution using fresh serum-free culture medium with no RA) for 90 minutes at 37°C, after which 100 μl of culture supernatants (in triplicate) were sampled for fluorescence emission analysis at 590nm using Varioskan LUX multimode microplate reader (ThermoFischer, Franklin, MA). The cells were then washed once with PBS to remove excess reagent and then replenished with fresh, serum-free medium. Cell number was calculated by interpolation using a standard curve for fluorescence values of 150,

100, 80, 60, 40, 20, 10, 5 x 10^4 cells. All values correspond to average ± SD of 3 independent experiments.

3.3. Stromal cell gene expression in RA-supplemented medium

Following 11 days of culture, RNA was extracted from the cells RNeasy Mini Kit (QIAGEN, UK) according to manufacturer specifications. The RNA was then treated with DNase to eliminate genomic DNA. Quality assessment of the RNA was performed using a Nanodrop 2000 spectrophotometer (Thermo Scientific, UK) to ensure the A_{260}/A_{280} ratio was within the range of 1.7 to 2.0 and the A_{260}/A_{280} was above 2:1. The RNA was then reverse-transcribed into cDNA with the RT2 First Strand kit (Qiagen, UK) according to manufacturer specifications in a TC-Plus thermal cycler (Techne, Staffordshire, UK). The resulting cDNA was then assessed using the Nanodrop to ensure purity and suitable concentration. The qPCR reaction was carried out using direct dye binding in the Eco Real-Time PCR System (Illumina, USA) and the appropriate primers (Table 1). The following cycles: 10 minute denaturation at 95°C, followed by 40x cycles of 10 seconds at 95°C, 30 seconds at 60°C and 15 seconds at 72°C. All values correspond to average ± SD of 3 independent experiments with expression of each gene of interest normalized to housekeeping gene GAPDH.

4. Results

4.1. Survival of healthy and keratoconic stromal cells with RA

When exposed to RA at a concentration of 1uM, limbal cells were able to proliferate (Fig. 9A). While the population of central cells did not increase, it didn't decrease either (Fig. 9B). Whether this was as a result of cells not dying or due to rates of proliferation and cell death cancelling each other out remains to be better understood. The addition of RA to serum free medium when culturing explant migrated cells had similar effects to those seen when culturing enzyme digested cells. The limbal cells showed a population increase when exposed to RA (Fig. 9C). The explant migrated central cells showed a high percentage increase in population, much higher than any other population (Fig. 9D). It should be noted however that these central cells have the poorest initial adherence (as low as 20%) and that therefore, any population increase is in fact quite small. This is a relevant finding however as it suggests that the enzyme digested central cells may proliferate rather than keep the cells already there alive. Keratoconic cells were also cultured in serum free medium supplemented with 1μM of RA. Keratoconic stromal cells proliferated when cultured with RA (Fig. 10), suggesting that a serum free model could be built using these culture conditions.

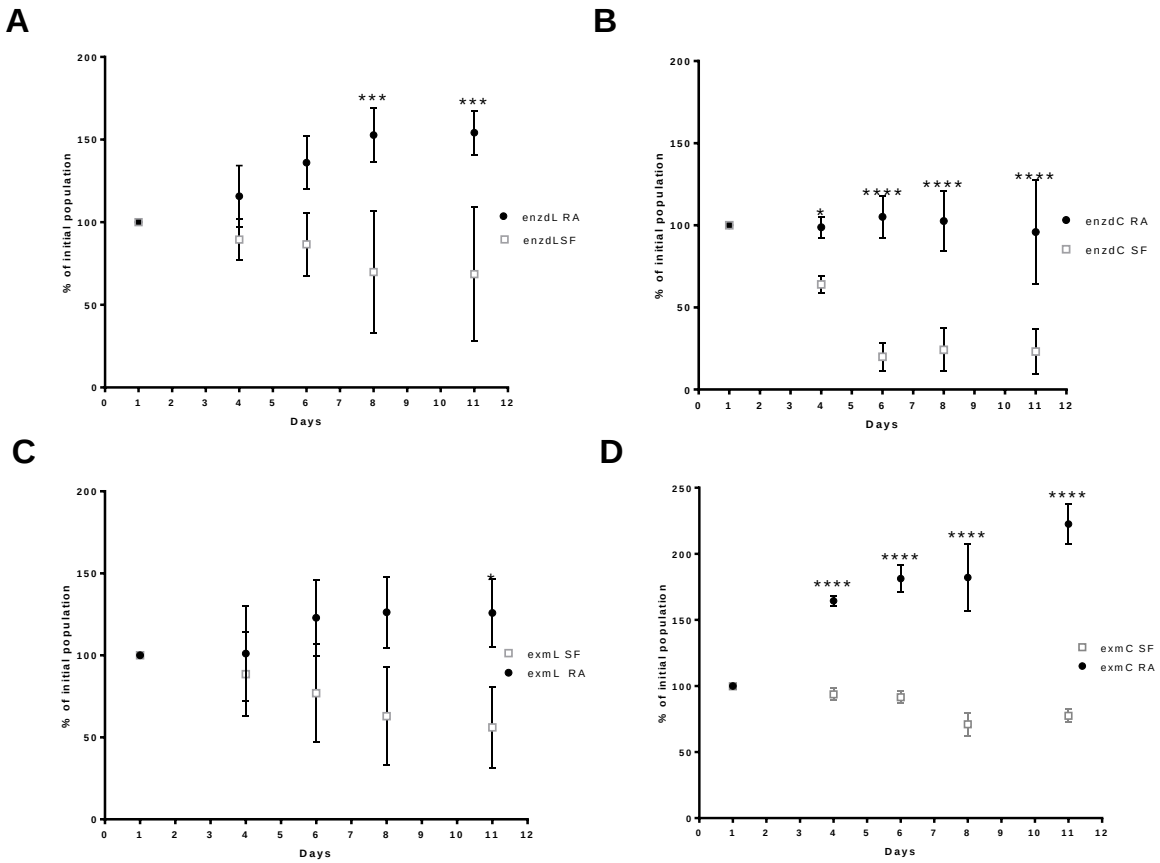

Figure 9: Survival of explant migrated and enzyme digested healthy stromal cells in retinoic acid serum- free medium as quantified by Alamar blue assay. Data was obtained from 3 experiments (n=3) per cell type, each with a different donor. (* for $p < 0.05$, ** for $p<0.005$, *** for $p<0.0005$, **** for $p<0.0001$).

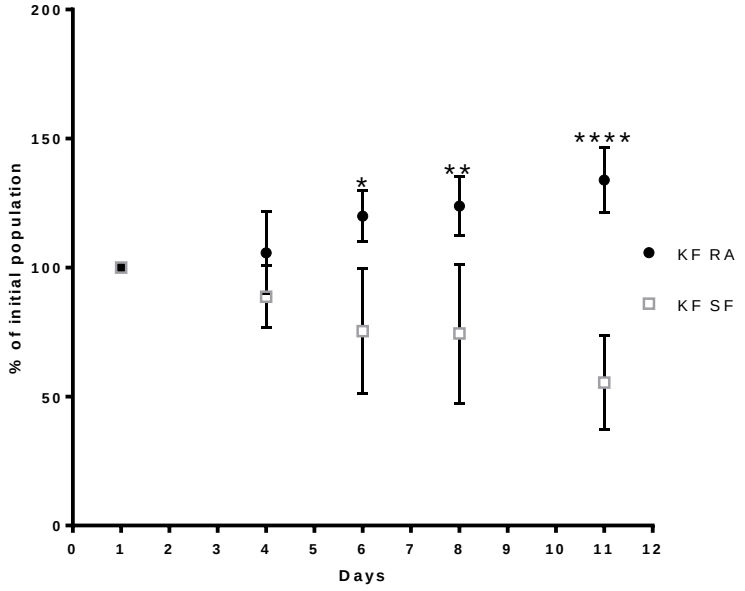

Figure 10: Survival of keratoconic stromal cells in RA serum- free medium as quantified by Alamar blue assay. Data was obtained from 3 experiments (n=3) per cell type, each with a different donor (* for $p < 0.05$, ** for p<0.005, *** for p<0.0005, **** for p<0.0001).

4.2. Gene expression of healthy and keratoconic stromal cells with RA

Multiple important keratocyte markers were assayed at the transcript level to determine whether RA had an effect on healthy stromal cells and keratoconic cells. Results showed that RA did have an effect on the expression profile of both healthy and keratoconic, with similar shifts in behaviour for both cell types. Expression of ALDH3 did change across all cell types with the addition of RA, significant difference was only detected in limbal and keratoconic cells (Fig 11N). KERA also showed higher expression in the presence of RA, with a statistically significant difference observed in all cell types except exmC (Fig. 11B). Decorin expression trended downwards when exposed to RA, with central cells like exmC, enzdL and KF seeming the most affected although with no statistical significance (Fig. 11A). MMP3 expression was only affected in enzyme digested cells, with the most change being seen in the limbal population (Fig. 11I). LUM expression is the first gene with both significant increases and decreases accompanying RA addition. The lower lumican expression initially seen in enzdL was increased while the higher expression in exmL was decreased (Fig. 11C). RA brought lumican expression in all cell types to a similar level, suggesting a bidirectional regulatory effect from RA. TIMP1 expression was significantly affected in enzdL, exmC, and KF (Fig. 11J). MMP1 expression was affected in both of the explant migrated cells types, decreasing in the limbal cells and increasing in the central cells (Fig. 11G). Genes involved in

matrix degradation seemed more reactive in explant migrated cell types although not in KF. This somewhat reinforces the identity of keratoconic cells having some unique behaviours despite being extracted through migration. Vimentin expression was driven down considerably, though not in a statistically significant manner, across all cell types with the most drastic change being observed in the central populations. The expression of αSMA was increased in the enzyme digested populations and was reduced in the explant migrated cells, with statistical significance observed in both cases. KF seemed to not react to RA in regard to its αSMA expression. RA receptor, RARA, (Greenbaum et al., 2017) expression in enzdL observed an increase in the presence of RA, no change could be seen in other cell types. Expression of Collagen I was reduced in enzdL and exmL while increasing in enzdC. Collagen V on the other hand seemed reduced across all cell types but only significantly for enzdL (Fig. 11 E and F). MMP2 expression seemed to have been most affected in the exmC populations, which is in line with previous changes in behaviour specific to explant migrated cells affecting matrix digestion-related genes (Fig. 11H). However, none of the MMP2 expression changes were deemed statistically significant. Finally, CD34 expression was reduced in all cell types following RA exposure with the exception of exmC (Fig. 11K).

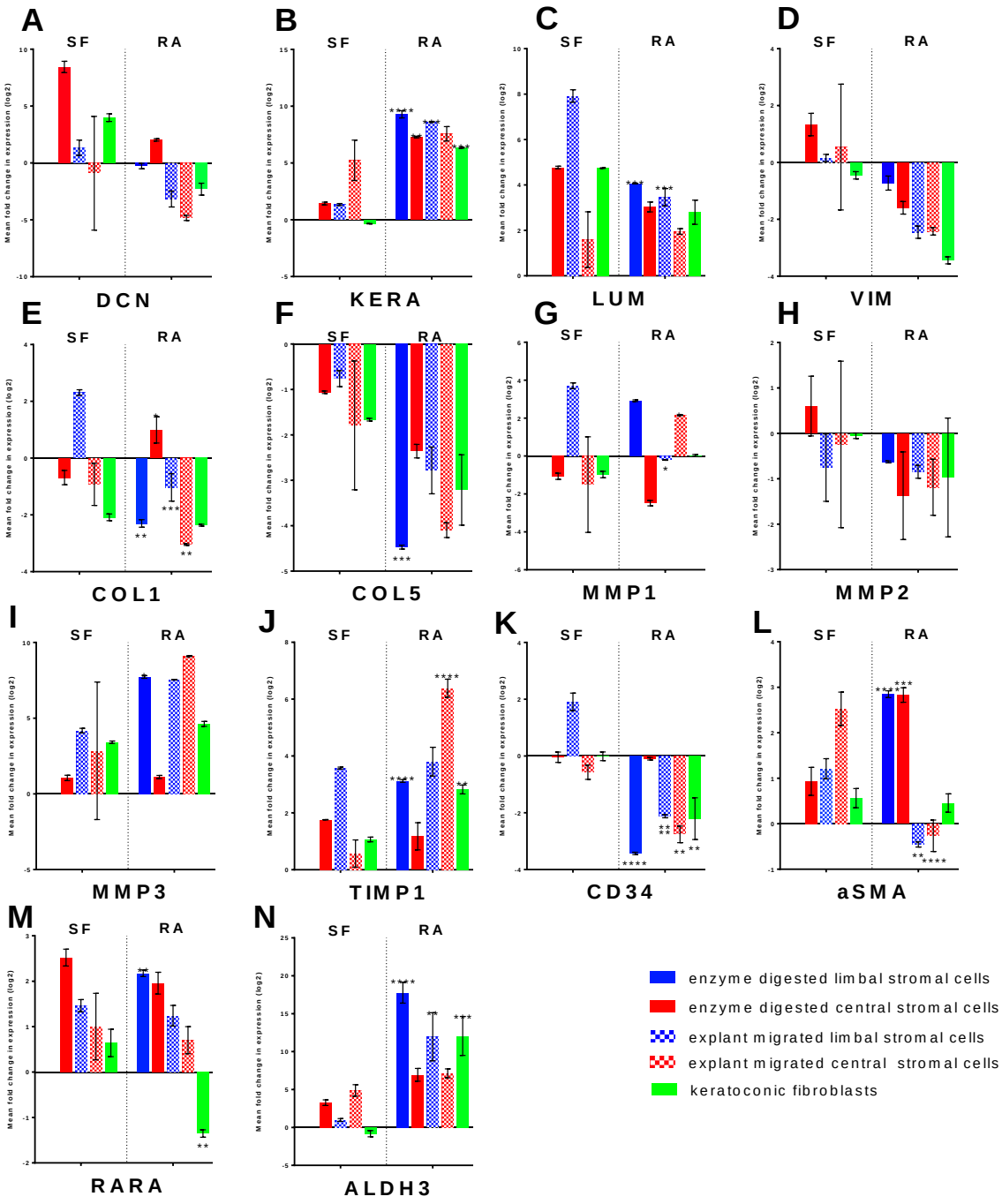

Figure 11 : Fold change in gene expression for healthy stromal cells and keratoconic fibroblasts cultured in serum-free medium without RA (left portion of graph) or with RA (right portion of graph) for 11 days. Gene expression was normalized relative to control group of enzyme-digested limbal cells in serum-free medium without RA (solid blue fill). Extraction methods were: enzyme digestion (solid fill) and explant migration (chequered fill) for healthy cells. Healthy limbal cells (blue), healthy central cells (red) and keratoconic cells (green)were assayed. Data (mean ±SD) were obtained from three independent experiments (n = 3) and

used one-way ANOVA to compare RA-supplemented culture to respective non-supplemented control (* for $p < 0.05$, ** for $p<0.005$, *** for $p<0.0005$, **** for $p<0.0001$).

5. Discussion

RA has already been studied for its role in guiding mesenchymal and corneal morphogenesis, as well as proliferation and differentiation of stromal cells (Gouveia and Connon, 2013; Abidin et al., 2015). At a concentration of 1µM, RA was found to cause proliferation and block migration in corneal stromal cells cultured in serum free environment. This made RA an interesting candidate for the maintenance of a stromal cell population *in vitro* without serum. At a concentration of 1µM, RA triggered proliferation in all cell populations assayed, with the exception of enzyme-digested central cells. While explant migrated central cells did show a large percentage increase in population, although their starting population was much smaller than other cell types assayed and any small increase in cell number would appear as a larger percentage increase. This was due to explant migrated central cells reacting very poorly to detachment and typically not reattaching if seeded into a serum free environment; the lower number of attached cells meant that a smaller amount of RNA was collected, a sufficient amount for analysis was still extracted. As for keratoconic cells, once again we see a behaviour very similar to limbal cells rather than central cells, with cell numbers increasing rather than stagnating. RA was therefore selected as one of the key supplements that will keep keratoconic cells alive in the model.

The addition of retinoic also had a significant impact on the expression of multiple genes essential to stromal cell function. Large increases where observed in the expression of ALDH3A1, a gene that codes for an aldehyde dehydrogenase responsible for the protection of corneal transparency. This protein composes a large portion of the corneal soluble protein content and its high expression when exposed to RA is encouraging as this suggests that *in vivo* behaviour may be occurring. Of interest is that, while the increases in ALDH3A1 were not deemed statistically significant, limbal cells exposed to RA reached higher concentrations of ALDH3A1 mRNA compared to their central counterparts. This suggests perhaps a greater sensitivity to RA in limbal cells, which keratoconic cells also share, further supporting the idea that keratoconic cells are limbal-like while residing in the corneal centre.

Another gene that showed notable increase is KERA, encoding for keratocan, a proteoglycan essential for corneal transparency. All stromal cells assayed, healthy and keratoconic, showed increased KERA expression when exposed to RA. Decorin, another important proteoglycan,

had its gene expression reduced by RA. Lastly, the proteoglycan lumican showed a varied response to RA based on the cell type. Taken together, these three leucine-rich proteoglycans indicate a shift in the organization of matrix produced by the cells. Previous research showed that keratan sulphate proteoglycans, like keratocan and lumican, are involved in the regulation of collagen fibril diameter while dermatan sulphate proteoglycan, like decorin, control interfibrillar spacing and lamellar adhesive properties of corneal collagens (Michelacci, 2003). The reduction in decorin expression and increase in keratocan expression could be interpreted as a cellular effort to regulate fibrillar diameter and foregoing some control of fibrillar spacing. The exact implication this would have in a 2D culture system's ECM over such a short timespan remains unclear.

Another facet of ECM maintenance affected by RA is the expression of matrix metalloproteinase-coding genes. MMP1, 2, and 3 were all affected to some degree. Explant migrated cells were the most significantly affected with an increase in MMP3 for both limbal and central explant migrated cells. MMP1 showed and increase for exmC but a decrease for exmL. Finally, while MMP2 was not found to increase or decrease significantly after addition of RA, the larger variations in MMP2 expression in healthy central cells disappeared after RA supplementation. Taken together this data seems to suggest that explant migrated cells became more involved in matrix degradation in the presence of RA. However, the expression of general MMP-inhibitor TIMP1 also changed with RA, particularly in exmC. It could be interpreted that while degradative pathways are more active in exmC, they are more heavily regulated or inhibited. The different reaction of limbal and central explant migrated cells to RA in regards to MMP1 may ultimately have the same result due to increased TIMP1 expression compensating for upregulated MMP1 in exmC. Of relevance is also that while KF where isolated using the exact same techniques and tissue location as exmC, the reactions to RA in respect to MMP gene expression are very different. A lack of sensitivity to environmental cues in guiding gene expression may be a novel facet of keratoconus at a cellular and it has previously been observed that TIMP1 shows reduced expression in keratoconic corneas (Riley et al., 1995).

The most important aspect of ECM-regulation is the production of collagen by the stromal cells. The addition of RA also affects the expression of genes coding for these essential ECM building materials. Collagen type I saw little change in all cell types with the exception of exmL, where a significant decrease in expression was observed after culture with RA. Collagen type V was reduced significantly in all cell types assayed. As collagen type I is the

predominant type in the corneal stroma (Ihanamaki et al., 2004), RA may be limiting the production of non-essential collagens rather than increasing production of type I. The reduction of collagen type V is still concerning as this collagen has a role in regulating the ultimate diameter of collagen fibrils (Birk, 2001), an important role in a tissue where fibril geometry dictates light scattering. It is possible that this reaction was a product of culture on plastic for a short period of time and that longer culture periods would have seen the stromal cells shift to a behaviour more focused on matrix re-organization with more type V being produced. Further work using collagen gel culture and longer culture periods was of interest in pursuing this investigation.

Inside the cells, the cytoskeleton and the forces that act upon it also seemed to be affected by the addition of RA. Vimentin, a cytoskeletal protein responsible for cell structure and movement (Mendez et al., 2010), was found to have reduced expression in all stromal cells, healthy and keratoconic. The effects on cell behaviour that loss of VIM expression may have had were difficult to interpret, as the protein's function is not inherent to the monomer produced by the gene, but rather to the organization of the protein into filaments within the cells. It should also be considered that two other major cytoskeletal proteins, tubulin and actin, may still give the cell structure in the absence of vimentin. Of interest is that low vimentin expression is typically associated with poor wound repair due to myofibroblast impairment (Eckes et al., 2000), meaning that RA may impair wound repair response in some manner.

The most commonly used marker of myofibroblastic differentiation for stromal cells is increased expression of αSMA, a contractile protein used in migration and wound closure (Torricelli et al., 2016). The addition of RA did alter αSMA expression, with enzyme-digested cells showing increased expression while explant migrated cells showed no significant reaction. KF did show some increased expression following RA addition, although variability was too high to conclude that RA significantly increased αSMA expression. In this case, KF seemed more similar to enzyme-digested cells rather than explant migrated cells despite KF being themselves explant migrated. Increased αSMA in enzdL and enzdC would suggest that the two cell populations are now more contractile or motile. As explant migrated cells likely possessed higher levels of αSMA in the first place due to their extraction method being biased towards more migratory cells, it may be that the gene expression was reduced to some degree by an inhibitor. In the future, extraction of stromal cells by explant migration could be

attempted with RA in order to find out if a greater number of cells can be isolated with potentially increased migration from the increased αSMA expression.

The RARA gene codes for the non-steroid hormone receptor retinoic acid receptor α. This receptor is typically bound to a co-repressor complex until stimulated by RA into binding with a co-activator, enabling a conformational change in the receptor. This change then allows the RA receptor heterodimer to become a transcription factor (Cvekl and Wang, 2009). In the cultured stromal cells assayed, only enzdL showed an increase in RARA expression after addition of RA. It is possible that enzdL stromal cells are more sensitive to RA presence, as seen by the much greater effect of RA on proliferation. It is possible that all other stromal cells already possess large enough amounts of RA receptors and do not require additional RARA production. Analysis of RA receptors and their dimer-forming partners at the protein level could inform on the effects of RA on transcription factor activation.

The final gene assessed, CD34, codes for a transmembrane protein. This protein is one of the most commonly used markers for hematopoietic and general mesenchymal stem cells lineages (Huss, 2000). In the cornea specifically, CD34 appears only on the stromal cells and is not detected on the epithelial or endothelial cells (Joseph et al., 2003). When RA was added to the serum-free cultures of stromal cells, CD34 expression was found to be lower in both explant-migrated and enzyme-digested limbal cells. While central cells and KF also seemed to have decreased levels of CD34, no statistical significance was detected. This decrease in CD34 could suggest differentiation and a shift in cell behaviour where limbal cells are more affected. This is somewhat in line with previous work that identified the limbal stroma as a stem cells niche.

Overall, the addition of RA was hypothesized to have multiple effects based on the new patterns of gene expression seen. RA seemed to stimulate greater ALDH3A1 production, which may protect the stromal cells from UV and oxidative stress. Important shifts in ECM maintenance and production where identified with more KERA and less DCN being expressed, suggesting a greater impact on fibrillar spacing and less control on fibril diameter. This is further supported by lower collagen type V expression, another controller of collagen fibril diameter. The degradation of matrix also seemed to be altered with MMPs gene being most affected in explant migrated cells. While exmC and exmL seemed to have different MMP expression profiles, the end results seemed similar due to increased expression of MMP-regulator TIMP1 in exmC. Cell contractility and cytoskeleton-related genes also

showed change with lower expression of cytoskeleton fibril monomer and greater expression of genes expressing αSMA. RARA and CD34 showed more change in limbal cells, suggesting that the limbus is host to cells that are more sensitive to environmental cues. Finally, while the theory that keratoconic cells are “limbal-like central cells” held promise when looking at changes in ALDH3A1 and αSMA expression, KF did show some differences from limbal cells in genes such as CD34 and DCN. The theory of poor limbal differentiation being a mechanism of keratoconus remains to be investigated. With the relative success of keeping keratoconic cells alive in serum-free conditions as well as causing gene expression that could considered similar as what is seen *in vivo,* the next step in model building can begin.

Chapter 6: Engineering a 3D Culture System

1. Abstract

Collagens within the stroma are responsible for the cornea's three most important attributes: transparency, light refraction and physical protection of the eye. The fibrillar collagen, produced by the stromal cells, is also thought to guide cell behaviours such as migration or alignment. The ECM collagen's properties and the behaviour of cells within affect and maintain each other (reciprocal arrangement) to such a degree that separating the two undoubtedly prevents proper function. Therefore, the construction of a stromal model should incorporate ECM to some degree to better reproduce *in vivo* cell behaviour. Fibrillar collagen type I was used to make compressed collagen gels (CCG), this collagen type was used to construct the model due to its natural abundance and structural importance in the human cornea. CCGs were chosen as a culture system due to their relative ease of manipulation, similarity to *in vivo* ECM (in terms of collagen type I content) and extensive previous research on use in cell culture. The culture system made using CCG and retinoic acid (RA) allowed for culture of healthy and keratoconic stromal cells for extended periods of time with gene expression similar to what may be observed *in vivo*. The addition of curvature as an environmental cue was also shown to have some effect on cell behaviour in the gels.

2. Introduction

2.1. Stromal architecture and function

The corneal stroma is a rigid and transparent piece of tissue that fulfils two primary functions: refraction of light and protection of the eye's inner contents. These functions are achieved through the organization of the collagen ECM, a highly organized and well-maintained tissue. Within the stroma are stacked collagen lamellae and inside these lamellae collagen fibres arranged parallel to each other. Typically, the fibres of adjacent lamellae will be ordered in different directions. Overall, the stromal collagen shows two preferred orientation orthogonal to each other. This results in an anisotropic stress response where the tissue shows less deformation when subjected to stress in the vertical direction (Xue et al., 2018). The fibrils in the cornea do also change shape as they near the limbus, fusing with the circumferential collagen (Meek and Boote, 2004). Cells and their products regulate collagen fibril nucleation, diameter and spacing in these lamellae. This is important as is avoids fibrosis, which would cause opacity. Proteoglycans like decorin or keratocan, other collagens like collagen type V and even MMPs are used to constantly remodel the stromal ECM (Holmes et al., 2018).

While the cells influence the matrix, the ECM also drives particular cell behaviour. Previous research has found that fibre's alignment, pressure, stiffness, and curvature all affect stromal cell behaviour (Gouveia et al., 2017, Kivanany et al., 2016). The construction of a stromal model should aim to reproduce the features exhibited by the natural tissue and improve upon the well appreciated limitations of traditional cell culture.

2.2. Influence of stromal ECM on cell behaviour

Previous isolations of stromal cells from the cornea found that some of the cells were capable of a large number of population doublings while still retaining the ability to produce essential components like keratocan (Du et al., 2005). In culture, these cells where capable of producing small amounts of stromal ECM but did not arrange this matrix into a functional tissue (Du et al., 2007). Spatial cues from whatever substrate the cells reside on likely provides the signals required for ECM organization into stromal tissue. The effects of aligned substrates has previously been investigated and it was found that on top of aligning cells, the ECM produced was made up of aligned fibrils with uniform diameters and regular interfibrillar spacing (Wu et al., 2012). This collagen architecture broadly replicated what can be seen in stromal lamellae, although the tissue lacked the curvature of the healthy cornea.

2.3. Use of collagen gels in model building

The most intuitive approach to biological model building is often to simply mimic the tissue architecture and properties found *in vivo* and then seeding primary cells within. This approach seemed very feasible, as the corneal stroma can be considered a simple thin disk of collagen matrix. Some specific features of the stroma are not easily duplicated though; the alignment of collagen fibrils and the very high density of collagen prove more complicated. One of the first attempts at using collagen precipitated from acetic acid found that these structures produced resembled matrix in natural mammalian soft-tissue (Elsdale and Bard, 1972). The application of this collagen gel-making method to the manufacture of stroma-like ECM produced a matrix where stromal cells organized in similar fashion to their in vivo counterparts (Minami et al., 1993). Newer approaches to tissue models found that compressing the collagen gel (Brown et al., 2005) allowed for mechanical properties that more closely resemble stiff tissue, such as skin or bladder (Hu et al., 2010, Engelhardt et al., 2010). Applying compression to the precipitated collagen gels produced material with better light transmittance and mechanical properties as well as more hospitable conditions to corneal epithelial and stromal cell (Kong et al., 2017, Mi et al., 2012). Compressed collagen gels or

CCGs present an attractive scaffold within which to culture stroma cells and model the native tissue.

2.4. Curvature as an environmental cue

Using substrate curvature alone to influence cell behaviour has been done for over a decade (Smeal et al., 2005). In most cases, cell alignment or direction of cell growth is affected. Somewhat recently, the effects of curvature on corneal stromal cells were studied and is was found that monolayers cultured on top of a domed surface would have aligned cells producing aligned ECM (Gouveia et al., 2017). Utilizing the curvature of the initial scaffold, as a cue to pattern cell alignment and subsequent ECM production is not only simple, it also creates a dome-shaped tissue very similar to the corneal stroma itself.

2.5. Model specifications and requirements

Traditional technologies are normally required to fulfil specific performance requirements. In tissue engineering and modelling, attempts have been made to develop similar standards. Typically, these standards involve recognising in vivo behaviour and applying these to a design-build-test framework. The initial design and build phases are simple enough, but the testing phase is where a model should prove its efficacy and then inform on any further designing. When it comes to keratoconus, the main characteristics verified in testing are: 1) stromal ECM thinning and 2) opacity in the cornea. A keratoconic model's success should be gauged by how well it reproduces these two criteria. The gene expression patterns and cell survival can inform on how pathologically the KF are behaving, informing on whether the model is suitable for any future research.

2.6. Aims

To construct a model of keratoconus in vitro, stromal cells need to be cultured in an environment that mimics the natural stroma. To this end, compressed collagen gels were used to culture the cells in a 3D environment. Gel curvature was also added to further affect cell behaviour.

3. Methods

3.1. Gel making and cell encapsulation

Healthy and keratoconic cells were encapsulated in compressed collagen gels as described in chapter 3, section 1.10. The resulting compressed collagen gels (CCG) were cultured in serum-free medium, the survival of the cells within was monitored using Alamar blue and the gene expression was assayed with qPCR after a month of culture.

3.2. Curved gel culture

To curve gels, freshly made CCGs containing stromal cells were gently detached from their original plate and draped over a glass dome of 10mm diameter. A metal washer was used to hold the gel in place during culture to prevent movement during feeding or plate movement.

3.3. Retinoic acid supplementation

To evaluate the effects of retinoic acid on cell survival, RA was added to serum free medium at a concentration of 0.5μM after being initially diluted from a powder stock (Merck, USA) to a concentration of 10mM in ethanol.

3.4. Stromal cell gene expression in compressed collagen gels

Following 30 days of culture, the gels were homogenized using 1ml Trizol and a syringe. Then 200μl of chloroform was added to the homogenized mixture and allowed to it for 15 minutes at room temperature. After this initial phase separation, the homogenized mix was centrifuged at 18000xG for 15 minutes. The mix was now separated into 3 phases; the top two phases containing genetic material were collected for RNA isolation and suspended in ethanol. RNA was extracted from the cells using the RNeasy Mini Kit (QIAGEN, UK) according to manufacturer specifications. The RNA was then treated with DNase to eliminate genomic DNA. Quality assessment of the RNA was performed using a Nanodrop 2000 spectrophotometer (Thermo Scientific, UK) to ensure the A_{260}/A_{280} ratio was within the range of 1.7 to 2.0 and the A_{260}/A_{280} was above 2:1. The RNA was then reverse-transcribed into cDNA with the RT2 First Strand kit (Qiagen, UK) according to manufacturer specifications in a TC-Plus thermal cycler (Techne, Staffordshire, UK). The resulting cDNA was then assessed using the Nanodrop to ensure purity and suitable concentration. The qPCR reaction was carried out using direct dye binding in the Eco Real-Time PCR System (Illumina, USA) and the appropriate primers (Table 1). The following cycles: 10 minutes of denaturation at 95°C,

followed by 40x cycles of 10 seconds at 95°C, 30 seconds at 60°C and 15 seconds at 72°C. All values correspond to average ± SD of 3 independent experiments with expression of each gene of interest normalized to housekeeping gene GAPDH.

4. Results

4.1. Survival of healthy and keratoconic stromal cells in gels

Stromal cells cultured in CCG perished at slower rates than cells seeded in identical amounts on flat plastic. After a month of culture in the collagen discs, the limbal, central and keratoconic cells all kept a population number above 40% of the initially seeded cells and with population numbers above 60% within the first 11 days (Fig. 12A, B and C). This contrasted with the 2D cultures where 50% remaining cell population or lower would be reached within 11 days for all cell types assayed (Fig. 6). It could therefore be said that CCG culture increased cell survival.

The addition of RA further improved the survival of stromal cells, bringing the final surviving percentage after 30 days of culture to around 80%. No difference in cell number during the first 11 days could be identified between CCG culture with and without RA. This is unlike 2D cultures where RA had an almost immediate positive effect on the cells (Fig. 9). Statistical comparison of serum-free conditions with and without RA for each cell type showed a significant difference in cell population when RA was added: enzdL with an overall p value of <0.0001, enzdC with a p value of 0.0036 and KF with a p value of 0.0113. Notably, all three cell types assayed: limbal, central and keratoconic, showed a population percentage that did not change much during the final week of culture, suggesting perhaps that a stable group of cells was established and could survive long term as was shown previously with limbal stromal cells in a 3d collagen gel (Abidin et al., 2015).

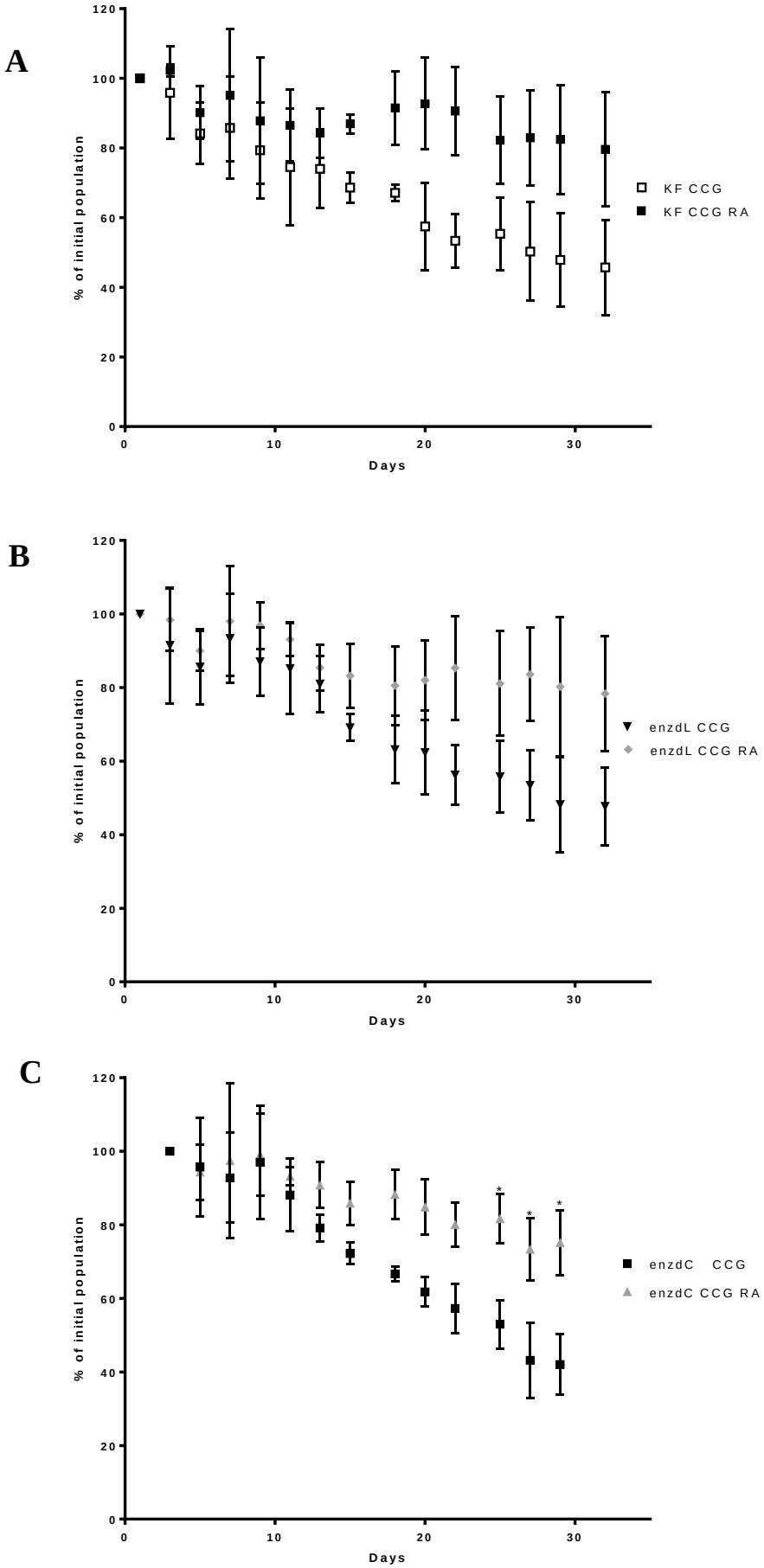

Figure 12: Survival of Keratoconic cells and enzyme digested limbal and central stromal cells in CCG with and without retinoic acid in serum- free medium as quantified by Alamar blue assay. Corrected p values (<0.05) calculated by ANOVA. Data was obtained from 3 experiments (n=3) per cell type, each with a different donor.

4.2. Gene expression of healthy and keratoconic stromal cells in gels

Multiple important keratocyte markers were assayed at the transcript level to determine whether culturing healthy stromal cells and keratoconic cells in CCGs affected gene expression. Results showed that CCG did have an effect on the expression profile of both healthy and keratoconic, with similar shifts in behaviour for both cell types. Expression of ALDH3 did increase significantly in limbal cells and in KFs, with the largest expressions of ALDH3 where observed in KF (Fig. 13N). Central cells did not show any change in ALDH3 expression following a month of culture in CCG. Keratocan gene expression followed a similar pattern with increasing expression in limbal and KF cells, with a statistically significant difference observed in the two cell types. Central cells did seem to change their Keratocan gene expression in gel culture with a significantly decreased expression (Fig. 13B). Decorin gene expression showed some significant increase in central and KF cells but the greatest increase in expression was observed in the limbal cells, which had the lowest initial expression of Decorin in flat cultures (Fig. 13A). MMP3 expression was significantly increased in all cell types, with the most pronounced expression being in the healthy cells (Fig. 13I). Lumican gene expression was increased in limbal cells following CCG culture. The opposite was observed in KF where CCG culture caused a decrease in Lumican expression (Fig. 13C). Central cells did not appear to change their expression of Lumican when cultured in gels. TIMP1 expression was significantly reduced in central and KF cells while limbal cells showed a significant increase in expression (Fig. 13J). Much like MMP3, the expression of MMP1 was significantly increased in all cell types cultured in CCG, the largest increase was noted in central cells (Fig. 13G). It should be noted however that far greater fold-increases in expression where observed in MMP3 expression. Vimentin gene expression was increased in limbal and KF with central cells experiencing a comparatively slight increase (Fig. 13D). Significant increases in αSMA expression were observed in all 3 cell types assayed, with the largest increases being in limbal and KF (Fig. 13L). RARA expression in 2D was highest in central cells, but culture in CCG caused expression to decrease significantly in these central cells until all three cell types appeared to express RARA at similar levels (Fig. 13M). Expression of both Collagen type I and V was very significantly reduced all cell types. MMP2 expression was reduced in all cell types, although only to a significant degree in limbal cells (Fig. 13H). This is the only MMP that didn’t see an increase when cultured in gels. Finally, CD34 expression was significantly reduced in all cell types following culture in CCG (Fig. 13K).

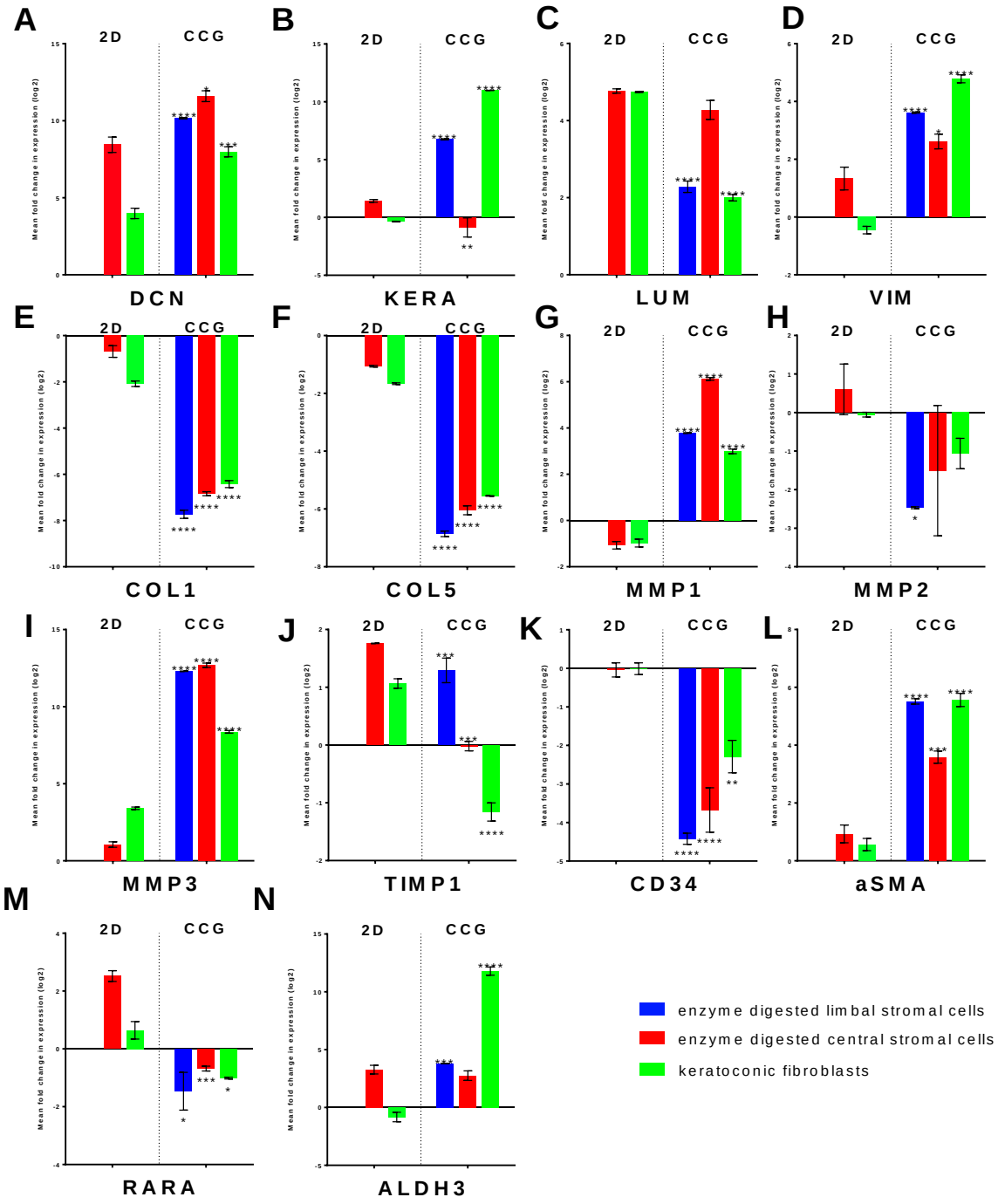

Figure 13: Fold change in gene expression for healthy limbal and central stromal cells and keratoconic fibroblasts cultured in serum-free medium on flat plastic for 11 days (left portion of graph) or within a compressed collagen gel for 30 days (CCG) (right portion of graph). Gene expression was normalized relative to control group of enzyme-digested limbal cells in serum-free medium cultured on flat plastic (left, solid blue fill). Cells assayed: enzyme digested limbal (blue solid fill), enzyme digested central cells (red solid fill) and keratoconic cells (green solid fill). Data (mean ±SD) were obtained from three independent experiments

(n = 3) and used one-way ANOVA to compare RA-supplemented culture to respective non-supplemented control (* for $p < 0.05$, ** for $p<0.005$, *** for $p<0.0005$, **** for $p<0.0001$).

4.3. Gene expression of healthy and keratoconic stromal cells in gels with retinoic acid

The addition of RA to the CCG culture of enzdL, enzdC and KF caused multiple changes in gene expression. Results showed that CCG did influence the expression profile of both healthy and keratoconic, with similar shifts in behaviour for both cell types. Expression of ALDH3 showed a large significant increase in limbal cells while KFs showed a small but significant decrease (Fig. 14N). Central cells showed a significant decrease in ALDH3 expression. Keratocan gene expression saw an increase in limbal cells but a decrease in KF while central cells showed a large increase following RA culture (Fig. 14B). Decorin and Vimentin gene expression was reduced in all cell populations upon addition of RA, mirroring the cell behaviour seen in 2D plastic cultures (Fig. 14A and D). The final proteoglycan assayed, Lumican, saw its gene expression increase for all cell types, although the largest rise was observed in limbal cells with a 40-fold increase while central cells and keratoconic cells showed 30-fold and 10-fold increases respectively (Fig. 14C). Both MMP1 and MMP3 gene expression was significantly reduced in all cell types when cultured in RA (Fig. 14G and I). MMP2 showed great variability across all repeats and no significant difference could be detected (Fig. 14H). The MMP regulator TIMP1 saw its gene expression increase in all cell types with exposure to RA (Fig. 14J). The expression of αSMA did not seem to be affected in any way for limbal and central cells but KF did show a significant decrease in the presence of RA (Fig. 14L). Expression of Collagens Type I and V was significantly increased in limbal, central and KF (Fig. 14E and F). Limbal cells showed the highest increases in both collagen types, reaching 100-fold increases. With the addition of RA, the expression of RARA did increase significantly in limbal cells and KF (Fig. 14M). Finally, CD34 expression increased significantly in limbal cell, increased in central cell, and showed no significant change in KF (Fig. 14K).

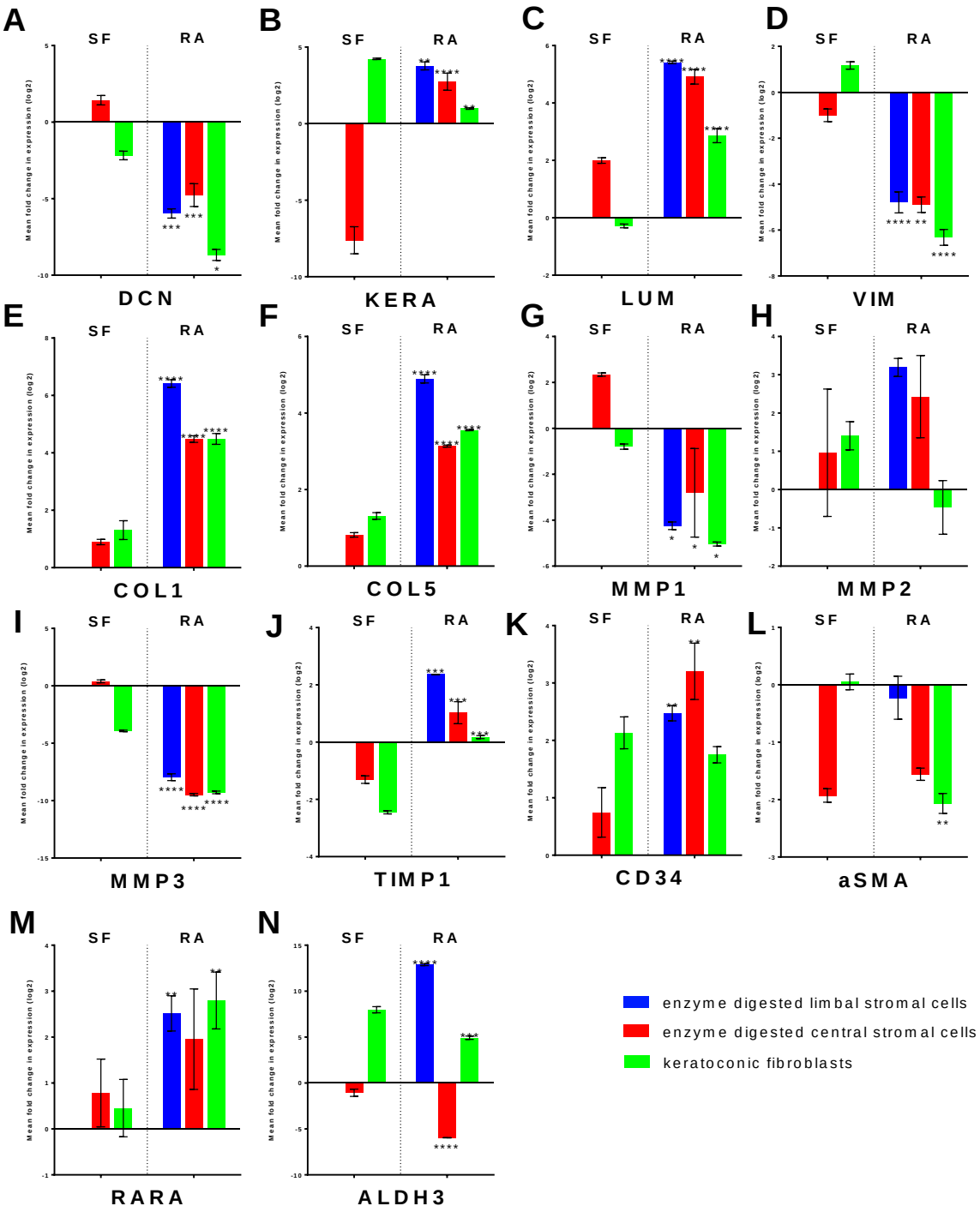

Figure 14: Fold change in gene expression for healthy limbal and central stromal cells and keratoconic fibroblasts cultured in CCG with serum-free medium either without RA (left portion of graph) or with RA (right portion of graph) for 30 days. Gene expression was normalized relative to control group of enzyme-digested limbal cells in serum-free medium cultured in CCG (left, solid blue fill). Cells assayed: enzyme digested limbal (blue solid fill), enzyme digested central cells (red solid fill) and keratoconic cells (green solid fill). Data (mean ±SD) were obtained from three independent experiments (n = 3) and used one-way

ANOVA to compare RA-supplemented culture to respective non-supplemented control (* for $p < 0.05$, ** for $p<0.005$, *** for $p<0.0005$, **** for $p<0.0001$).

4.3. Gene expression of healthy and keratoconic stromal cells in curved gels

By curving the gel, the cells are cultured in, a curved CCG (cCCG) was made. The final addition of curvature as an environmental cue to the model did have some effects on the gene expression of limbal stromal cells and keratoconic stromal cells both in the absence of RA (Fig. 15) and in the presence of RA (Fig. 16). Expression of ALDH3 was not impacted by curvature in gels with no RA (Fig. 15N). EnzdL in cCCG with RA did show a significant decrease in ALDH3 expression compared to flat CCG with RA (Fig. 16N). Keratocan gene expression was not significantly affected by curvature either with or without RA (Fig. 15B, Fig. 16B), although some increase could be seen for limbal cells without RA and for KF with RA. Larger variability in KERA expression was observed in cCCG RA. Decorin expression seemed to be reduced by curvature in both KF and enzdL, though not significantly (Fig. 15A, Fig. 16A). Vimentin expression in the absence of RA saw a large significant decrease due to curvature but only for KF, enzdL had a small increase in VIM in cCCG (Fig. 15D). The cCCG RA did caused a decrease in VIM expression for limbal cells and an increase for KF (Fig. 16D). Lumican gene expression did not seem responsive to curvature in the presence of RA but in the absence of RA, curvature did lead to an increase in LUM expression for KF (Fig. 15C). Expression of MMP3 was not significantly affected by curvature in either the presence (Fig. 16I) or absence of RA (Fig.15I). MMP1 expression was significantly reduced by CCG curvature but only in the presence of RA (Fig. 16G), this effect of curvature could not be observed in the absence of RA (Fig. 15G). This suggests that curvature had an effect on MMP1 that RA enables. MMP2 was significantly increased for both enzdL and KF in cCCG but in cCCG RA (Fig. 15H), enzdL saw a decrease while KF saw no change (Fig. 16H). This suggests that curvature influenced MMP2 that RA was then able to prevent. The last actor in the metalloproteinase-related genes assayed, TIMP1, saw its expression significantly decrease in both enzdL and KF in cCCG (Fig. 15J). In cCCG RA however, only enzdL showed a significant decrease compared to CCG RA (Fig. 16J). Curvature increased the expression of Collagen type I in enzdL but only in cCCG without RA (Fig. 15E). Expression of Collagen V was significantly increased by curvature in both enzdL and KF (Fig. 15F). In cCCG RA, neither of the collagen gene expression were affected. The expression of αSMA was reduced in KF in in the absence of RA (Fig. 15L) but increased in the presence of RA (Fig. 16L). EnzdL expression of αSMA was not affected by curvature in the absence of RA (Fig. 15L) but saw a decrease in the presence of RA (Fig. 16L). This

difference in αSMA shows that the two cell types are not identical. Expression of RARA increased in KF but only in the absence of RA (Fig. 16M). No change in was seen in RARA expression in the presence of RA (Fig. 16M). Finally, expression of CD34 increased in KF by curvature in the absence of RA (Fig. 15K) while the presence of RA lead to a decrease in enzdL's CD34 expression (Fig. 16K).

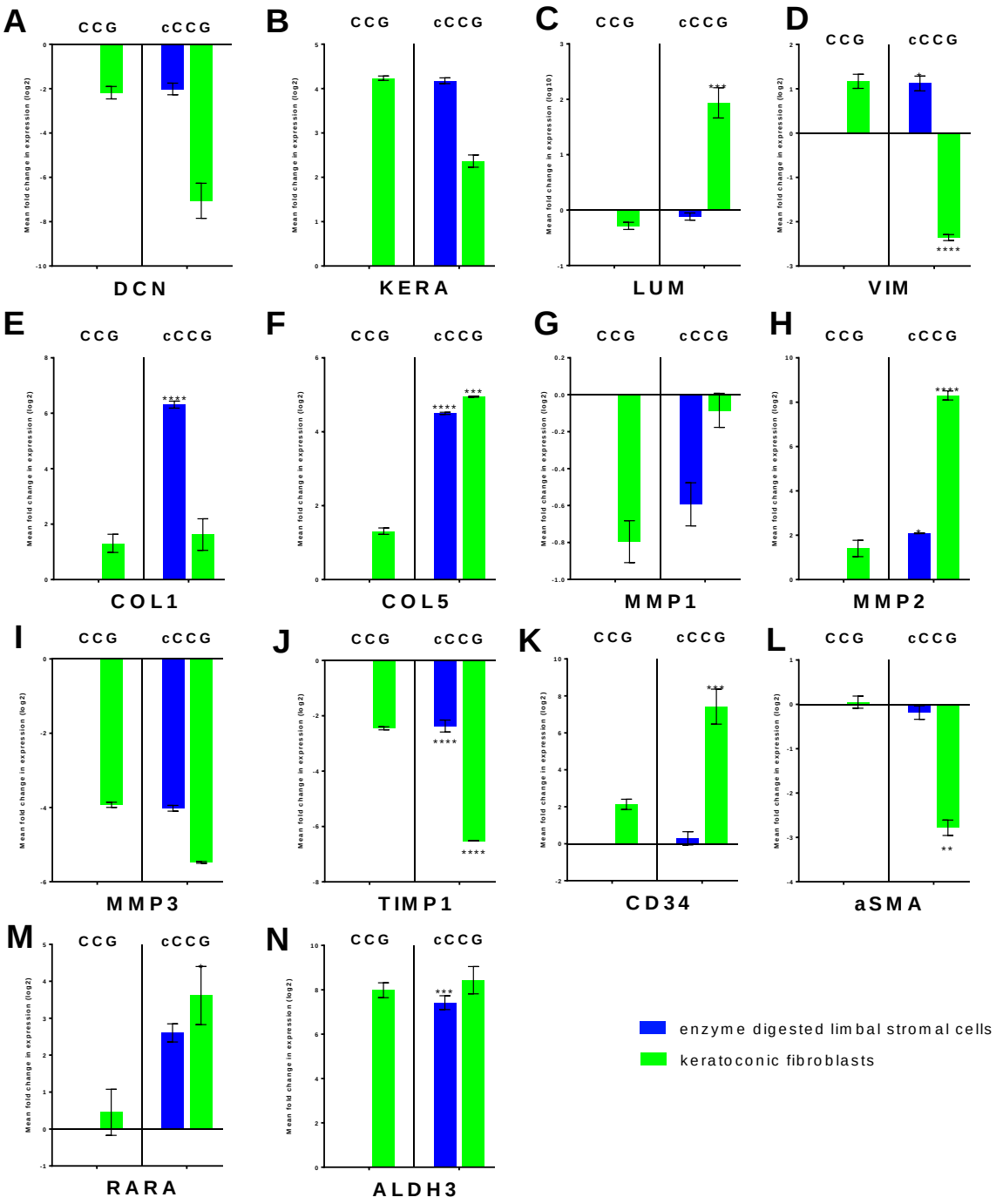

Figure 15: Fold change in gene expression for healthy limbal stromal cells and keratoconic fibroblasts cultured either in flat CCG (left portion, denoted by solid line) or in curved CCG (right portion, denoted by solid line). Each type of gel was subjected to culture without RA. Gene expression was normalized relative to control group of enzyme-digested limbal cells in serum-free medium cultured in CCG (leftmost, solid blue fill). Cells assayed: enzyme digested limbal (blue solid fill) and keratoconic cells (green solid fill). Data (mean ±SD) were obtained from three independent experiments (n = 3) and used one-way ANOVA to compare RA-supplemented culture to respective non-supplemented control (* for $p < 0.05$, ** for $p<0.005$, *** for $p<0.0005$, **** for $p<0.0001$).

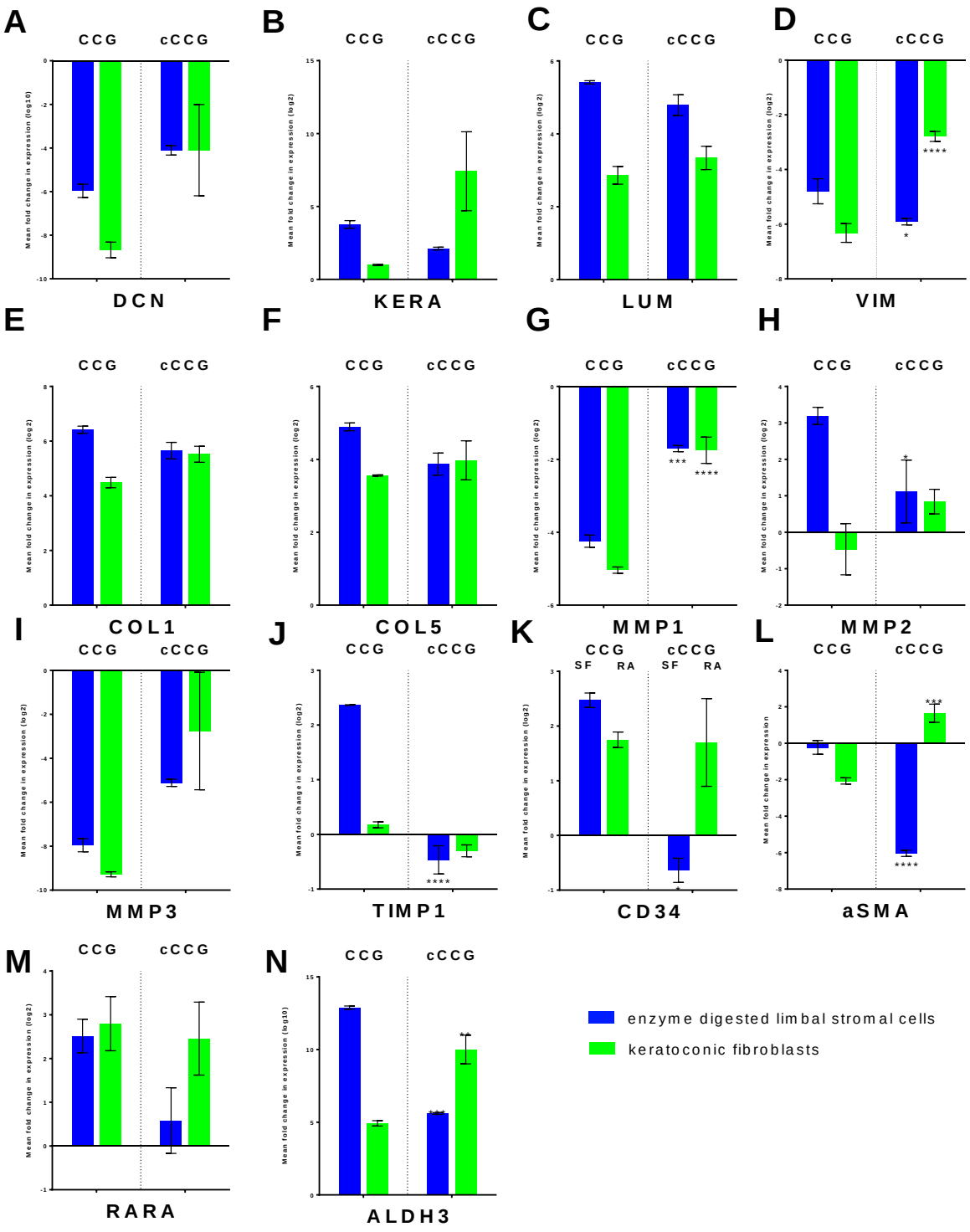

Figure 16: Fold change in gene expression for healthy limbal stromal cells and keratoconic fibroblasts cultured either in flat CCG (left portion, denoted by solid line) or in curved CCG (right portion, denoted by dotted line). Each type of gel cultured with RA. Gene expression was normalized relative to control group of enzyme-digested limbal cells in serum-free medium cultured in CCG (leftmost solid blue fill of Fig. 15). Cells assayed: enzyme digested limbal (blue solid fill) and keratoconic cells (green solid fill). Data (mean ±SD) were obtained from three independent experiments (n = 3) and used one-way ANOVA to compare RA-

supplemented culture to respective non-supplemented control (* for $p < 0.05$, ** for $p<0.005$, *** for $p<0.0005$, **** for $p<0.0001$).

5. Discussion

5.1. Comparison of 2D to CCG culture

The corneal stroma is a transparent spherical cap of highly organized collagen maintained by the stromal cells within. When constructing a tissue model, the cells, ECM and secreted factors are the three most basic quantities to consider. The cells were first approached with regards to their isolation method and what may constitute a proper healthy control. The secreted factor or the stroma were reproduced to some extent by omitting serum and adding factors such as ascorbic acid, ITS and RA. Finally, the ECM portion was approached with simple compressed discs of collagen, CCG. With its well documented compatibility with fibroblasts and similarity to the tissue of origin, collagen type I was the obvious choice for a simple culture scaffold (Sheu et al., 2001). Within these disks, the stromal cells behaved very differently than when cultured on tissue-culture plastic (TCP). Survival was the most striking change with a greater percent of the initially seeded population surviving in the serum-free medium. Previous culture on TCP showed that on average, 50% of cells would perish in the first 11 days while in CCG, none of the assayed cell population saw a drop below 60%. Even after a month of culture, no population, healthy or keratoconic, dropped below 40%. Although, there still remained a decrease in cell population, even with culture in these gels. Addition of RA to the medium further enhanced cell survival with central, limbal and keratoconic cells all retaining significantly larger populations after 30 days. In most cases, more than 80% of the initially seeded population survived. Interestingly, in reaction to the RA population growth no longer seemed occur in the CCG as it had in 2D. Instead, RA maintained a population of cells alive within the gels over the full month they were assayed. It is likely the cells could have survived even longer. This is promising as it is expected that cells in vivo are not constantly growing in number, rather they are maintaining a stable population through controlled division and apoptosis.

While a positive effect on survival is encouraging, there remained the issue of gene expression profile for the three cell types: central, limbal and keratoconic. The principal protective protein in the cornea that offsets oxidative stress, ALDH3A1, was greatly increased in both limbal and keratoconic cells, although KF did show such a large amount of variance that the increase could not be classified as significant. This is somewhat encouraging as high

production of the protein could be regarded as a corneal fibroblastic behaviour. Central cells however, did not show any change in expression of this crucial protein. The exact reason for a lack of reaction on the part of central cells is unclear although it could be hypothesized that since central cells initially expressed the highest amount of ALDH3 prior to CCG culture, the cells are already at their maximum production. In the cornea, these cells are the most vulnerable due to their location and terminal differentiation, therefore requiring the most ALDH3A1 possible. The shift in ALDH3A1 expression when cultured in CCG also further reinforces the idea of limbal healthy cells and central keratoconic cells share an identity to some degree.

As well as protecting themselves, the stromal cells now have an ECM to maintain as provided by the CCG. The production of various crosslinkers and collagens allows for an assessment of this activity. Keratocan showed more evidence of a similarity between limbal and KF cells, although this time a statistically significant difference could be observed in both cell types. Central cells did not seem to change their expression of KERA when cultured CCG, although once again the expression on KERA in flat surface culture was highest in central cells and may already be at it maximum, incapable of increased even when cultured in CCG. For central cells, this trend continues with VIM and LUM. DCN showed an increase for central cells but the variability was too great to draw statistical significance. In regard to crosslinker production (KERA, VIM, LUM and DCN), central cells seemed to outperform limbal and keratoconic cells on flat surface culture but shows little to no reaction to the new CCG environment. Limbal cells on the other hand showed great reactivity in regard to production of the four crosslinkers when cultured in CCG. Along with the previously mentioned KERA increase, LUM, VIM and, DCN all significantly increased. It appears that limbal cells have a greater capacity for change in regard to the strengthening of existing matrix. The changes in regard to environmental cues suggest a less differentiated state with room for adaptation rather than a fixed set of gene expressions, as observed so far in central cells. Keratoconic cells initially seemed to follow limbal cells by increasing KERA, VIM, and DCN expression when cultured in CCG, although the DCN increase was not significant due to large variance. However, LUM expression was found to drop in KF following CCG culture. Since these KF are diseased cells, showing a loss of expression in one of the important proteoglycans for corneal functions could be seen as encouraging in regard to model building. Although whether this is the correct kind of pathological behaviour remains to be seen. Expression of collagen type 1 and 5 dropped dramatically in the three cell types when cultured in CCG, it

stands to reason that once in ECM, the cells need not produce as much matrix to house themselves.

Continuing in the ECM maintenance functionality of these stromal cells, expression of MMP and MMP-associated TIMP1 was also affected by culture in CCG. In limbal, central and keratoconic the expression of MMP1 and MMP3 was very significantly increased, particularly MMP3. Out of the three cell types, central cells appeared to yield the largest increase in MMP1 and MMP3 expression following CCG culture. MMP2 expression seemed unaffected in central and keratoconic cells but a significant decrease was observed in limbal cells. The MMP regulator TIMP1 saw its expression decrease in both central and keratoconic stromal cells while limbal cells had a non-significant increase. Overall, all stromal cells seem to be more active in the deconstruction of ECM following culture in ECM rather than on plastic which is to be expected. In this facet of ECM maintenance, KF seem to mimic limbal cells in the production of MMP1 and MMP3 but then appear most similar to central cells in the expression of TIMP1 and MMP2. With keratoconus being a disease where the corneal stroma loses a large portion of ECM, it could have been expected that MMP expression would be highest in KF and with minimal expression of the MMP-regulator. This was not the case, although more facets of the model remain to be explored and more factors added.

In the past, it has been shown that culturing fibroblasts in a 3D environment enriches the mechanical activity of the cells (Rhee, 2009). With αSMA being one of the principal ways for cells to mechanically interact with the environment, the expression of the gene was of interest. In all three cell types, αSMA expression was increased. However, the increase was highest in keratoconic and limbal cells while central cells showed only a relatively modest 20-fold increase in expression. Once again, KF appeared to behave more like limbal cells than central cells, this time in regards to expression of a gene related to migration and contractility. Expression of RARA seemed to decrease in all three cell types to some degree but the only significant decrease was seen in central cells. There is no obvious explanation as to why culture of stromal cells in CCG would cause a reduction in the expression of a retinoic acid signalling factor. Lastly, CD34 saw a significant reduction in all three cell types assayed, although this is likely due to the difference in culture time between 2D and 3D cultures, the former lasting 11 days while the latter went on for a month.

5.2. Comparison of CCG with and without RA

Addition of RA to culture medium enhanced survival of limbal, central and keratoconic stromal cells in CCG. Along with the increase in the percentage of viable cells, RA also caused some changes in gene expression. Expression of ALDH3 was increased in limbal cells and decreased in central cells while KF did not appear affected. The reaction of all 3 kinds of stromal cells in CCG was unlike that of cells cultured on flat plastic where a large increase in ALDH3 was observed upon addition of RA. This could mean that gel culture interferes to some extent with RA signalling or, considering the ALDH3 increase due to CCG culture alone, gel culture is sufficient to drive ALDH3 expression up to a cap in the case of KF. That RA did manage to greatly increase ALDH3 expression in limbal cells suggests a greater potential for ALDH3 production in these cells, while central cells and keratoconic cells may have less potential and therefore be more vulnerable to oxidative stress. The expression profile of keratoconic cells harvested from the limbus would prove very interesting in this instance to discern if a lack of ALDH3 expression is innate to all KF cells or due to a more central identity of the KF. However, availability of such cells is scarce and collection poses some issue.

Expression of crosslinker genes changed in all cell types after CCG RA culture. VIM and DCN both saw significant drops for all cell types once RA was added to the CCG culture system. This mimics what was observed in 2D upon addition of RA as both VIM and DCN expression dropped in that instance too. LUM expression was increased in CCG by the addition of RA. This was unlike what had been observed in 2D where, upon addition of RA, LUM expression had only increased in limbal cells while decreasing in central and KF. In CCG, the largest increase was in limbal and central cells while KF cells showed only a very small increase. A larger reaction to RA in the case of LUM seems to be exclusive to healthy cells. This, taken in conjunction with the decrease of KF's LUM expression upon culture in CCG, would suggest that LUM is a gene particularly affected in the keratoconic disease pathway. A deficiency in lumican production has previously been investigated as a way of modelling keratoconus in animals, although results proved inconclusive with no definitive similarities between lumican-deficient mouse corneas and keratoconic tissue (Shao et al., 2011). Analysis of lumican at a protein level in response to RA and CCG culture would no doubt aid in further elucidating just how relevant this is to keratoconus. KERA expression was also affected with a clear healthy/keratoconic divide. In the case of KERA, limbal and central cells both showed increased expression while KF's expression decreased with the addition of RA to the CCG. This is unlike the 2D culture system where the addition of RA

prompted large increases in KERA expression for all cell types. It should be noted that when introduced to the CCG environment, KF saw the largest increase in KERA expression, and with the addition of RA both healthy cells and KF now express similar amounts of KERA. In regards to the expression of both collagen type I and V, the two genes had their expression significantly increase in all donors upon addition of RA, suggesting greater ECM production capacity in the stromal cells. Limbal cells in particular saw the largest increase in both types of collagen while the healthy central and keratoconic central cells both had a smaller increase.

Following the production and crosslinking of ECM, the degradation of ECM by MMP and associated regulators seemed to decrease as seen by the expression patterns of the stromal cells in CCG RA. When introduced to the CCG, MMP1 and MMP3 expressions both saw large increase for healthy and keratoconic cells. When RA was added to the CCG, MMP1 and MMP3 expression both decreased significantly. This was also accompanied by an increase in TIMP1 expression across all donors. While MMP2 still remained highly variable, some significantly higher expression was noted in limbal cells and central cells had some increase though not variable. Meanwhile, KF seemed to little change in MMP2 expression. In the 2D culture system, no decrease in the expression of MMPs could be seen upon addition of RA, even though past research seems conclusive that MMP1 should definitely see a reduction following RA addition (Pardo and Selman, 2005). Only in 3D culture, where the cells where stimulated to produce a larger amount of MMPs due to the surrounding ECM, could a large RA-induced change be seen in MMP expression.

RARA expression seemed to have increased in all cell types with the addition of RA, although the large variance prevents any statistical significance. The increases in RARA expression in the presence of RA do seem more pronounced in 3D than in 2D but due to the large variance it is difficult to draw a conclusion regarding the effect of CCG on the cellular reaction to RA. When introduced to CCG, all three types of cells (enzdL, enzdC and KF) showed increased αSMA expression, with central cells showing only a modest increase while limbal and KF showed a higher increase. With the addition of RA, limbal and central cell expression of αSMA did not change but KF expression of αSMA now most resembles central cells. Finally, CD34 expression increased in the two healthy cell types but no the KF, although the increase in healthy central cells was too variable to be significant. This could be interpreted as RA maintaining some degree of cell plasticity but only in healthy cells, meaning that KF may not be able to possess traits typically associated with higher CD34 expression such as progenitor localization and niche anchoring (Joseph et al., 2003).

5.3. Comparison of flat and curved CCG in the presence and absence of RA

Curvature as an environmental cue has been shown to affect cell alignment and ECM fibre alignment. While in the past there has been evidence that curvature could affect corneal stromal cell gene expression, particularly ALDH3 and key crosslinkers, it was after the stromal cells had produced aligned matrix with mechanical and chemical properties very different from the planar control (Gouveia et al., 2017). In the experiment presented here, the cells were not allowed to produce their own matrix from a curved or planar template for several months before assaying gene expression (as collagen was included from the start). Only healthy limbal cells and KF were assayed here. The effects of RA were also assayed in the new curved CCG by comparing flat versus curved with RA as well as flat versus curved without RA. Curvature seemed to have some effect on gene expression. ALDH3 expression was decreased in healthy cells in cCCG relative to the flat CCG with RA. ALDH3 expression in KF did seem to increase although the variance meant that there was no statistical significance. Loss of ALDH3 would certainly expose the cells to greater oxidative stress where they *in vivo*. Additionally, this goes against the previous observation made on limbal stromal cells grown on a curved surface, where ALDH3 expression was found to have increased (Gouveia et al., 2017). The ALDH3 expression we observed on flat surface with RA was more in line with previous data, as an increase in expression was observed relative to the no-RA control.

With regards to the crosslinkers, KERA saw an increase for healthy cells when cultured in cCCG compared to CCG, however this same increase was not noted when comparing the flat and curved gels in the presence of RA. In KF, a decrease was noted in KERA expression that once again was only seen in the absence on RA and although a much greater expression of KERA seemed to have occurred in cCCG RA, there was no statistical significance noted. DCN as well showed no difference between CCG and cCCG when RA was present but when comparing flat and curved gels in the absence of RA, both healthy and KF showed a decrease in DCN. VIM continued the pattern of RA either preventing or obscuring curvature-stimulated expression changes as only the non-RA supplemented CCG showed a difference between flat and curved. In the case of VIM, a decrease was noted for KF while an increase was seen in healthy cells. LUM bucks the trend by showing no statistically significant difference whatsoever. ECM production as measured by expression of collagen types I and V did also seem affected by curvature. In the case of collagen type 1, increased expression was only seen for healthy cells in the absence of RA. In the case of collagen type V, a large

increase in expression was seen for healthy cells and KF when the gel was curved without RA present. In cCCG RA, healthy cells did show some decrease in collagen type V expression. While previous research on gene expression of stromal cells on curved surface is limited, the past data was conclusive in showing an increase in all the crosslinkers and collagens assayed here. It is likely that short culture, encapsulating the cells rather than culturing the cells on the surface, and allowing a templated ECM to form lead to these differences.

The expression of MMPs and TIMP1 was also affect by curvature. Without RA and when the CCG was curved, decreases in MMP1, MMP3 and TIMP1 were observed in limbal cells. In KF under the same conditions similar decreases were noted in MMP3 and TIMP1 showed a marked decrease, but an increase was seen in MMP1 and MMP2. When RA was added to the cCCG, limbal cells saw an increase in MMP1 and MMP3 while still observing a reduction in TIMP1. KF in the same RA cCCG conditions only saw a reduction in MMP3. There appeared to be different reactions to curvature based on whether or not RA was present. The best example is MMP3 expression, where in the flat gels a clear anti-MMP3 effect of RA can be observed, but in curved gels the levels of MMP3 appear not to change when RA is added. MMP1 expression does show some distinct anti-MMP1 effect of RA that persists in curved, although to a lesser degree. It would seem that the curved CCG culture system rendered the stromal somewhat less sensitive to the effects of RA, whether that is an effect of curvature alone is difficult to ascertain.

As seen is almost all other culture conditions, RARA remains a very variable expressed gene. However, in the cCCG without any RA present, some increase in RA-receptor's gene expression was seen. Expression of αSMA showed change only in KF, where culture in cCCG caused a reduction, although this was not seen in cCCG RA. Finally, the improved limbal cell CD34 expression that was seen in flat CCG in the presence of RA could not be detected in curved CCG with RA. Overall, the exact effect of curvature was complex although there seemed to be a pattern of curvature seemingly desensitizing the stromal cells to RA, causing effects that were previously seen in flat gels to vanish. It remains to be seen whether curved or flat gels best allow the stromal cells to emulate the *in vivo* counterparts.

One the repeating correlation seen in this experiment was the inverse relationship between KERA and MMP1. With almost every change in culture conditions and in all cell type, a decrease in KERA would coincide with a large increase in MMP1. Starting with the shift from 2D to 3D culture, where central cells showed no increase in KERA expression yet

produced the largest increased in MMP1 expression. Then, with the addition of RA to the 3D cultures, the same central cells showed the greatest increase in KERA and the greatest decrease in MMP1. When the gels went from flat to curved gels, limbal cells showed increased KERA accompanied by decreasing MMP1. KF experiencing the same shift from flat to curved showed decreasing KERA followed by increasing MMP1. Very little research has been done concerning the absence of KERA and its effects, although one study did find that KERA expression decrease did deform the cornea without affecting the expression of other cross-linker proteins (Liu et al., 2003). Keratocan's role as a determinant of collagen fibril size and spacing is well documented, suggesting that without KERA expression fibril size would increase causing stromal swelling. The inverse was observed with the absence of KERA leading to thinner corneas (Liu et al., 2003). In the past, experiments using KERA and LUM knockouts found that while both produced animals with thinner corneas, only the LUM mutant could be suitably explained due to reduced collagen biosynthesis and lower keratocyte count (Chakravarti et al., 2000). Previous research showed that the expression of keratocan is in some way modulated by lumican, another proteoglycan of the same family (Carlson et al., 2005). However, in our experiments KERA expression seemed to behave independently of increased or decreased LUM expression. It would certainly be interesting to find out if KERA knockout models have altered expression of MMP1, to further investigate the regulatory role of KERA on MMP gene expression. It is possible that the increased MMP1 expression in the absence of KERA is to blame for the thin corneas observed in KERA mutant animals. Importantly, the KERA-MMP1 correlation did not include TIMP1, the more obvious MMP regulator, or include the other MMPs to the same degree. It could be theorized that within the cornea, RA can affect MMP1 expression specifically either via KERA or through an intermediary that governs these two genes closely.

Chapter 7: Validation of the Artificial Stromal Model

1. Abstract

Tissue engineering as a field has provided tools and techniques necessary to construct biological equivalents of tissues and systems found in living organisms. From this development of complex cell culture systems arose the field of disease modelling. This field provides the unique challenge of replicating faulty cell and tissue behaviours outside of the host environment. Having ourselves managed to culture keratoconic cells in a cornea-like set of conditions, it remains to be seen how valid this culture system is and how applicable it is to modelling use. Although healthy and keratoconic stromal cells were cultured successfully, some problems were notable. The expression of certain genes seen *in vivo* could not be recapitulated *in vitro*, particularly in the case of MMP2 and CD34. However, the combined use of retinoic acid and compressed collagen gels did seem to bring the gene expression profile of stromal cells to a state closest to that observed *in vivo*. With this in mind, the culture conditions laid out in previous chapter could be used to assemble a stromal model of keratoconus and offer a platform on which to continue developing a more complex corneal disease model.

2. Introduction

2.1. Hallmarks of keratoconus gene expression in vivo

The characteristics of keratoconus that were previously mentioned in the literature review chapter could broadly be separated into two categories: the diagnostics signs that include deformation, iron deposition and membrane breaks; and the molecular characteristics that include increased presence of inflammatory molecules or loss of ALDH3. The latter of the two categories constitutes behaviour that this model aims to replicate *in vitro*. Whether the model is capable of recapitulating the differences seen between healthy and keratoconic cells *in vivo* was used as a measure of this model's success and validity. The comparison between healthy limbal stromal cells and keratoconic stromal cells focused particularly on the gene expression of: crosslinker proteins, ALDH3A1, MMP and collagen. Each of these has been reported as dysregulated in the keratoconic cornea.

Keratocan is an abundant proteoglycan found in the corneal stroma and is responsible for collagen fibril size and spacing. The expression of keratocan is closely tied to lumican, another proteoglycan of the same family (Carlson et al., 2005). Keratocan is exclusive to the cornea and its expression is considered a marker of keratocyte function (Foster et al., 2014).

Reports state that keratocan along with other crosslinking proteoglycans such as vimentin and decorin, are all upregulated in the keratoconic stroma albeit with some molecular structural alterations (Funderburgh et al., 1998, Yam et al., 2019).

The loss of collagen is another change in the stromal environment. Whether this is due to increased enzyme activity, decrease in collagen production or shift in type of collagen produced is uncertain, although all three of these characteristics have been observed at some point in keratoconic corneas. Increased collagenase and gelatinase activity in keratoconic corneal buttons have been noted for a long time (Kao et al., 1982, Rehany et al., 1982). With further research, the implications of the inflammatory system became clearer, although the exact sequence of events is still unclear and interleukins may play either an initiating or supporting role (Balasubramanian et al., 2010). With regards to collagen production, an obvious shift is seen in the case of scar tissue, where collagen type III is more abundant that the usual collagen type I (Newsome et al., 1981). However, scars are a secondary consequence of keratoconus rather than part of the disease itself. Normally present in the healthy stroma is collagen type V, an intermediary linker and spacer for collagen type I fibrils. In keratoconus, collagen type V reportedly sees a marked decrease (Chaerkady et al., 2013).

In regards to enzyme production, increased expression of MMP genes and the activity of the produced proteins have been noted on several occasions. Accompanying this increase in proteolytic activity is a decrease in regulatory protein activity, particularly TIMP-1 (Balasubramanian et al., 2010). The collagenase MMP1 has been reported as showing increased expression (Seppala et al., 2006), targeting collagen types I and III in particular within the stroma. Stromelysin MMP3 has been reported as showing no significant difference in its keratoconic gene expression relative to a healthy control (Saghizadeh et al., 2001). Gelatinases like MMP2 have also been investigated as a culprit of matrix degradation since some native collagens like collagen type IV and V are vulnerable to the enzyme. Bowman's layer in particular would be a target due to its higher collagen type IV content and since breaks in this layer are a hallmark of keratoconus, investigating gelatinase is relevant (Collier, 2001). Previous research did find that MMP2 expression was not significantly increased and the produced enzyme was mainly found in its inactive state (Fini et al., 1992). The enzyme-regulator TIMP1 showed a decrease in expression in keratoconic corneas (Kenney et al., 2005). Interestingly, TIMP1 polymorphisms have been correlated with keratoconus incidence, meaning that while any change in expression may not reflect protein function, in this case it is a particularly applicable consideration (Saravani et al., 2017).

Nuclear retinoic acid receptors are divided in two classes: RXR and RAR, which bind together to form a heterodimer involved in the detection of retinoic acid. Mutant mice lacking the expression of either RXR or RAR showed abnormal corneal development and deformations (Kastner et al., 1994). While the gene hasn't been tied to keratoconus and its expression hasn't been extensively studied, it remains a gene of interest (Rong et al., 2017).
The activation of keratocytes into myofibroblasts is characterized by the increased expression of alpha smooth muscle actin (α SMA). The contractile myofibroblasts are essential to wound closure as they may bridge the wound gap and pull the edges together. Myofibroblasts, like other corneal stromal cells, will produce ECM crosslinkers and MMPs to remodel damaged stroma (Ebihara et al., 2007). Myofibroblasts play an essential role in wound healing of the cornea, however these differentiated cell states are also associated with pathological processes like corneal haze and scarring (Connon et al., 2003). In keratoconus, no major association with α SMA has been established although the gene itself remains an excellent marker of cell identity.
Through cataloguing these established gene expression hallmarks of keratoconus, it may be possible to judge a disease model's worth in reproducing these characteristics.

2.2. Previous keratoconus models and their validity

The strict definition of a disease model is typically: an animal or cells that will display all or some of the pathological processes that can be normally be observed in human patients. The purpose of the disease model is to aid in understanding how the disease develops and provide testing for potential treatment. In the work presented here, the model is a population of keratoconic cells that have been submitted to conditions similar to those they would be *in vivo*. When healthy cells were submitted to the same conditions, they adopted gene expression and survival behaviour similar to what may be observed *in vivo*. While this culture system seems able to model the corneal stroma, its validity in regards to modelling keratoconus remains in question.
Like almost all in vitro models, keratoconus began its *in vitro* studies as a simple monolayer of primary cells and the initial investigations with this system found that the keratoconic stromal behaved differently in culture, particularly in the production of some cross-linkers and collagens (Yue et al., 1979). Further work then aimed to reproduce features of the stromal environment in an attempt to mitigate the effects of culture on keratoconic cell behaviour (Gouveia and Connon, 2013). These features included serum-free medium and supplements like retinoic or ascorbic acid and lead to further discoveries regarding the gene expression and

protein secretion of the cells. Some work was done with non-primary cells in order to overcome the need for a reliable source of donor tissue. One example is the use of induced pluripotent stem cells (iPSC) combined with viral reprogramming to yield cells with keratoconic features (Joseph et al., 2016). How reliable this approach is with regards to reproducing the molecular and cell interactions of keratoconus is debatable, although the benefits of easy availability are obvious. For the sake of this experiment, primary cells were used as tissue was readily available and any model-building effort benefits from having components from the originally studied system. The next obvious consideration was that the cornea itself is a large piece of tissue composed of multiple layers of ECM assembled by the cells within and its properties are determinants of cell behaviour. While the construction of healthy corneal models has progressed to a point where multilayer tissues have been constructed with relative success, the keratoconic cornea has had few attempts at modelling in a 3D manner. A model of keratoconus was a constructed using cell-generated matrix to investigate the relevance of 3D culture on the modelling of keratoconus (Karamichos et al., 2012). Although the culture in question used serum medium, convincing evidence showed that a 3D culture system caused drastic changes in cell behaviour and may be more desirable in future modelling of keratoconus.

The validity of these models was assessed by how well particular characteristics of keratoconus were reproduced *in vitro* and how closely the cell environment resembled the *in vivo* conditions. Similar criteria were used to judge the validity of the model built in our experiments. Importantly, the model was compared to two ethnic groups of keratoconus patients: European Caucasians and Saudi Arabian Arabs. The different incidence of the keratoconus suggests potentially different genetic profiles for the disease. Comparing the model to two different profiles also helps in deciding the future development that may be taken in refining the model.

2.3. Aims

Having assembled a 3D culture system for healthy and keratoconic cells, it remained to be seen how well the disease behaviour and corneal environment could be replicated. To assess these criteria, qPCR of healthy cells immediately after extraction was used as a baseline to which set of culture conditions was compared. This allowed us to find the set of culture conditions that best enable the natural stromal cell expression. As a second measure, RNA-Seq was used to compare keratoconic cells grown in our model to keratoconic harvested from patients. The degrees of similarity between the two may be interpreted as a measure of the model's relative success.

3. Method

3.1. Quantitative PCR

RNA had previously been collected from healthy enzyme-digested limbal stromal cells (enzdL). This included RNA isolated directly after cell isolation (enzdL FRESH) as well as RNA isolated after culture in conditions described over the course of the previous chapters (RA, CCG, cCCG). Quality assessment of the RNA was performed using a Nanodrop 2000 spectrophotometer (Thermo Scientific, UK) to ensure the A_{260}/A_{280} ratio was within the range of 1.7 to 2.0 and the A_{260}/A_{280} was above 2:1. The RNA was then reverse-transcribed into cDNA with the RT2 First Strand kit (Qiagen, UK) according to manufacturer specifications in a TC-Plus thermal cycler (Techne, Staffordshire, UK). The resulting cDNA was then assessed using the Nanodrop to ensure purity and suitable concentration. The qPCR reaction was carried out using direct dye binding in the Eco Real-Time PCR System (Illumina, USA) and the appropriate primers (Table 1). The following cycles: 10 minutes of denaturation at 95°C, followed by 40x cycles of 10 seconds at 95°C, 30 seconds at 60°C and 15 seconds at 72°C. All values correspond to average ± SD of 3 independent experiments with expression of each gene of interest normalized to housekeeping gene GAPDH.

3.2. RNA-Seq

Three donor cell lines of keratoconic stromal cells were cultured in curved collagen gels with retinoic acid for 30 days before the RNA was extracted and quantified as previously described. Dr. Shukti Chakravarti and her group as part of an on-going collaboration then processed these 3 samples. The sequenced RNA bulk data was then returned along with data from keratoconic patients (12 middle-eastern and 3 European). The sample group of cultured cells was then compared to each of the two patient sample groups to assess model transcriptome similarity to patient transcriptome. The method used was: FastQC version 0.11.8 (and multiqc) for read quality control, Salmon version 0.14.1 for mapping to the human (hg38) transcriptome and DESeq2 bioconductor version release 3.9 for differential expression analysis. Cutadapt 2.4 was used to trim Illumina sequencing adaptors.

4. Results

4.1. Quantitative PCR

The purpose of this comparison was to identify which set of culture conditions could best reproduce the gene expression seen in the freshly extracted cells. This was used as a measure of how well our environmental conditions are stimulating cell *in vitro* to behave like the *in vivo* source population. Results showed that no one set of culture conditions could force the cells to behave like the freshly extracted baseline. However, some conditions did come closer. CCG RA in particular caused the stromal cell's expression of 11 out of 14 assayed genes to not be statistically different from the fresh stromal cells. Limbal stromal cells cultured in flat compressed collagen gels and fed with serum-free medium supplemented with retinoic acid behave mostly like the same cells in their native environment. There were some genes whose expression could not be returned to *in vivo* levels: CD34, MMP2 and KERA. In the case of CD34 and MMP2 in particular, the levels plummeted and never recovered no matter the culture conditions (Figure 16). KERA expression did show varying degrees of recovery with CCG RA coming the closest to the original expression levels, although the difference remained significant. In almost every culture condition, retinoic acid had a positive effect on the gene expression of the limbal stromal cells. Comparing SF and SFRA as well as CCG and CCG RA, we can see that the number of genes expressed significantly differently decreases, from 7 to 5 in SF and 7 to 3 in CCG (Table 2). Retinoic acid certainly seems to be a most effective supplement with 3D culture further empowering the effect.

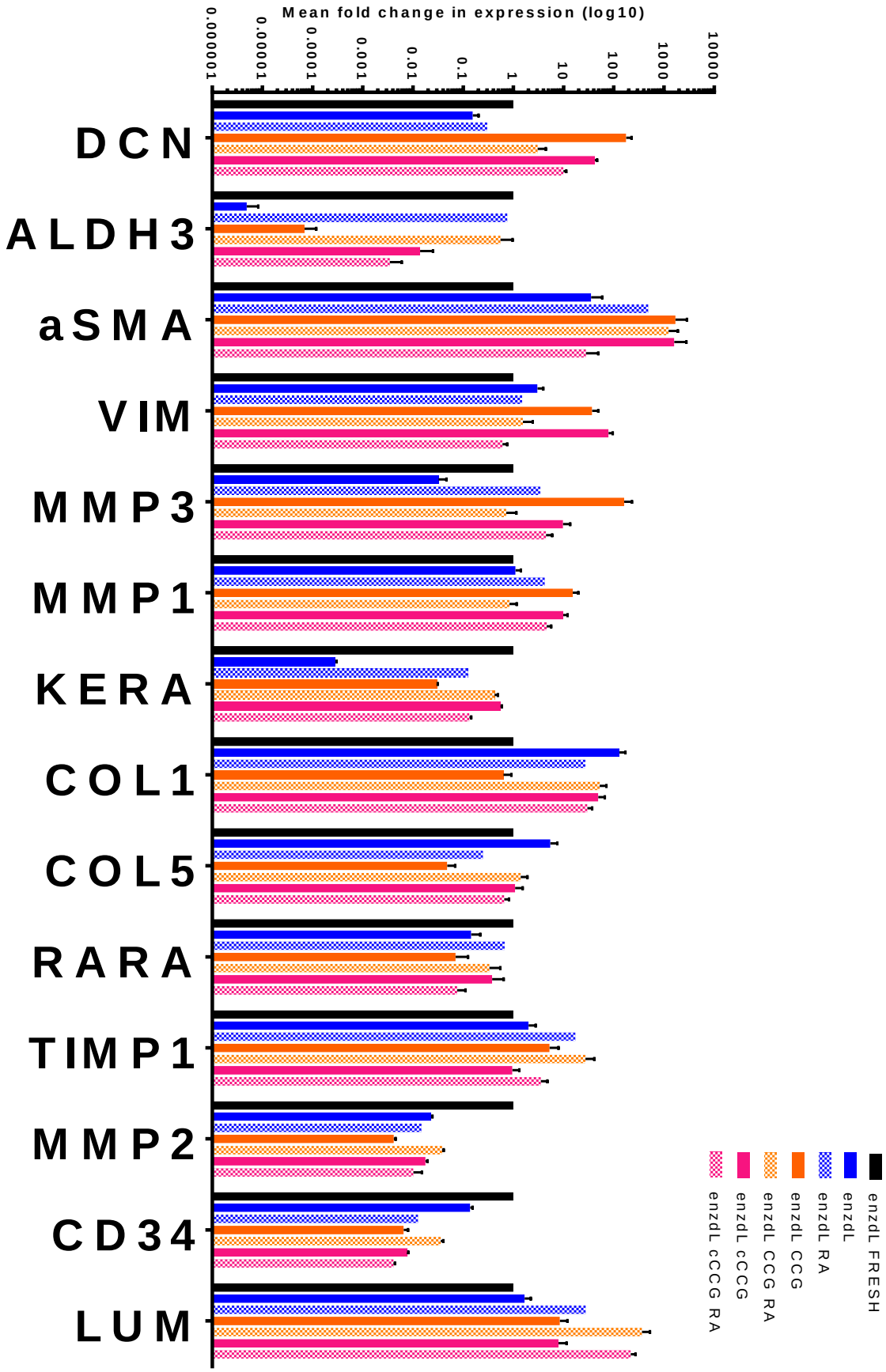

Figure 17: Gene expression of enzyme-digested healthy limbal stromal cells in various culture conditions relative to freshly extracted limbal stromal cells. The model conditions are: SF = serum-free medium only, CCG = compressed collagen gel, cCCG = curved CCG. RA indicates the presence of retinoic acid in the culture medium.

	SF	SF RA	CCG	CCG RA	cCCG	cCCG RA
DCN	0.003	0.015	0.070	0.281	0.011	0.022
ALDH3A1	< 0.0001	0.785	< 0.0001	0.387	< 0.0001	< 0.0001
aSMA	0.277	0.295	0.285	0.200	0.311	0.326
VIM	0.160	0.509	0.093	0.599	0.043	0.116
MMP3	< 0.0001	0.480	0.145	0.576	0.142	0.142
MMP1	0.777	0.430	0.085	0.662	0.053	0.081
KERA	< 0.0001	< 0.0001	< 0.0001	0.013	0.007	< 0.0001
COL1	0.091	0.138	0.315	0.107	0.109	0.057
COL5	0.160	0.017	< 0.0001	0.521	0.871	0.167
RARA	0.008	0.464	0.003	0.089	0.141	0.001
TIMP1	0.319	0.117	0.247	0.196	0.908	0.181
MMP2	< 0.0001	< 0.0001	< 0.0001	< 0.0001	< 0.0001	< 0.0001
CD34	< 0.0001	< 0.0001	< 0.0001	< 0.0001	< 0.0001	< 0.0001
LUM	0.344	0.093	0.167	0.151	0.192	0.053

Table 2: Results of multiple t-tests comparing the freshly isolated limbal stromal cells to the cells cultured in the various model conditions (SF = serum-free medium only, CCG = compressed collagen gel, cCCG = curved CCG) RA indicates the presence of retinoic acid in the culture medium. Hexes highlighted in yellow denote a gene expression statistically different from fresh cells as $p < 0.05$.

4.2. RNA-Seq

Initially principal component analysis (PCA) was used to identify general differences in transcription profile (Fig. 17). As was expected, cells from similar patient groups and cells cultures in the model each formed their own cluster and it is clear that the model shows some differences from both patient samples.

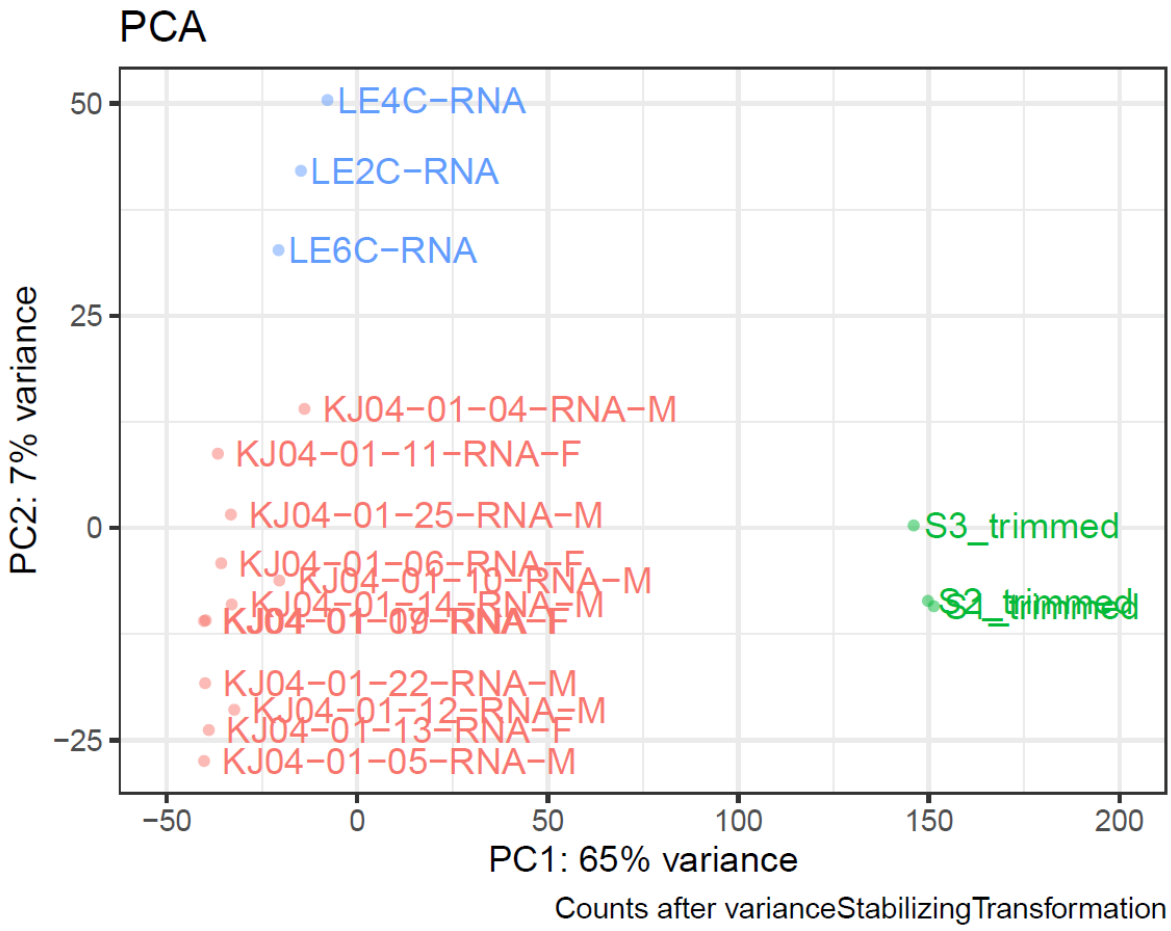

Figure 18: Principal component analysis showing transcriptional variance among the two patient groups and the model, with the model being the most different. European Caucasian keratoconus patients in blue, Saudi Arabian keratoconus patients in red, model samples in green.

Analysis showed that out of the 41256 genes expressed in the both the European patients and model samples, 15446 genes were expressed significantly differently than in the model (Fig. 18B and 18D). Among those differently expressed genes, 6511 were reduced while 8935 were increased. Comparing the Saudi patients and models samples showed 41241 genes expressed in both with 17498 genes expressed differently than in the model (Fig. 18A and 18C). Among those differently expressed genes, 7420 were reduced while 10078 were increased. In both cases, a greater variety of gene seem to be highly expressed in the patients than in the model.

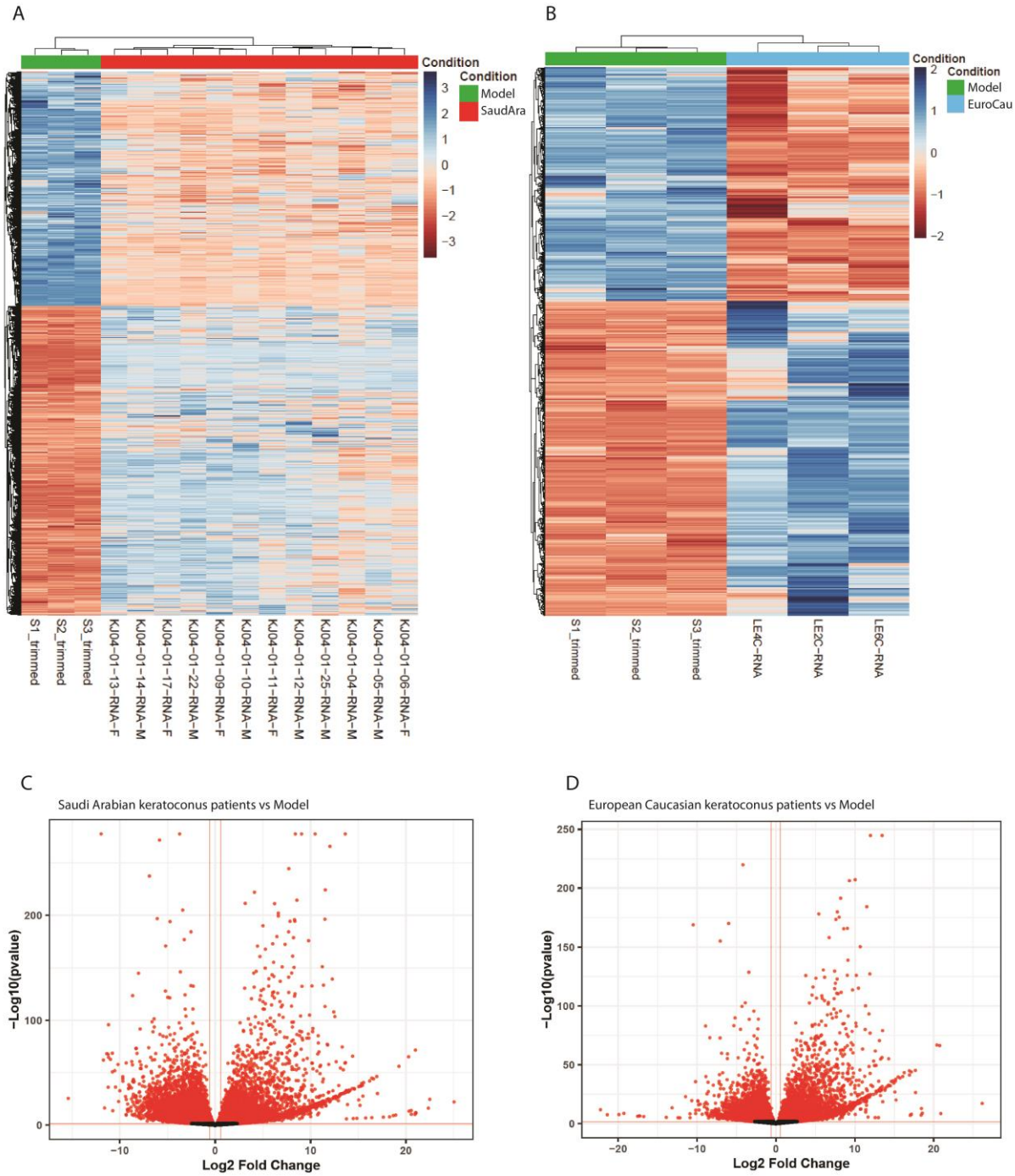

Figure 19: Heat map of all significantly enriched (blue) and depleted (red) genes for: (A) Saudi Arabian patient samples (red) vs model (green) and (B) European Caucasian patient samples (blue) vs model (green). Volcano plots DESeq2 analysis of: (C) Saudi Arabian patient samples vs Model samples and (D) European Caucasian patient samples vs Model samples.

Having deduced that the model's keratoconic cells are overall very different from the patient's keratoconic cells and that fewer genes are highly expressed in the models, specific genes of interest can now be identified for further investigation.

	European Caucasian vs Model		Saudi Arabian vs Model	
Gene	**p value**	**log2 Fold Change**	**p value**	**log2 Fold Change**
DCN	0.044927125	-1.178472402	3.29E-08	-3.496993351
ALDH3A1	0	13.46295866	0	13.63122549
aSMA	1.59E-30	-7.023091821	4.69E-41	-6.525173326
VIM	0.006896053	-1.868566265	6.44E-08	-3.694583534
MMP3	0.406381146	-0.582736576	0.004436869	-3.028269
MMP1	0.001424595	-4.092874712	4.52E-10	-8.5558165
KERA	0.390831194	-0.477554619	0.00276404	-1.889882
COL1 α2 chain	5.04E-06	-6.996375	1.52E-05	-5.03760894
COL5 α3 chain	2.40E-13	-6.286702246	1.89E-25	2.943493325
RARA	0.00176206	-0.831695125	5.21E-13	-1.602180527
TIMP1	5.65E-56	-6.154045006	2.84E-94	-6.385010565
MMP2	6.53E-08	-7.730155267	4.61E-08	-6.417490231
CD34	0.050206499	1.203552768	0.9851764	-0.008425096
LUM	1.13E-05	-3.916611417	2.27E-09	-4.501190344

Table 3: Fold change and associated p value for genes of interest as gathered by RNA-Seq comparing model samples and each of the two patient groups. Non-significant p values (>0.05) are highlighted.

The genes initially investigated in qPCR expression analysis were also investigated in RNA-Seq (Table 3). Caucasian patients expressed similar levels of KERA, MMP3 and CD34 to what was seen in models. In Arabic patients, only CD34 was expressed at similar levels to the model. ALDH3A1 in particular showed much greater expression in the patient groups than in the model. Genes that are commonly associated with matrix degradation like MMP1, MMP2 and MMP3 were less expressed in the patient groups, with the exception of MMP3 in Caucasian patients. While the patient groups seemed to have generally similar correlations relative to the model, some genes had an increasing fold change compared one patient group and a decreasing fold change compared to the other patient group. Collagen type V for example was reduced relative to the model in Caucasians but increased in Saudi Arabians.

log2 Fold Change	p value	Gene name	Gene description
-19.88976747	1.93E-08	RXRB	retinoid X receptor beta
-8.690919235	3.28E-08	RARRES2	retinoic acid receptor responder 2
-10.19005893	2.13E-36	ACTG2	actin, gamma 2, smooth muscle, enteric
-9.798855765	1.02E-16	CRYGN	crystallin gamma N
12.9455653	1.35E-28	CRYBG2	crystallin beta-gamma domain containing 2
25.03310458	7.52E-23	HSPA1B	heat shock protein family A member 1B

Table 4: Selection of European Caucasian patient genes that showed particularly large fold changes relative to the model.

log2 Fold Change	p value	Gene name	Gene description
-9.340588868	1.26E-10	RXRB	retinoid X receptor beta
-9.692303314	5.29E-45	CRYGN	crystallin gamma N
13.04666632	9.61E-30	CRYBG2	crystallin beta-gamma domain containing 2
26.14215665	6.64E-18	HSPA1B	heat shock protein family A member 1B

Table 5: Selection of Saudi Arabian patient genes that showed particularly large fold changes relative to the model.

As RNA-Seq allows for the identification of a very large number of transcribed genes, it was possible to look through the significantly different results for interesting genes where expression showed large fold changes. These genes are the outliers particularly visible in Figure 18C and 18D. When initially surveying the data, large changes could be seen in numerous keratin genes relative to the model. This suggests that the patient sample contained epithelial cells, as epithelium the main producer of this particular protein and stromal cells produce relatively little keratin. Two crystallins were found to be expressed very differently in the model relative to the patient samples: crystallin gamma N and a member of the crystallin beta-gamma family, with the former being more expressed in the model while the latter is more expressed in the patient samples. HSPA1B, a member of the HSP70 family of chaperone proteins also showed greater expression in patients than in the model. Retinoic acid associated proteins had their gene expression show up as lower in the patients than in the model. Finally, another smooth muscle actin, ACTG2 was shown to be expressed more in the model.

5. Discussion

By using freshly extracted limbal stromal cells as a baseline and comparing the gene expression of the same limbal cells cultured in various conditions we have found what set of conditions cause cells to behave most like the *in vivo* counterparts. The most obvious weaknesses of this validation method are: 1) that this method involved healthy and not

keratoconic cells; and 2) that all we have shown is that CCG RA as a culture condition can stimulate healthy behaviour from healthy limbal stromal cells. As the aim of our work was to design a disease model, healthy behaviour is not necessarily desirable and the same CCG RA conditions may simply rescue the keratoconic behaviour of the diseased stromal cells. This initial analysis of culture conditions did show that CCG RA would be the best candidate model system for further refinement and development into a more complete model of the healthy stroma, perhaps culminating into a corneal model. The most obvious next step would be the 3 genes that could not be expressed to their original levels: KERA, MMP2 and CD34. The exact reasons why these gene expression levels fell are somewhat unclear. In the case of CD34, it has previously been observed that culture in serum medium led to a loss of CD34 expression that could not be recovered (Perrella et al., 2007). It seems likely that the initial bulking phase in serum medium to produce large numbers of cells led to an irreversible loss of CD34 expression. Avoiding serum culture seems difficult, as large numbers of cells are needed for the construction of models, be it disease model or healthy tissue model.

An important consideration in regards to the qPCR approach to model validation presented here is that CCG RA was only confirmed as a potential model of the healthy stroma, not the keratoconic stroma. It may very well be that if fresh keratoconic cells were compared to keratoconic cells cultured in this model, the two could be completely different. The model could be forcing healthy behaviour from the stromal cells cultured within. It is possible for example that the RA concentration in keratoconic corneas is somehow altered, leading to or supporting the disease. The concentration of RA used here may be rescuing the keratoconic behaviour. RA concentration in particular is mentioned as, to the authors knowledge, it has never been investigated in keratoconic corneas. The acquisition of fresh keratoconic cells to form a gene expression baseline would be the most obvious next step if qPCR were to continue being used as a model validation method.

RNA-Seq is a powerful technique used to identify gene expression across the large range and build a transcriptomic identity of cells or tissues. In this instance, we used RNA-Seq to identify differences in gene expression between our model and two ethnically distinct groups of keratoconus patients. This was done in order to assess the validity of the model constructed as well as identify particular target genes that may need to be pursued further as design of this model continues. PCA initially showed that the model's transcription profile did not resemble either of the patient groups. Also, as predicted, there was some difference between the two patient groups, however this remains to be further explored in future work.

While the keratoconic model showed overall little similarity with either patient group, narrowing gene expression profile down to the 14 genes previously assayed in our qPCR analysis showed that the European Caucasian group was most similar, or rather "least different", with three genes expression appearing similar in both model and patients.

Keratin presence has been documented in the stroma (Xuan et al., 2016) although the high level of multiple keratin types (keratin types 24, 6, 3, 14, 12 and 5) suggests that the epithelia's gene expression was also part of the analysis. If that is the case, it could mean that the comparison between model and patient sample is not ideal, as the model does not yet integrate the epithelium in culture. Future work may aim to redo the validation after eliminating epithelial gene expression or add epithelial cells to the model. The challenge of obtaining keratoconic epithelial cells and culturing these for any significant period of time remains to be tackled.

Some crystallins were found to be more expressed in the model system, particularly crystallin gamma N and crystalline (CRYGN) beta-gamma domain containing 2 (CRYBG2). Crystallins are an important family of proteins for corneal and lens function in humans and vertebrates in general. However, crystallin gamma N is an oddity in primates and humans, it simply isn't expressed due a highly conserved stop codon mutation that sometimes leads to a longer, non-functional transcript. The exact reason why a large fold change occurred suggesting the model expressed a protein that likely doesn't occur in human cornea is unclear and somewhat concerning, considering that building a model requires the cells to behave at least like human cells. The second crystallin of interest was CRYBG2, a member of the crystallin beta-gamma family with no single clear functional role. The more well documented member of this family, like gamma-S and beta-S crystallins, seem to be involved in actin binding within the lens (Quax-Jeuken et al., 1985, Fan et al., 2012). Similar to chaperone proteins, this specific family of crystallins seems to be shepherding larger oligomers to prevent aggregation (Wistow, 2012). A similarly functioning gene was also found to be lacking in the model and more present in the patients, HSPA1B. HSPA1B codes for a chaperone protein and a member of the Hsp70 family, a highly conserved ubiquitous group of molecular chaperones (Radons, 2016). HSPA1B, like most heat shock proteins, expression is well documented as being stress inducible and having increased expression during immune activity (Lindquist and Craig, 1988). The lack of chaperone protein gene expression in our model could indicate a lack of stress. The cells were harvested from diseased tissue and cultivated in optimal conditions, similar to what may be found in a healthy cornea, as

exemplified by the qPCR comparison of cultured healthy cells and fresh healthy cells. It may be that reintroducing as element of stress, potentially immune or inflammatory, could recapitulate more keratoconic gene expression *in vitro*. Experiments utilizing stress-modulation have already shown some success in reproducing keratoconus-like transcription profiles (Soiberman et al., 2019).

Throughout the gene expression analysis of keratoconic cells with qPCR, alpha smooth muscle actin or αSMA was repeatedly used as a marker of myofibroblastic differentiation. A particularly large rise was seen when first culturing keratoconic cells in gels and comparison to patients showed a decisive increase in αSMA expression in the model. ACTG2 is another smooth muscle actin that had apparently increased due to model culture, the cells definitely appear to be more contractile and likely more myofibroblastic. This differentiation could be considered a target for future development of the model.

A final remarkable set of genes that saw great difference in comparing patient and model were those associated with retinoic acid, particularly RXRB and to a lesser extent RARRES2. RXRB is a nuclear retinoic acid receptor that dimerizes with other retinoic acid receptors, such as the previously mentioned RARA. RXRB is the most abundantly expressed of the six retinoic acid receptors in the cornea and is the only one that doesn't show dynamic expression patterns (Mori et al., 2001). However, its absence seems to have no effect, as null mutant animals do not exhibit abnormal eyes (Kastner et al., 1996). The significance of increased RXRB expression in the model system is difficult to interpret, as while absence of RXRB has been investigated, excess has not. Taken in its entirety, the RNA-Seq validation provided some sobering insight into how much remains to be done in order to build an ideal model while also indicating new avenues of investigation for future experiments. The model may yet be developed into a better reflection of the patient eye through epithelium integration and controlled stress induction among other techniques.

Chapter 8: Conclusions and Future Directions

1. Conclusions

In this thesis we have assembled a culture system comprising of compressed collagen gels and serum-free medium supplemented with retinoic acid to culture primary keratoconic stromal cells for the purpose of disease modelling.

Initially we investigated the effects of extraction method and location on the behaviour of the extracted population. We found that central and limbal cells differ in their survival and gene expression in all culture conditions, even after bulking in serum. We also found that while keratoconic cells were extracted from the central button via explant migration, they show very little similarity to healthy cells extracted from the same location with the same method. Instead, keratoconic cells most resembled the limbal cells extracted via enzyme digestion. This led to an initial theory that keratoconic cells were to some extent "displaced" limbal cells that may not have differentiated into the more function-orientated central cell identity. Further comparison between the limbal and keratoconic cells did show that there were some still some differences between the two cell types and that keratoconic cell possessed their own identity, at least as presented by analysis of gene expression. The differences observed among the six distinct populations of stromal cells we isolated constitute an interesting consideration for any future work utilising primary stromal cells. The variety in behaviour, survival and gene expression, shows that the data derived from cell extracted by enzyme digestion may not be easily compared to data derived from cells that were explant migrated. Considering that the differences seen here were in tissue from the same donor (center and limbus from the same cornea, explant migration and enzyme digestion from the left and right corneas), using different donors and different extraction methods could no doubt yield greatly different cell identities. Establishing the effects of cell extraction method and location would aid future analysis of the work done on stromal cells and even build towards a standardisation effort in the techniques surrounding primary stromal cell extraction.

Following the extraction of the stromal cells, we sought to maintain a large population alive *in vitro*, as a first step towards model construction. Retinoic acid (RA) proved entirely effective in that pursuit and even lead to proliferation of stromal cells in serum-free conditions. RA seemed to affect the expression of ALDH3A1 the most, with very significant increases in expression being seen in all cell types upon addition of RA.

One of the first model requirements decided in the planning phase was that the culture system would be 3D to emulate the stromal tissue. This was achieved using one of the most thoroughly documented biomaterials: collagen. By compressing the collagen gel, we obtained a thin, semi-transparent disc reminiscent of the corneal stroma. The cells within behaved very differently than when cultured on flat plastic. Increases were seen in the expression of genes coding for digestive enzymes and crosslinkers, suggesting that cells were now remodelling the surrounding matrix. Also, of interest is that the toxicity threshold of retinoic acid seemed to change with 3D culture. This seems relevant particularly in future experimental planning and understanding previous work that compared 2D and 3D systems. Indeed, if the sensitivity of stromal cells could change for retinoic acid, what other supplement could be having a different effect in 3D?

Analysis of the gene expression profiles of healthy limbal cells revealed that compressed collagen gels and retinoic acid provided an environment that best simulated natural stromal cells behaviour in serum-free conditions. To then further refine the model, curvature was suggested as an additional environmental cue. Curving gels prove to have little beneficial effect in modelling the healthy cornea, as gene expression patterns seemed distant from the baseline control. It would seem that flat gels performed better that curved gels, although it is difficult to discern the exact mechanics underlying this difference in response.

The inverse relationship observed in KERA and MMP, where KERA increase while MMP1 drops, was also noteworthy. The absence of KERA results in deformation of the cornea but without impacting the expression of other crosslinkers and collagens. This is unlike LUM absence, which did reduce collagen expression. KERA absence must have deformed the cornea via another mechanism, potentially MMP1. MMP1 appears suspect due to our observation that with every KERA expression increase, MMP1 expression decreases. Further investigation into the relationship between these two genes and their expressed proteins could prove fruitful in elucidating the degradative regulation of the cornea.

The work presented here is supported a small number of samples (3 samples of keratoconic tissue and 3 samples of 3 healthy tissue), this means that any variations across donors would greatly affect results. The healthy samples were also all female and with an average age of 75; while the keratoconic sample age and sex were unknown, based on demographic data they were likely males in around the age of 30. It is very possible that differences seen between the two groups (healthy and keratoconic) were entirely due to age, sex, or a combination of both.

While some effort was made to support differences seen with literature, future experiments should aim to collect healthy tissue from young donors of both sexes and, if possible, from multiple ethnicities.

It is known and documented that the corneal stroma changes with age. Increases in haziness and density are usually observed clinically as patients age, even in healthy individuals (Stocker & Moore, 1975; Weale, 1963). Within the stromal matrix, the collagen fibrils also change with age showing dysregulation in spacing (Kanai & Kaufman, 1973). Interfibrillar spacing often decreased with age, accompanied by increased collagen glycation and greater presence of glycation end-products (Malik et al., 1992). Interestingly these glycation changes would contribute to a stiffer tissue and are posited to be the main reasons why keratoconus does not progress in older patients. This means that differences observed here between a likely young keratoconic donor group and an aged healthy control group may be due to aging, particularly with regards to interfibrillar spacing-related gene like collagen type V.

The final test of the model with RNA-Seq by comparing the cultured keratoconic cells to real samples harvested from two patient groups revealed that the model differs greatly from the patient tissue. While it is possible that patient samples had epithelial tissue adding an extra dimension to the complex transcriptome, the evident difference in stromal cell specific genes confirm the model is far from perfect. Further engagement of a keratoconic cell identity could no doubt still be achieved *in vitro* thought the use of environmental conditions such as stress, epithelial cells, low-glucose or even a shaped mould.

The construction of a stromal model and its subsequent troubleshooting has allowed us to identify specific gene expression patterns that were then used to assess a model of keratoconus. The data presented raised several questions regarding the mechanism involved in cell maintenance *in vitro* and the different cell populations *in vivo*. The study of stromal cell extraction method and location presented here would certainly be of great use to the entire field of corneal research during experimental planning. Extracting and culturing the right cell for an experiment is important and the basic characterisation shown here supports this importance regarding stromal cells. Concerning the construction of keratoconus models, the work done here sets new parameters of success by identifying particular targets in the form of gene expressions.

2. Future directions

Early in the work on isolation of stromal cells from the cornea it was found that keratoconic cells consistently behaved like enzyme digested limbal cells. This was particularly obvious in the case of survival and the expression of a few genes. The nature of this similarity could not be fully explored here and remains a tantalizing comparison. If the disease is partly due to relocation or poor differentiation of limbal cells in the corneal centre, this could have significant implications in future treatment design. For now, it remains an interesting observation.

As with all model designing experiment, the obvious next step is the addition of more signals or traits found in the original disease system into the model in order to best replicate the disease. In the case of a corneal model, adding the two missing cell populations, epithelial and endothelial cells, could prove difficult yet result in a more realistic model of the cornea as a whole. Another obvious feature to change is the glucose concentration of the medium. Previous work did show that lower glucose concentrations closer to what is observed in the stroma can enhance cell survival and expression of CD34, a particular marker we could not express at *in vivo* levels in our model (Foster et al., 2015). Greater and more varied characterization efforts of the model throughout these design phases would be of great help in discerning what each condition is causing in the cells. Proteomics in particular would be of interest, as the transcriptomic data presented in this work could prove useful in comparing translation and transcription. While a greater number of patient tissue samples would be obviously desirable, a greater diversity in ethnic sources and sex effects would be of value. This is because some previous research has found evidence of sex affecting gene expression in the keratoconic cornea (You et al., 2018). As for ethnicity, specific groups have been determined to be more at risk than others and may even develop conditions associated with keratoconus (Georgiou et al., 2004). Since the goal of this model is partly to build greater understanding of the disease, as many samples as possible should collected from diverse sources. The extraction techniques, assays, data and observations exposed here would no doubt be of use in the future design of an even better model of keratoconus or the corneal stroma.

References

ABIDIN, F. Z., GOUVEIA, R. M. & CONNON, C. J. 2015. Application of retinoic acid improves form and function of tissue engineered corneal construct. *Organogenesis,* 11**,** 122-36.

ADAMIS, A. P., FILATOV, V., TRIPATHI, B. J. & TRIPATHI, R. C. 1993. Fuchs Endothelial Dystrophy of the Cornea. *Survey of Ophthalmology,* 38**,** 149-168.

AMENTO, E. P. & BECK, L. S. 1991. TGF-beta and wound healing. *Ciba Found Symp,* 157**,** 115-23; discussion 123-9.

ANDRADE, F. E. C., COVRE, J. L., RAMOS, L., HAZARBASSANOV, R. M., SANTOS, M. S. D., CAMPOS, M., GOMES, J. A. P. & GIL, C. D. 2018. Evaluation of galectin-1 and galectin-3 as prospective biomarkers in keratoconus. *Br J Ophthalmol*.

ARNAL, E., PERIS-MARTINEZ, C., MENEZO, J. L., JOHNSEN-SORIANO, S. & ROMERO, F. J. 2011. Oxidative stress in keratoconus? *Invest Ophthalmol Vis Sci,* 52**,** 8592-7.

ASSIRI, A. A., YOUSUF, B. I., QUANTOCK, A. J. & MURPHY, P. J. 2005. Incidence and severity of keratoconus in Asir province, Saudi Arabia. *Br J Ophthalmol,* 89**,** 1403-6.

ATANASSOV, C. L., SEILER, N. & REBEL, G. 1998. Reduction of ammonia formation in cell cultures by L-alanyl-L-glutamine requires optimization of the dipeptide concentration. *Journal of Biotechnology,* 62**,** 159-162.

BALASUBRAMANIAN, S. A., PYE, D. C. & WILLCOX, M. D. 2010. Are proteinases the reason for keratoconus? *Curr Eye Res,* 35**,** 185-91.

BALASUBRAMANIAN, S. A., PYE, D. C. & WILLCOX, M. D. 2013. Effects of eye rubbing on the levels of protease, protease activity and cytokines in tears: relevance in keratoconus. *Clin Exp Optom,* 96**,** 214-8.

BARNES, D. & SATO, G. 1980. Methods for growth of cultured cells in serum-free medium. *Anal Biochem,* 102**,** 255-70.

BEALES, M. P., FUNDERBURGH, J. L., JESTER, J. V. & HASSELL, J. R. 1999. Proteoglycan synthesis by bovine keratocytes and corneal fibroblasts: maintenance of the keratocyte phenotype in culture. *Invest Ophthalmol Vis Sci,* 40**,** 1658-63.

BIRK, D. E. 2001. Type V collagen: heterotypic type I/V collagen interactions in the regulation of fibril assembly. *Micron,* 32**,** 223-37.

BOOTE, C., KAMMA-LORGER, C. S., HAYES, S., HARRIS, J., BURGHAMMER, M., HILLER, J., TERRILL, N. J. & MEEK, K. M. 2011. Quantification of collagen organization in the peripheral human cornea at micron-scale resolution. *Biophys J,* 101**,** 33-42.

BRANCH, M. J., HASHMANI, K., DHILLON, P., JONES, D. R., DUA, H. S. & HOPKINSON, A. 2012. Mesenchymal stem cells in the human corneal limbal stroma. *Invest Ophthalmol Vis Sci,* 53**,** 5109-16.

BROWN, R. A., WISEMAN, M., CHUO, C. B., CHEEMA, U. & NAZHAT, S. N. 2005. Ultrarapid engineering of biomimetic materials and tissues: Fabrication of nano- and microstructures by plastic compression. *Advanced Functional Materials,* 15**,** 1762-1770.

BUILLES, N., BECHETOILLE, N., JUSTIN, V., DUCERF, A., AUXENFANS, C., BURILLON, C., SERGENT, M. & DAMOUR, O. 2006. Development of an optimised culture medium for keratocytes in monolayer. *Biomed Mater Eng,* 16**,** S95-S104.

BUREAU, J., FABRE, E. J., HECQUET, C., POULIQUEN, Y. & LORANS, G. 1993. Modification of prostaglandin E2 and collagen synthesis in keratoconus fibroblasts, associated with an increase of interleukin 1 alpha receptor number. *C R Acad Sci III,* 316**,** 425-30.

CANNON, D. J. & FOSTER, C. S. 1978. Collagen crosslinking in keratoconus. *Invest Ophthalmol Vis Sci,* 17**,** 63-5.

CAO, Z., SAID, N., AMIN, S., WU, H. K., BRUCE, A., GARATE, M., HSU, D. K., KUWABARA, I., LIU, F. T. & PANJWANI, N. 2002. Galectins-3 and -7, but not galectin-1, play a role in re-epithelialization of wounds. *J Biol Chem,* 277**,** 42299-305.

CARLSON, E. C., LIU, C. Y., CHIKAMA, T., HAYASHI, Y., KAO, C. W., BIRK, D. E., FUNDERBURGH, J. L., JESTER, J. V. & KAO, W. W. 2005. Keratocan, a cornea-specific keratan sulfate proteoglycan, is regulated by lumican. *J Biol Chem,* 280**,** 25541-7.

CARRINGTON, L. M. & BOULTON, M. 2005. Hepatocyte growth factor and keratinocyte growth factor regulation of epithelial and stromal corneal wound healing. *J Cataract Refract Surg,* 31**,** 412-23.

CHAERKADY, R., SHAO, H., SCOTT, S. G., PANDEY, A., JUN, A. S. & CHAKRAVARTI, S. 2013. The keratoconus corneal proteome: loss of epithelial integrity and stromal degeneration. *J Proteomics,* 87**,** 122-31.

CHAKRAVARTI, S., PETROLL, W. M., HASSELL, J. R., JESTER, J. V., LASS, J. H., PAUL, J. & BIRK, D. E. 2000. Corneal opacity in lumican-null mice: defects in collagen fibril structure and packing in the posterior stroma. *Invest Ophthalmol Vis Sci,* 41**,** 3365-73.

CHAURASIA, S. S., KAUR, H., DE MEDEIROS, F. W., SMITH, S. D. & WILSON, S. E. 2009. Reprint of "Dynamics of the expression of intermediate filaments vimentin and desmin during myofibroblast differentiation after corneal injury". *Exp Eye Res,* 89**,** 590-6.

CHEN, J., LI, H., SUNDARRAJ, N. & WANG, J. H. 2007. Alpha-smooth muscle actin expression enhances cell traction force. *Cell Motil Cytoskeleton,* 64**,** 248-57.

CHEN, S., MIENALTOWSKI, M. J. & BIRK, D. E. 2015. Regulation of corneal stroma extracellular matrix assembly. *Exp Eye Res,* 133**,** 69-80.

CHWA, M., ATILANO, S. R., HERTZOG, D., ZHENG, H., LANGBERG, J., KIM, D. W. & KENNEY, M. C. 2008. Hypersensitive response to oxidative stress in keratoconus corneal fibroblasts. *Invest Ophthalmol Vis Sci,* 49**,** 4361-9.

COLLIER, S. A. 2001. Is the corneal degradation in keratoconus caused by matrix-metalloproteinases? *Clin Exp Ophthalmol,* 29**,** 340-4.

CONNON, C. J., MARSHALL, J., PATMORE, A. L., BRAHMA, A. & MEEK, K. M. 2003. Persistent haze and disorganization of anterior stromal collagen appear unrelated following phototherapeutic keratectomy. *J Refract Surg,* 19**,** 323-32.

CORDOVA, B., MORATO, R., IZQUIERDO, D., PARAMIO, T. & MOGAS, T. 2010. Effect of the addition of insulin-transferrin-selenium and/or L-ascorbic acid to the in vitro maturation of prepubertal bovine oocytes on cytoplasmic maturation and embryo development. *Theriogenology,* 74**,** 1341-8.

CULLEN, J. F. & BUTLER, H. G. 1963. Mongolism (Down's Syndrome) and Keratoconus. *Br J Ophthalmol,* 47**,** 321-30.

CVEKL, A. & WANG, W. L. 2009. Retinoic acid signaling in mammalian eye development. *Exp Eye Res,* 89**,** 280-91.

DAVIDSON, A. E., HAYES, S., HARDCASTLE, A. J. & TUFT, S. J. 2014. The pathogenesis of keratoconus. *Eye (Lond),* 28**,** 189-95.

DE TOLEDO, J. A., DE LA PAZ, M. F., BARRAQUER, R. I. & BARRAQUER, J. 2003. Long-term progression of astigmatism after penetrating keratoplasty for keratoconus: evidence of late recurrence. *Cornea,* 22**,** 317-23.

DU, Y., FUNDERBURGH, M. L., MANN, M. M., SUNDARRAJ, N. & FUNDERBURGH, J. L. 2005. Multipotent stem cells in human corneal stroma. *Stem Cells,* 23**,** 1266-75.

DU, Y., SUNDARRAJ, N., FUNDERBURGH, M. L., HARVEY, S. A., BIRK, D. E. & FUNDERBURGH, J. L. 2007. Secretion and organization of a cornea-like tissue in vitro by stem cells from human corneal stroma. *Invest Ophthalmol Vis Sci,* 48**,** 5038-45.

DUA, H. S. & AZUARA-BLANCO, A. 2000. Limbal stem cells of the corneal epithelium. *Surv Ophthalmol,* 44**,** 415-25.

DULBECCO, R. & FREEMAN, G. 1959. Plaque production by the polyoma virus. *Virology,* 8**,** 396-7.

EAGLE, H. 1955. Nutrition needs of mammalian cells in tissue culture. *Science,* 122**,** 501-14.

EAGLE, H. 1959. Amino acid metabolism in mammalian cell cultures. *Science,* 130**,** 432-7.

EBIHARA, N., MATSUDA, A., NAKAMURA, S., MATSUDA, H. & MURAKAMI, A. 2011. Role of the IL-6 classic- and trans-signaling pathways in corneal sterile inflammation and wound healing. *Invest Ophthalmol Vis Sci,* 52**,** 8549-57.

EBIHARA, N., YAMAGAMI, S., CHEN, L., TOKURA, T., IWATSU, M., USHIO, H. & MURAKAMI, A. 2007. Expression and function of toll-like receptor-3 and -9 in human corneal myofibroblasts. *Invest Ophthalmol Vis Sci,* 48**,** 3069-76.

ECKES, B., COLUCCI-GUYON, E., SMOLA, H., NODDER, S., BABINET, C., KRIEG, T. & MARTIN, P. 2000. Impaired wound healing in embryonic and adult mice lacking vimentin. *J Cell Sci,* 113 (Pt 13)**,** 2455-62.

ELDER, M. J. 1994. Leber congenital amaurosis and its association with keratoconus and keratoglobus. *J Pediatr Ophthalmol Strabismus,* 31**,** 38-40.

ELSDALE, T. & BARD, J. 1972. Collagen substrata for studies on cell behavior. *J Cell Biol,* 54**,** 626-37.

ENGELHARDT, E. M., STEGBERG, E., BROWN, R. A., HUBBELL, J. A., WURM, F. M., ADAM, M. & FREY, P. 2010. Compressed collagen gel: a novel scaffold for human bladder cells. *J Tissue Eng Regen Med,* 4**,** 123-30.

ENGLER, C., CHAKRAVARTI, S., DOYLE, J., EBERHART, C. G., MENG, H., STARK, W. J., KELLIHER, C. & JUN, A. S. 2011. Transforming growth factor-beta signaling pathway activation in Keratoconus. *Am J Ophthalmol,* 151**,** 752-759 e2.

ESPANA, E. M., HE, H., KAWAKITA, T., DI PASCUALE, M. A., RAJU, V. K., LIU, C. Y. & TSENG, S. C. 2003. Human keratocytes cultured on amniotic membrane stroma preserve morphology and express keratocan. *Invest Ophthalmol Vis Sci,* 44**,** 5136-41.

FAN, J., DONG, L., MISHRA, S., CHEN, Y., FITZGERALD, P. & WISTOW, G. 2012. A role for gammaS-crystallin in the organization of actin and fiber cell maturation in the mouse lens. *FEBS J,* 279**,** 2892-904.

FEIZI, S., JAVADI, M. A. & REZAEI KANAVI, M. 2012. Recurrent keratoconus in a corneal graft after deep anterior lamellar keratoplasty. *J Ophthalmic Vis Res,* 7**,** 328-31.

FERNANDEZ-PEREZ, J. & AHEARNE, M. 2019. Influence of Biochemical Cues in Human Corneal Stromal Cell Phenotype. *Curr Eye Res,* 44**,** 135-146.

FINI, M. E. & STRAMER, B. M. 2005. How the cornea heals: cornea-specific repair mechanisms affecting surgical outcomes. *Cornea,* 24**,** S2-S11.

FINI, M. E., YUE, B. Y. & SUGAR, J. 1992. Collagenolytic/gelatinolytic metalloproteinases in normal and keratoconus corneas. *Curr Eye Res,* 11**,** 849-62.

FLECKMAN, P., DALE, B. A. & HOLBROOK, K. A. 1985. Profilaggrin, a high-molecular-weight precursor of filaggrin in human epidermis and cultured keratinocytes. *J Invest Dermatol,* 85**,** 507-12.

FLEIGE, S., WALF, V., HUCH, S., PRGOMET, C., SEHM, J. & PFAFFL, M. W. 2006. Comparison of relative mRNA quantification models and the impact of RNA integrity in quantitative real-time RT-PCR. *Biotechnol Lett,* 28**,** 1601-13.

FOSTER, J., WU, W. H., SCOTT, S. G., BASSI, M., MOHAN, D., DAOUD, Y., STARK, W. J., JUN, A. S. & CHAKRAVARTI, S. 2014. Transforming growth factor beta and insulin signal changes in stromal fibroblasts of individual keratoconus patients. *PLoS One,* 9**,** e106556.

FOSTER, J. W., GOUVEIA, R. M. & CONNON, C. J. 2015. Low-glucose enhances keratocyte-characteristic phenotype from corneal stromal cells in serum-free conditions. *Sci Rep,* 5**,** 10839.

FRANCIS, G. L. 2010. Albumin and mammalian cell culture: implications for biotechnology applications. *Cytotechnology,* 62**,** 1-16.

FUCHS, E. & GREEN, H. 1981. Regulation of terminal differentiation of cultured human keratinocytes by vitamin A. *Cell,* 25**,** 617-25.

FUJII, A., SHEARER, T. R. & AZUMA, M. 2015. Galectin-3 enhances extracellular matrix associations and wound healing in monkey corneal epithelium. *Exp Eye Res,* 137**,** 71-8.

FUNDERBURGH, J. L., FUNDERBURGH, M. L. & DU, Y. 2016. Stem Cells in the Limbal Stroma. *Ocul Surf,* 14**,** 113-20.

FUNDERBURGH, J. L., HEVELONE, N. D., ROTH, M. R., FUNDERBURGH, M. L., RODRIGUES, M. R., NIRANKARI, V. S. & CONRAD, G. W. 1998. Decorin and biglycan of normal and pathologic human corneas. *Invest Ophthalmol Vis Sci,* 39**,** 1957-64.

FUNDERBURGH, J. L., MANN, M. M. & FUNDERBURGH, M. L. 2003. Keratocyte phenotype mediates proteoglycan structure: a role for fibroblasts in corneal fibrosis. *J Biol Chem,* 278**,** 45629-37.

FUNDERBURGH, M. L., DU, Y., MANN, M. M., SUNDARRAJ, N. & FUNDERBURGH, J. L. 2005. PAX6 expression identifies progenitor cells for corneal keratocytes. *FASEB J,* 19**,** 1371-3.

GAGE, P. J., RHOADES, W., PRUCKA, S. K. & HJALT, T. 2005. Fate maps of neural crest and mesoderm in the mammalian eye. *Investigative Ophthalmology & Visual Science,* 46**,** 4200-4208.

GALVIS, V., SHERWIN, T., TELLO, A., MERAYO, J., BARRERA, R. & ACERA, A. 2015. Keratoconus: an inflammatory disorder? *Eye (Lond),* 29**,** 843-59.

GEARING, A. J., BECKETT, P., CHRISTODOULOU, M., CHURCHILL, M., CLEMENTS, J., DAVIDSON, A. H., DRUMMOND, A. H., GALLOWAY, W. A., GILBERT, R., GORDON, J. L. & ET AL. 1994. Processing of tumour necrosis factor-alpha precursor by metalloproteinases. *Nature,* 370**,** 555-7.

GEORGIEV, G. A., EFTIMOV, P. & YOKOI, N. 2017. Structure-function relationship of tear film lipid layer: A contemporary perspective. *Exp Eye Res,* 163**,** 17-28.

GEORGIOU, T., FUNNELL, C. L., CASSELS-BROWN, A. & O'CONOR, R. 2004. Influence of ethnic origin on the incidence of keratoconus and associated atopic disease in Asians and white patients. *Eye (Lond),* 18**,** 379-83.

GODEFROOIJ, D. A., DE WIT, G. A., UITERWAAL, C. S., IMHOF, S. M. & WISSE, R. P. 2017. Age-specific Incidence and Prevalence of Keratoconus: A Nationwide Registration Study. *Am J Ophthalmol,* 175**,** 169-172.

GONDHOWIARDJO, T. D., VAN HAERINGEN, N. J., VOLKER-DIEBEN, H. J., BEEKHUIS, H. W., KOK, J. H., VAN RIJ, G., PELS, L. & KIJLSTRA, A. 1993. Analysis of corneal aldehyde dehydrogenase patterns in pathologic corneas. *Cornea,* 12**,** 146-54.

GONZALEZ-ANDRADES, M., ALONSO-PASTOR, L., MAURIS, J., CRUZAT, A., DOHLMAN, C. H. & ARGUESO, P. 2016. Establishment of a novel in vitro model of stratified epithelial wound healing with barrier function. *Sci Rep,* 6**,** 19395.

GORDON-SHAAG, A., MILLODOT, M., SHNEOR, E. & LIU, Y. 2015. The genetic and environmental factors for keratoconus. *Biomed Res Int,* 2015**,** 795738.

GOUVEIA, R. M. & CONNON, C. J. 2013. The effects of retinoic acid on human corneal stromal keratocytes cultured in vitro under serum-free conditions. *Invest Ophthalmol Vis Sci,* 54**,** 7483-91.

GOUVEIA, R. M., KOUDOUNA, E., JESTER, J., FIGUEIREDO, F. & CONNON, C. J. 2017. Template Curvature Influences Cell Alignment to Create Improved Human Corneal Tissue Equivalents. *Advanced Biosystems,* 1.

GREENBAUM, C., ATKINSON, M., BAIDAL, D., BATTAGLIA, M., BINGLEY, P., BOSI, E., BUCKNER, J., CLEMENTS, M., COLMAN, P., DIMEGLIO, L., EVANS-MOLINA, C., GITELMAN, S., GOLAND, R., GOTTLIEB, P., HEROLD, K., KNIP, M., KRISCHER, J., LERNMARK, A., MOORE, W., MORAN, A., MUIR, A., PALMER, J., PEAKMAN, M., PHILIPSON, L., RASKIN, P., REDONDO, M., RODRIGUEZ, H., RUSSELL, W., SPAIN, L., SCHATZ, D. A., SOSENKO, J., WHERRETT, D., WILSON, D., WINTER, W., ZIEGLER, A., ANDERSON, M., ANTINOZZI, P., BENOIST, C., BLUM, J., BOURCIER, K., CHASE, P., CLARE-SALZLER, M., CLYNES, R., COWIE, C., EISENBARTH, G., FATHMAN, C. G., GRAVE, G., HARRISON, L., HERING, B., INSEL, R., JORDAN, S., KAUFMAN, F., KAY, T., KENYON, N., KLINES, R., LACHIN, J., LESCHEK, E., MAHON, J., MARKS, J. B., MONZAVI, R., NANTO-SALONEN, K., NEPOM, G., ORBAN, T., PARKMAN, R., PESCOVITZ, M., PEYMAN, J., PUGLIESE, A., RIDGE, J., ROEP, B., RONCAROLO, M., SAVAGE, P., SIMELL, O., SHERWIN, R., SIEGELMAN, M., SKYLER, J. S., THOMAS, J., TRUCCO, M., WAGNER, J., BOURCIER, K., GREENBAUM, C. J., KRISCHER, J. P., LESCHEK, E., RAFKIN, L., SPAIN, L., COWIE, C., FOULKES, M., INSEL, R., KRAUSE-STEINRAUF, H., LACHIN, J. M., MALOZOWSKI, S., PEYMAN, J., RIDGE, J., SAVAGE, P., SKYLER, J. S., ZAFONTE, S. J., GREENBAUM, C. J., RAFKIN, L., SOSENKO, J., SKYLER, J. S.,

KENYON, N. S., et al. 2017. Effect of Oral Insulin on Prevention of Diabetes in Relatives of Patients With Type 1 Diabetes A Randomized Clinical Trial. *Jama-Journal of the American Medical Association,* 318**,** 1891-1902.

HAM, R. G. & MCKEEHAN, W. L. 1979. Medium and growth requirements. *Methods Enzymol,* 58**,** 44-93.

HAYASHI, S., OSAWA, T. & TOHYAMA, K. 2002a. Comparative observations on corneas, with special reference to Bowman's layer and Descemet's membrane in mammals and amphibians. *J Morphol,* 254**,** 247-58.

HAYASHI, S., OSAWA, T. & TOHYAMA, K. 2002b. Comparative observations on corneas, with special reference to Bowman's layer and Descemet's membrane in mammals and amphibians. *Journal of Morphology,* 254**,** 247-258.

HECK, D. E., VETRANO, A. M., MARIANO, T. M. & LASKIN, J. D. 2003. UVB light stimulates production of reactive oxygen species: unexpected role for catalase. *J Biol Chem,* 278**,** 22432-6.

HELMY, M. H., ISMAIL, S. S., FAYED, H. & EL-BASSIOUNI, E. A. 2000. Effect of selenium supplementation on the activities of glutathione metabolizing enzymes in human hepatoma Hep G2 cell line. *Toxicology,* 144**,** 57-61.

HENRIKSSON, J. T., MCDERMOTT, A. M. & BERGMANSON, J. P. 2009. Dimensions and morphology of the cornea in three strains of mice. *Invest Ophthalmol Vis Sci,* 50**,** 3648-54.

HOLMES, D. F., LU, Y., STARBORG, T. & KADLER, K. E. 2018. Collagen Fibril Assembly and Function. *Curr Top Dev Biol,* 130**,** 107-142.

HOU, Y., LE, V. N. H., TOTH, G., SIEBELMANN, S., HORSTMANN, J., GABRIEL, T., BOCK, F. & CURSIEFEN, C. 2018. UV light crosslinking regresses mature corneal blood and lymphatic vessels and promotes subsequent high-risk corneal transplant survival. *Am J Transplant*.

HU, K., SHI, H., ZHU, J., DENG, D., ZHOU, G., ZHANG, W., CAO, Y. & LIU, W. 2010. Compressed collagen gel as the scaffold for skin engineering. *Biomed Microdevices,* 12**,** 627-35.

HUIJSKENS, M. J., WALCZAK, M., SARKAR, S., ATRAFI, F., SENDEN-GIJSBERS, B. L., TILANUS, M. G., BOS, G. M., WIETEN, L. & GERMERAAD, W. T. 2015. Ascorbic acid promotes proliferation of natural killer cell populations in culture systems applicable for natural killer cell therapy. *Cytotherapy,* 17**,** 613-20.

HUSS, R. 2000. Isolation of primary and immortalized CD34-hematopoietic and mesenchymal stem cells from various sources. *Stem Cells,* 18**,** 1-9.

IHANAMAKI, T., PELLINIEMI, L. J. & VUORIO, E. 2004. Collagens and collagen-related matrix components in the human and mouse eye. *Prog Retin Eye Res,* 23**,** 403-34.

IONESCU, C., CORBU, C. G., TANASE, C., JONESCU-CUYPERS, C., NICULA, C., DASCALESCU, D., CRISTEA, M. & VOINEA, L. M. 2016. Inflammatory Biomarkers Profile as Microenvironmental Expression in Keratoconus. *Dis Markers,* 2016**,** 1243819.

JARVELAINEN, H., SAINIO, A. & WIGHT, T. N. 2015. Pivotal role for decorin in angiogenesis. *Matrix Biol,* 43**,** 15-26.

JEON, K. I., HINDMAN, H. B., BUBEL, T., MCDANIEL, T., DEMAGISTRIS, M., CALLAN, C. & HUXLIN, K. R. 2018. Corneal myofibroblasts inhibit regenerating nerves during wound healing. *Sci Rep,* 8**,** 12945.

JESTER, J. V. 2008. Corneal crystallins and the development of cellular transparency. *Semin Cell Dev Biol,* 19**,** 82-93.

JESTER, J. V. & HO-CHANG, J. 2003. Modulation of cultured corneal keratocyte phenotype by growth factors/cytokines control in vitro contractility and extracellular matrix contraction. *Exp Eye Res,* 77**,** 581-92.

JESTER, J. V., PETROLL, W. M. & CAVANAGH, H. D. 1999. Corneal stromal wound healing in refractive surgery: the role of myofibroblasts. *Prog Retin Eye Res,* 18**,** 311-56.

JHANJI, V., SHARMA, N. & VAJPAYEE, R. B. 2011. Management of keratoconus: current scenario. *Br J Ophthalmol,* 95**,** 1044-50.

JOSEPH, A., HOSSAIN, P., JHAM, S., JONES, R. E., TIGHE, P., MCINTOSH, R. S. & DUA, H. S. 2003. Expression of CD34 and L-selectin on human corneal keratocytes. *Invest Ophthalmol Vis Sci,* 44**,** 4689-92.

JOSEPH, R., SRIVASTAVA, O. P. & PFISTER, R. R. 2016. Modeling Keratoconus Using Induced Pluripotent Stem Cells. *Investigative Ophthalmology & Visual Science,* 57**,** 3685-3697.

KANAI A, KAUFMAN HE. Electron microscopic studies of corneal stroma: aging changes of collagen fibers. Ann. Ophthalmol. 1973;5:285–287.

KAO, W. W., VERGNES, J. P., EBERT, J., SUNDAR-RAJ, C. V. & BROWN, S. I. 1982. Increased collagenase and gelatinase activities in keratoconus. *Biochem Biophys Res Commun,* 107**,** 929-36.

KARAMICHOS, D., HUTCHEON, A. E., RICH, C. B., TRINKAUS-RANDALL, V., ASARA, J. M. & ZIESKE, J. D. 2014. In vitro model suggests oxidative stress involved in keratoconus disease. *Sci Rep,* 4**,** 4608.

KARAMICHOS, D., HUTCHEON, A. E. & ZIESKE, J. D. 2011. Transforming growth factor-beta3 regulates assembly of a non-fibrotic matrix in a 3D corneal model. *J Tissue Eng Regen Med,* 5**,** e228-38.

KARAMICHOS, D., RICH, C. B., ZAREIAN, R., HUTCHEON, A. E., RUBERTI, J. W., TRINKAUS-RANDALL, V. & ZIESKE, J. D. 2013. TGF-beta3 stimulates stromal matrix assembly by human corneal keratocyte-like cells. *Invest Ophthalmol Vis Sci,* 54**,** 6612-9.

KARAMICHOS, D., ZAREIAN, R., GUO, X., HUTCHEON, A. E., RUBERTI, J. W. & ZIESKE, J. D. 2012. Novel in Vitro Model for Keratoconus Disease. *J Funct Biomater,* 3**,** 760-775.

KASTNER, P., GRONDONA, J. M., MARK, M., GANSMULLER, A., LEMEUR, M., DECIMO, D., VONESCH, J. L., DOLLE, P. & CHAMBON, P. 1994. Genetic analysis of RXR alpha developmental function: convergence of RXR and RAR signaling pathways in heart and eye morphogenesis. *Cell,* 78**,** 987-1003.

KASTNER, P., MARK, M., LEID, M., GANSMULLER, A., CHIN, W., GRONDONA, J. M., DECIMO, D., KREZEL, W., DIERICH, A. & CHAMBON, P. 1996. Abnormal spermatogenesis in RXR beta mutant mice. *Genes Dev,* 10**,** 80-92.

KENNEY, M. C., CHWA, M., ATILANO, S. R., TRAN, A., CARBALLO, M., SAGHIZADEH, M., VASILIOU, V., ADACHI, W. & BROWN, D. J. 2005. Increased levels of catalase and cathepsin V/L2 but decreased TIMP-1 in keratoconus corneas: evidence that oxidative stress plays a role in this disorder. *Invest Ophthalmol Vis Sci,* 46**,** 823-32.

KIJLSTRA, A. & KUIZENGA, A. 1994. Analysis and function of the human tear proteins. *Adv Exp Med Biol,* 350**,** 299-308.

KIM, W. J., MOHAN, R. R., MOHAN, R. R. & WILSON, S. E. 1999. Effect of PDGF, IL-1alpha, and BMP2/4 on corneal fibroblast chemotaxis: expression of the platelet-derived growth factor system in the cornea. *Invest Ophthalmol Vis Sci,* 40**,** 1364-72.

KIVANANY, P. B., GROSE, K. C. & PETROLL, W. M. 2016. Temporal and spatial analysis of stromal cell and extracellular matrix patterning following lamellar keratectomy. *Exp Eye Res,* 153**,** 56-64.

KIVANANY, P. B., GROSE, K. C., TIPPANI, M., SU, S. & PETROLL, W. M. 2018. Assessment of Corneal Stromal Remodeling and Regeneration after Photorefractive Keratectomy. *Sci Rep,* 8**,** 12580.

KODAMA, R., YANG, X., ARAKI, T., SATO, M., IWASHIGE, S., TANIGAWA, Y., UCHIMURA, M., ISHIMARU, K., SASAKI, Y., KAMIMURA, Y. & MAEDA, H. 2010. Keratoconus in a cynomolgus monkey. *J Toxicol Pathol,* 23**,** 53-8.

KOK, Y. O., TAN, G. F. & LOON, S. C. 2012. Review: keratoconus in Asia. *Cornea,* 31**,** 581-93.

KOLB, H. 1995. Gross Anatomy of the Eye. *In:* KOLB, H., FERNANDEZ, E. & NELSON, R. (eds.) *Webvision: The Organization of the Retina and Visual System.* Salt Lake City (UT).

KOMAI, Y. & USHIKI, T. 1991. The three-dimensional organization of collagen fibrils in the human cornea and sclera. *Invest Ophthalmol Vis Sci,* 32**,** 2244-58.

KONG, B., SUN, W., CHEN, G., TANG, S., LI, M., SHAO, Z. & MI, S. 2017. Tissue-engineered cornea constructed with compressed collagen and laser-perforated electrospun mat. *Sci Rep,* 7**,** 970.

LACKNER, E. M., MATTHAEI, M., MENG, H., ARDJOMAND, N., EBERHART, C. G. & JUN, A. S. 2014. Design and analysis of keratoconus tissue microarrays. *Cornea,* 33**,** 49-55.

LAGALI, N., GERMUNDSSON, J. & FAGERHOLM, P. 2009. The role of Bowman's layer in corneal regeneration after phototherapeutic keratectomy: a prospective study using in vivo confocal microscopy. *Invest Ophthalmol Vis Sci,* 50**,** 4192-8.

LEVINGS, R. L. & WESSMAN, S. J. 1991. Bovine viral diarrhea virus contamination of nutrient serum, cell cultures and viral vaccines. *Dev Biol Stand,* 75**,** 177-81.

LI, D. Q. & TSENG, S. C. 1997. Differential regulation of keratinocyte growth factor and hepatocyte growth factor/scatter factor by different cytokines in human corneal and limbal fibroblasts. *J Cell Physiol,* 172**,** 361-72.

LINDQUIST, S. & CRAIG, E. A. 1988. The heat-shock proteins. *Annu Rev Genet,* 22**,** 631-77.

LIU, C. Y., BIRK, D. E., HASSELL, J. R., KANE, B. & KAO, W. W. 2003. Keratocan-deficient mice display alterations in corneal structure. *J Biol Chem,* 278**,** 21672-7.

LJUBIMOV, A. V. & SAGHIZADEH, M. 2015. Progress in corneal wound healing. *Prog Retin Eye Res,* 49**,** 17-45.

LOH, A., HADZIAHMETOVIC, M. & DUNAIEF, J. L. 2009. Iron homeostasis and eye disease. *Biochim Biophys Acta,* 1790**,** 637-49.

LYON, D., MCKAY, T. B., SARKAR-NAG, A., PRIYADARSINI, S. & KARAMICHOS, D. 2015. Human Keratoconus Cell Contractility is Mediated by Transforming Growth Factor-Beta Isoforms. *J Funct Biomater,* 6**,** 422-38.

MAGUIRE, L. J. & BOURNE, W. M. 1989. Corneal topography of early keratoconus. *Am J Ophthalmol,* 108**,** 107-12.

MALIK NS, MOSS SJ, AHMED N, FURTH AJ, WALL RS, MEEK KM. Ageing of the human corneal stroma: structural and biochemical changes. Biochim. Biophys. Acta. 1992;1138:222–228.

MARCELO, C. L. & MADISON, K. C. 1984. Regulation of the expression of epidermal keratinocyte proliferation and differentiation by vitamin A analogs. *Arch Dermatol Res,* 276**,** 381-9.

MAURICE, D. M. 1957. The structure and transparency of the cornea. *J Physiol,* 136**,** 263-86.

MAZZOTTA, C., BALESTRAZZI, A., TRAVERSI, C., BAIOCCHI, S., CAPOROSSI, T., TOMMASI, C. & CAPOROSSI, A. 2007. Treatment of progressive keratoconus by riboflavin-UVA-induced cross-linking of corneal collagen: ultrastructural analysis by

Heidelberg Retinal Tomograph II in vivo confocal microscopy in humans. *Cornea,* 26**,** 390-7.

MEEK, K. M. & BOOTE, C. 2004. The organization of collagen in the corneal stroma. *Exp Eye Res,* 78**,** 503-12.

MELLO, C. B., RAMOS, L., GIMENES, A. D., ANDRADE, T. R., OLIANI, S. M. & GIL, C. D. 2015. Immunomodulatory effects of galectin-1 on an IgE-mediated allergic conjunctivitis model. *Invest Ophthalmol Vis Sci,* 56**,** 693-704.

MENDEZ, M. G., KOJIMA, S. & GOLDMAN, R. D. 2010. Vimentin induces changes in cell shape, motility, and adhesion during the epithelial to mesenchymal transition. *FASEB J,* 24**,** 1838-51.

MI, S. L., DAVID, A. L., CHOWDHURY, B., JONES, R. R., HAMLEY, I. W., SQUIRES, A. M. & CONNON, C. J. 2012. Tissue Engineering a Fetal Membrane. *Tissue Engineering Part A,* 18**,** 373-381.

MICHELACCI, Y. M. 2003. Collagens and proteoglycans of the corneal extracellular matrix. *Braz J Med Biol Res,* 36**,** 1037-46.

MIKULA, E., WINKLER, M., JUHASZ, T., BROWN, D. J., SHOA, G., TRAN, S., KENNEY, M. C. & JESTER, J. V. 2018. Axial mechanical and structural characterization of keratoconus corneas. *Exp Eye Res,* 175**,** 14-19.

MINAMI, Y., SUGIHARA, H. & OONO, S. 1993. Reconstruction of cornea in three-dimensional collagen gel matrix culture. *Invest Ophthalmol Vis Sci,* 34**,** 2316-24.

MIOTTO, M., GOUVEIA, R. M., IONESCU, A. M., FIGUEIREDO, F., HAMLEY, I. W. & CONNON, C. J. 2019. 4D Corneal Tissue Engineering: Achieving Time-Dependent Tissue Self-Curvature through Localized Control of Cell Actuators. *Advanced Functional Materials,* 29.

MISHIMA, S. 1965. Some Physiological Aspects of the Precorneal Tear Film. *Arch Ophthalmol,* 73**,** 233-41.

MOLLER-PEDERSEN, T., CAVANAGH, H. D., PETROLL, W. M. & JESTER, J. V. 2000. Stromal wound healing explains refractive instability and haze development after photorefractive keratectomy: a 1-year confocal microscopic study. *Ophthalmology,* 107**,** 1235-45.

MORI, M., GHYSELINCK, N. B., CHAMBON, P. & MARK, M. 2001. Systematic immunolocalization of retinoid receptors in developing and adult mouse eyes. *Invest Ophthalmol Vis Sci,* 42**,** 1312-8.

MULLER, L. J., PELS, E. & VRENSEN, G. F. 2001. The specific architecture of the anterior stroma accounts for maintenance of corneal curvature. *Br J Ophthalmol,* 85**,** 437-43.

MULLER, L. J., PELS, L. & VRENSEN, G. F. 1995. Novel aspects of the ultrastructural organization of human corneal keratocytes. *Invest Ophthalmol Vis Sci,* 36**,** 2557-67.

MUSSELMANN, K., ALEXANDROU, B., KANE, B. & HASSELL, J. R. 2005. Maintenance of the keratocyte phenotype during cell proliferation stimulated by insulin. *J Biol Chem,* 280**,** 32634-9.

NAGASE, H. & WOESSNER, J. F., JR. 1999. Matrix metalloproteinases. *J Biol Chem,* 274**,** 21491-4.

NAKAMURA, K., KUROSAKA, D., YOSHINO, M., OSHIMA, T. & KUROSAKA, H. 2002. Injured corneal epithelial cells promote myodifferentiation of corneal fibroblasts. *Invest Ophthalmol Vis Sci,* 43**,** 2603-8.

NEWSOME, D. A., FOIDART, J. M., HASSELL, J. R., KRACHMER, J. H., RODRIGUES, M. M. & KATZ, S. I. 1981. Detection of specific collagen types in normal and keratoconus corneas. *Invest Ophthalmol Vis Sci,* 20**,** 738-50.

NEZZAR, H., CHIAMBARETTA, F., MARCEAU, G., BLANCHON, L., FAYE, B., DECHELOTTE, P., RIGAL, D. & SAPIN, V. 2007. Molecular and metabolic retinoid pathways in the human ocular surface. *Mol Vis,* 13**,** 1641-50.

NIELSEN, J. S. & MCNAGNY, K. M. 2008. Novel functions of the CD34 family. *Journal of Cell Science,* 121**,** 3683-3692.

OJEDA, J. L., VENTOSA, J. A. & PIEDRA, S. 2001. The three-dimensional microanatomy of the rabbit and human cornea. A chemical and mechanical microdissection-SEM approach. *J Anat,* 199**,** 567-76.

ORWIN, E. J. & HUBEL, A. 2000. In vitro culture characteristics of corneal epithelial, endothelial, and keratocyte cells in a native collagen matrix. *Tissue Eng,* 6**,** 307-19.

OTTEN, J., BOKEMEYER, C. & FIEDLER, W. 2010. Tgf-Beta superfamily receptors-targets for antiangiogenic therapy? *J Oncol,* 2010**,** 317068.

PACELLA, E., PACELLA, F., DE PAOLIS, G., PARISELLA, F. R., TURCHETTI, P., ANELLO, G. & CAVALLOTTI, C. 2015. Glycosaminoglycans in the human cornea: age-related changes. *Ophthalmol Eye Dis,* 7**,** 1-5.

PAPPA, A., ESTEY, T., MANZER, R., BROWN, D. & VASILIOU, V. 2003. Human aldehyde dehydrogenase 3A1 (ALDH3A1): biochemical characterization and immunohistochemical localization in the cornea. *Biochem J,* 376**,** 615-23.

PARDO, A. & SELMAN, M. 2005. MMP-1: the elder of the family. *Int J Biochem Cell Biol,* 37**,** 283-8.

PATEL, S., MCLAREN, J., HODGE, D. & BOURNE, W. 2001. Normal human keratocyte density and corneal thickness measurement by using confocal microscopy in vivo. *Invest Ophthalmol Vis Sci,* 42**,** 333-9.

PERRELLA, G., BRUSINI, P., SPELAT, R., HOSSAIN, P., HOPKINSON, A. & DUA, H. S. 2007. Expression of haematopoietic stem cell markers, CD133 and CD34 on human corneal keratocytes. *Br J Ophthalmol,* 91**,** 94-9.

PETROLL, W. M., CAVANAGH, H. D. & JESTER, J. V. 2004. Dynamic three-dimensional visualization of collagen matrix remodeling and cytoskeletal organization in living corneal fibroblasts. *Scanning,* 26**,** 1-10.

PIATIGORSKY, J. 1998. Multifunctional lens crystallins and corneal enzymes. More than meets the eye. *Ann N Y Acad Sci,* 842**,** 7-15.

PINNAMANENI, N. & FUNDERBURGH, J. L. 2012. Concise review: Stem cells in the corneal stroma. *Stem Cells,* 30**,** 1059-63.

POLISETTY, N., FATIMA, A., MADHIRA, S. L., SANGWAN, V. S. & VEMUGANTI, G. K. 2008. Mesenchymal cells from limbal stroma of human eye. *Mol Vis,* 14**,** 431-42.

POOLE, C. A., BROOKES, N. H. & CLOVER, G. M. 2003. Confocal imaging of the human keratocyte network using the vital dye 5-chloromethylfluorescein diacetate. *Clin Exp Ophthalmol,* 31**,** 147-54.

PRIYADARSINI, S., MCKAY, T. B., SARKER-NAG, A. & KARAMICHOS, D. 2015. Keratoconus in vitro and the key players of the TGF-beta pathway. *Mol Vis,* 21**,** 577-88.

QUANTOCK, A. J., BOOTE, C., SIEGLER, V. & MEEK, K. M. 2003. Collagen organization in the secondary chick cornea during development. *Invest Ophthalmol Vis Sci,* 44**,** 130-6.

QUAX-JEUKEN, Y., DRIESSEN, H., LEUNISSEN, J., QUAX, W., DE JONG, W. & BLOEMENDAL, H. 1985. beta s-Crystallin: structure and evolution of a distinct member of the beta gamma-superfamily. *EMBO J,* 4**,** 2597-602.

RABINOWITZ, Y. S. 1998. Keratoconus. *Surv Ophthalmol,* 42**,** 297-319.

RADONS, J. 2016. The human HSP70 family of chaperones: where do we stand? *Cell Stress Chaperones,* 21**,** 379-404.

RAISKUP, F., THEURING, A., PILLUNAT, L. E. & SPOERL, E. 2015. Corneal collagen crosslinking with riboflavin and ultraviolet-A light in progressive keratoconus: ten-year results. *J Cataract Refract Surg,* 41**,** 41-6.

RAJASAGI, N. K., SURYAWANSHI, A., SEHRAWAT, S., REDDY, P. B., MULIK, S., HIRASHIMA, M. & ROUSE, B. T. 2012. Galectin-1 reduces the severity of herpes simplex virus-induced ocular immunopathological lesions. *J Immunol,* 188**,** 4631-43.

REHANY, U., LAHAV, M. & SHOSHAN, S. 1982. Collagenolytic activity in keratoconus. *Ann Ophthalmol,* 14**,** 751-4.

REICHL, S., BEDNARZ, J. & MULLER-GOYMANN, C. C. 2004. Human corneal equivalent as cell culture model for in vitro drug permeation studies. *Br J Ophthalmol,* 88**,** 560-5.

REINACH, P. S. & POKORNY, K. S. 2008. The corneal epithelium: clinical relevance of cytokine-mediated responses to maintenance of corneal health. *Arq Bras Oftalmol,* 71**,** 80-6.

RHEE, S. 2009. Fibroblasts in three dimensional matrices: cell migration and matrix remodeling. *Exp Mol Med,* 41**,** 858-65.

RILEY, G. P., HARRALL, R. L., WATSON, P. G., CAWSTON, T. E. & HAZLEMAN, B. L. 1995. Collagenase (MMP-1) and TIMP-1 in destructive corneal disease associated with rheumatoid arthritis. *Eye (Lond),* 9 (Pt 6)**,** 703-18.

ROBINS, S. P. 2007. Biochemistry and functional significance of collagen cross-linking. *Biochem Soc Trans,* 35**,** 849-52.

ROCHELS, R. 1979. [Acute keratoconus in mongolism (author s transl)]. *Albrecht Von Graefes Arch Klin Exp Ophthalmol,* 212**,** 117-28.

ROEDER, B. A., KOKINI, K., STURGIS, J. E., ROBINSON, J. P. & VOYTIK-HARBIN, S. L. 2002. Tensile mechanical properties of three-dimensional type I collagen extracellular matrices with varied microstructure. *J Biomech Eng,* 124**,** 214-22.

ROLANDO, M. & ZIERHUT, M. 2001. The ocular surface and tear film and their dysfunction in dry eye disease. *Surv Ophthalmol,* 45 Suppl 2**,** S203-10.

ROMERO, M. D., MUINO, J. C., BIANCO, G. A., FERRERO, M., JUAREZ, C. P., LUNA, J. D. & RABINOVICH, G. A. 2006. Circulating anti-galectin-1 antibodies are associated with the severity of ocular disease in autoimmune and infectious uveitis. *Invest Ophthalmol Vis Sci,* 47**,** 1550-6.

ROMERO-JIMENEZ, M., SANTODOMINGO-RUBIDO, J. & WOLFFSOHN, J. S. 2010. Keratoconus: a review. *Cont Lens Anterior Eye,* 33**,** 157-66; quiz 205.

RONG, S. S., MA, S. T. U., YU, X. T., MA, L., CHU, W. K., CHAN, T. C. Y., WANG, Y. M., YOUNG, A. L., PANG, C. P., JHANJI, V. & CHEN, L. J. 2017. Genetic associations for keratoconus: a systematic review and meta-analysis. *Sci Rep,* 7**,** 4620.

SAGHIZADEH, M., BROWN, D. J., CASTELLON, R., CHWA, M., HUANG, G. H., LJUBIMOVA, J. Y., ROSENBERG, S., SPIRIN, K. S., STOLITENKO, R. B., ADACHI, W., KINOSHITA, S., MURPHY, G., WINDSOR, L. J., KENNEY, M. C. & LJUBIMOV, A. V. 2001. Overexpression of matrix metalloproteinase-10 and matrix metalloproteinase-3 in human diabetic corneas: a possible mechanism of basement membrane and integrin alterations. *Am J Pathol,* 158**,** 723-34.

SAHEBJADA, S., SCHACHE, M., RICHARDSON, A. J., SNIBSON, G., DANIELL, M. & BAIRD, P. N. 2014. Association of the hepatocyte growth factor gene with keratoconus in an Australian population. *PLoS One,* 9**,** e84067.

SARAVANI, R., YARI, D., SARAVANI, S. & HASANIAN-LANGROUDI, F. 2017. Correlation between the COL4A3, MMP-9, and TIMP-1 polymorphisms and risk of keratoconus. *Jpn J Ophthalmol,* 61**,** 218-222.

SCHWARZ, W. & KEYSERLINGK, D. G. 1966. [On the fine structure of the human cornea with special reference to the problem of transparency]. *Z Zellforsch Mikrosk Anat,* 73**,** 540-8.

SCHWIEGERLING, J. 1997. Cone dimensions in keratoconus using Zernike polynomials. *Optom Vis Sci,* 74**,** 963-9.

SEPPALA, H. P., MAATTA, M., RAUTIA, M., MACKIEWICZ, Z., TUISKU, I., TERVO, T. & KONTTINEN, Y. T. 2006. EMMPRIN and MMP-1 in keratoconus. *Cornea,* 25**,** 325-30.

SHAO, H., CHAERKADY, R., CHEN, S., PINTO, S. M., SHARMA, R., DELANGHE, B., BIRK, D. E., PANDEY, A. & CHAKRAVARTI, S. 2011. Proteome profiling of wild type and lumican-deficient mouse corneas. *J Proteomics,* 74**,** 1895-905.

SHARIF, R., FOWLER, B. & KARAMICHOS, D. 2018. Collagen cross-linking impact on keratoconus extracellular matrix. *PLoS One,* 13**,** e0200704.

SHERWIN, T. & BROOKES, N. H. 2004. Morphological changes in keratoconus: pathology or pathogenesis. *Clin Exp Ophthalmol,* 32**,** 211-7.

SHETTY, R., SHARMA, A., PAHUJA, N., CHEVOUR, P., PADMAJAN, N., DHAMODARAN, K., JAYADEV, C., R, M. M. A. N., GHOSH, A. & NALLATHAMBI, J. 2017. Oxidative stress induces dysregulated autophagy in corneal epithelium of keratoconus patients. *PLoS One,* 12**,** e0184628.

SHEU, M. T., HUANG, J. C., YEH, G. C. & HO, H. O. 2001. Characterization of collagen gel solutions and collagen matrices for cell culture. *Biomaterials,* 22**,** 1713-9.

SIDNEY, L. E., BRANCH, M. J., DUNPHY, S. E., DUA, H. S. & HOPKINSON, A. 2014. Concise Review: Evidence for CD34 as a Common Marker for Diverse Progenitors. *Stem Cells,* 32**,** 1380-1389.

SIGGEL, R., CHRISTOFI, E., GIASOUMI, F., ADLER, W., SIEBELMANN, S., BACHMANN, B., CURSIEFEN, C. & HEINDL, L. M. 2019. Changes in Corneal Biomechanical Properties After Descemet Membrane Endothelial Keratoplasty. *Cornea,* 38**,** 964-969.

SIVAK, J. M. & FINI, M. E. 2002. MMPs in the eye: emerging roles for matrix metalloproteinases in ocular physiology. *Prog Retin Eye Res,* 21**,** 1-14.

SMEAL, R. M., RABBITT, R., BIRAN, R. & TRESCO, P. A. 2005. Substrate curvature influences the direction of nerve outgrowth. *Ann Biomed Eng,* 33**,** 376-82.

SMITH, J. W. & FRAME, J. 1969. Observations on the collagen and proteinpolysaccharide complex of rabbit cornea stroma. *J Cell Sci,* 4**,** 421-36.

SNIBSON, G. R. 2010. Collagen cross-linking: a new treatment paradigm in corneal disease - a review. *Clin Exp Ophthalmol,* 38**,** 141-53.

SOIBERMAN, U. S., SHEHATA, A. E. M., LU, M. X., YOUNG, T., DAOUD, Y. J., CHAKRAVARTI, S., JUN, A. S. & FOSTER, J. W. 2019. Small Molecule Modulation of the Integrated Stress Response Governs the Keratoconic Phenotype In Vitro. *Invest Ophthalmol Vis Sci,* 60**,** 3422-3431.

SPOERL, E., MROCHEN, M., SLINEY, D., TROKEL, S. & SEILER, T. 2007. Safety of UVA-riboflavin cross-linking of the cornea. *Cornea,* 26**,** 385-9.

SRIDHAR, M. S. 2018. Anatomy of cornea and ocular surface. *Indian J Ophthalmol,* 66**,** 190-194.

STOCKER FW, MOORE LW., Jr Detecting changes in the cornea that come with age. Geriatrics. 1975;30:57–59. , 63–64, 67–69.

SUURONEN, E. J., NAKAMURA, M., WATSKY, M. A., STYS, P. K., MULLER, L. J., MUNGER, R., SHINOZAKI, N. & GRIFFITH, M. 2004. Innervated human corneal equivalents as in vitro models for nerve-target cell interactions. *FASEB J,* 18**,** 170-2.

TACHIBANA, M., OKAMOTO, M., SAKAMOTO, M. & MATSUSHIMA, Y. 2002. Hereditary keratoconus-like keratopathy in Japanese wild mice mapped to mouse Chromosome 13. *Mamm Genome,* 13**,** 692-5.

TAKAHASHI, T., LORD, B., SCHULZE, P. C., FRYER, R. M., SARANG, S. S., GULLANS, S. R. & LEE, R. T. 2003. Ascorbic acid enhances differentiation of embryonic stem cells into cardiac myocytes. *Circulation,* 107**,** 1912-6.

TOMIDOKORO, A., OSHIKA, T., AMANO, S., HIGAKI, S., MAEDA, N. & MIYATA, K. 2000. Changes in anterior and posterior corneal curvatures in keratoconus. *Ophthalmology,* 107**,** 1328-32.

TONG, L., CORRALES, R. M., CHEN, Z., VILLARREAL, A. L., DE PAIVA, C. S., BEUERMAN, R., LI, D. Q. & PFLUGFELDER, S. C. 2006. Expression and regulation of cornified envelope proteins in human corneal epithelium. *Invest Ophthalmol Vis Sci,* 47**,** 1938-46.

TORRICELLI, A. A., MARINO, G. K., SANTHANAM, A., WU, J., SINGH, A. & WILSON, S. E. 2015. Epithelial basement membrane proteins perlecan and nidogen-2 are up-regulated in stromal cells after epithelial injury in human corneas. *Exp Eye Res,* 134**,** 33-8.

TORRICELLI, A. A., SANTHANAM, A., WU, J., SINGH, V. & WILSON, S. E. 2016. The corneal fibrosis response to epithelial-stromal injury. *Exp Eye Res,* 142**,** 110-8.

TOTI, P., TOSI, G. M., TRAVERSI, C., SCHURFELD, K., CARDONE, C. & CAPOROSSI, A. 2002a. CD-34 stromal expression pattern in normal and altered human corneas. *Ophthalmology,* 109**,** 1167-71.

TOTI, P., TOSI, G. M., TRAVERSI, C., SCHURFELD, K., CARDONE, C. & CAPOROSSI, A. 2002b. CD-34 stromal expression pattern in normal and altered human corneas. *Ophthalmology,* 109**,** 1167-1171.

TSUBOTA, K., MASHIMA, Y., MURATA, H., SATO, N. & OGATA, T. 1995. Corneal Epithelium in Keratoconus. *Cornea,* 14**,** 77-83.

TUFT, S. J. & COSTER, D. J. 1990. The corneal endothelium. *Eye (Lond),* 4 (Pt 3)**,** 389-424.

VALLABH, N. A., ROMANO, V. & WILLOUGHBY, C. E. 2017. Mitochondrial dysfunction and oxidative stress in corneal disease. *Mitochondrion,* 36**,** 103-113.

VAN DER VALK, J., MELLOR, D., BRANDS, R., FISCHER, R., GRUBER, F., GSTRAUNTHALER, G., HELLEBREKERS, L., HYLLNER, J., JONKER, F. H., PRIETO, P., THALEN, M. & BAUMANS, V. 2004. The humane collection of fetal bovine serum and possibilities for serum-free cell and tissue culture. *Toxicol In Vitro,* 18**,** 1-12.

VEGA-ESTRADA, A., ALIO, J. L. & PLAZA-PUCHE, A. B. 2015. Keratoconus progression after intrastromal corneal ring segment implantation in young patients: Five-year follow-up. *J Cataract Refract Surg,* 41**,** 1145-52.

WANG, Y., RABINOWITZ, Y. S., ROTTER, J. I. & YANG, H. 2000. Genetic epidemiological study of keratoconus: evidence for major gene determination. *Am J Med Genet,* 93**,** 403-9.

WEALE RA. The Aging Eye. London: Hoeber Medical Division, Harper & Row; 1963.

WENG, J., LIANG, Q., MOHAN, R. R., LI, Q. & WILSON, S. E. 1997. Hepatocyte growth factor, keratinocyte growth factor, and other growth factor-receptor systems in the lens. *Invest Ophthalmol Vis Sci,* 38**,** 1543-54.

WESSMAN, S. J. & LEVINGS, R. L. 1999. Benefits and risks due to animal serum used in cell culture production. *Dev Biol Stand,* 99**,** 3-8.

WILLIAMS, A. L. & BOHNSACK, B. L. 2015. Neural crest derivatives in ocular development: Discerning the eye of the storm. *Birth Defects Research Part C-Embryo Today-Reviews,* 105**,** 87-95.

WILSON, S. E. 2012. Corneal myofibroblast biology and pathobiology: generation, persistence, and transparency. *Exp Eye Res,* 99**,** 78-88.

WILSON, S. E., CHEN, L., MOHAN, R. R., LIANG, Q. & LIU, J. 1999. Expression of HGF, KGF, EGF and receptor messenger RNAs following corneal epithelial wounding. *Exp Eye Res,* 68**,** 377-97.

WILSON, S. E., HE, Y. G., WENG, J., LI, Q., MCDOWALL, A. W., VITAL, M. & CHWANG, E. L. 1996. Epithelial injury induces keratocyte apoptosis: hypothesized role for the interleukin-1 system in the modulation of corneal tissue organization and wound healing. *Exp Eye Res,* 62**,** 325-7.

WILSON, S. E. & HONG, J. W. 2000. Bowman's layer structure and function: critical or dispensable to corneal function? A hypothesis. *Cornea,* 19**,** 417-20.

WILSON, S. E., NETTO, M. & AMBROSIO, R., JR. 2003. Corneal cells: chatty in development, homeostasis, wound healing, and disease. *Am J Ophthalmol,* 136**,** 530-6.

WISTOW, G. 2012. The human crystallin gene families. *Hum Genomics,* 6**,** 26.

WOJCIK, K. A., SYNOWIEC, E., JIMENEZ-GARCIA, M. P., KAMINSKA, A., POLAKOWSKI, P., BLASIAK, J., SZAFLIK, J. & SZAFLIK, J. P. 2013. Polymorphism of the transferrin gene in eye diseases: keratoconus and Fuchs endothelial corneal dystrophy. *Biomed Res Int,* 2013**,** 247438.

WOLLENSAK, G., SPOERL, E. & SEILER, T. 2003. Riboflavin/ultraviolet-a-induced collagen crosslinking for the treatment of keratoconus. *Am J Ophthalmol,* 135**,** 620-7.

WRANA, J. L., ATTISANO, L., CARCAMO, J., ZENTELLA, A., DOODY, J., LAIHO, M., WANG, X. F. & MASSAGUE, J. 1992. TGF beta signals through a heteromeric protein kinase receptor complex. *Cell,* 71**,** 1003-14.

WU, J., DU, Y., WATKINS, S. C., FUNDERBURGH, J. L. & WAGNER, W. R. 2012. The engineering of organized human corneal tissue through the spatial guidance of corneal stromal stem cells. *Biomaterials,* 33**,** 1343-52.

XUAN, M., WANG, S., LIU, X., HE, Y., LI, Y. & ZHANG, Y. 2016. Proteins of the corneal stroma: importance in visual function. *Cell Tissue Res,* 364**,** 9-16.

XUE, C., XIANG, Y., SHEN, M., WU, D. & WANG, Y. 2018. Preliminary Investigation of the Mechanical Anisotropy of the Normal Human Corneal Stroma. *J Ophthalmol,* 2018**,** 5392041.

YAM, G. H., FUEST, M., ZHOU, L., LIU, Y. C., DENG, L., CHAN, A. S., ONG, H. S., KHOR, W. B., ANG, M. & MEHTA, J. S. 2019. Differential epithelial and stromal protein profiles in cone and non-cone regions of keratoconus corneas. *Sci Rep,* 9**,** 2965.

YAM, G. H., WILLIAMS, G. P., SETIAWAN, M., YUSOFF, N. Z., LEE, X. W., HTOON, H. M., ZHOU, L., FUEST, M. & MEHTA, J. S. 2017. Nerve regeneration by human corneal stromal keratocytes and stromal fibroblasts. *Sci Rep,* 7**,** 45396.

YANG, A. Y., CHOW, J. & LIU, J. 2018. Corneal Innervation and Sensation: The Eye and Beyond. *Yale J Biol Med,* 91**,** 13-21.

YOSHIDA, S., SHIMMURA, S., NAGOSHI, N., FUKUDA, K., MATSUZAKI, Y., OKANO, H. & TSUBOTA, K. 2006. Isolation of multipotent neural crest-derived stem cells from the adult mouse cornea. *Stem Cells,* 24**,** 2714-2722.

YOU, J., CORLEY, S. M., WEN, L., HODGE, C., HOLLHUMER, R., MADIGAN, M. C., WILKINS, M. R. & SUTTON, G. 2018. RNA-Seq analysis and comparison of corneal epithelium in keratoconus and myopia patients. *Sci Rep,* 8**,** 389.

YOU, J., WEN, L., ROUFAS, A., HODGE, C., SUTTON, G. & MADIGAN, M. C. 2015. Expression of HGF and c-Met Proteins in Human Keratoconus Corneas. *J Ophthalmol,* 2015**,** 852986.

YU, F. S., YIN, J., XU, K. & HUANG, J. 2010. Growth factors and corneal epithelial wound healing. *Brain Res Bull,* 81**,** 229-35.

YU, Q. & STAMENKOVIC, I. 2000. Cell surface-localized matrix metalloproteinase-9 proteolytically activates TGF-beta and promotes tumor invasion and angiogenesis. *Genes Dev,* 14**,** 163-76.

YUE, B. Y., BAUM, J. L. & SMITH, B. D. 1979. Collagen synthesis by cultures of stromal cells from normal human and keratoconus corneas. *Biochem Biophys Res Commun,* 86**,** 465-72.

ZANON CDE, F., SONEHARA, N. M., GIROL, A. P., GIL, C. D. & OLIANI, S. M. 2015. Protective effects of the galectin-1 protein on in vivo and in vitro models of ocular inflammation. *Mol Vis,* 21**,** 1036-50.

ZHANG, J., ZHANG, L., HONG, J., WU, D. & XU, J. 2015. Association of Common Variants in LOX with Keratoconus: A Meta-Analysis. *PLoS One,* 10**,** e0145815.

ZIAEI, H., JAFARINASAB, M. R., JAVADI, M. A., KARIMIAN, F., POORSALMAN, H., MAHDAVI, M., SHOJA, M. R. & KATIBEH, M. 2012. Epidemiology of keratoconus in an Iranian population. *Cornea,* 31**,** 1044-7.

ZIERHUT, M., CADENAS, E. & RAO, N. A. 2008. *Free radicals in ophthalmic disorders,* New York, Informa Healthcare.

ZIESKE, J. D., GUIMARAES, S. R. & HUTCHEON, A. E. 2001. Kinetics of keratocyte proliferation in response to epithelial debridement. *Exp Eye Res,* 72**,** 33-9.